DANMARKS OG GRØNLANDS GEOLOGISKE UNDERSØGELSE RAPPORT 2017/5

Architecture and mineral potential of the Paleoproterozoic Karrat Group, West Greenland

Results of the 2016 Season

Diogo Rosa, Michelle Dewolfe, Pierpaolo Guarnieri, Jochen Kolb,
Crystal LaFlamme, Camille Partin, Sara Salehi,
Erik Vest Sørensen, Simon Thaarup,
Kristine Thrane & Robert Zimmermann

GEOLOGICAL SURVEY OF DENMARK AND GREENLAND
DANISH MINISTRY OF ENERGY, UTILITIES AND CLIMATE

GEUS

DANMARKS OG GRØNLANDS GEOLOGISKE UNDERSØGELSE RAPPORT 2017/5

Architecture and mineral potential of the Paleoproterozoic Karrat Group, West Greenland

Results of the 2016 Season

Diogo Rosa, Michelle Dewolfe, Pierpaolo Guarnieri, Jochen Kolb,
Crystal LaFlamme, Camille Partin, Sara Salehi,
Erik Vest Sørensen, Simon Thaarup,
Kristine Thrane & Robert Zimmermann

GEOLOGICAL SURVEY OF DENMARK AND GREENLAND
DANISH MINISTRY OF ENERGY, UTILITIES AND CLIMATE

Contents

Contents 3

Abstract 5

Background and logistical setup 7

Remote sensing 9

Oblique aerial photography (Photoflying) 9
Drone-borne surveys 12
Hyperspectral Imaging 13
Instruments 13
Targets and in-field logistics 13
Processing 15
Methods 16
Spectroscopy 17
Results 18

Archean 24

Stratigraphy of the Karrat Group 27

Undifferentiated Karrat Group (north of Upernavik) 28
Qeqertarssuaq Formation 33
Qaarsukassak Formation 38
Mârmorilik Formation 45
Kangilleq Formation 52
Nûkavsak Formation 63

Intrusive Rocks 71

Prøven Intrusive Complex (PIC) 71
Crustal melting, melt migration, and S-type pluton formation 71
Post-kinematic pegmatite dykes 72
Nutaarmiut gabbro complex 73

Structural Geology 75

Northern Domain 77
Prøven Domain 82
Kangiusap Kuua-Ukkusissat Fjord Domain 83
Umiammakku-Inngia Fjord Domain 85
Alfred Wegeners Halvø-Kangerlussuaq Fjord Domain 85
Nunaarsussuaq-Maarmorilik Domain 86

Economic Geology 92

Nûkavsak/Kangilleq VMS 92

Qaarsukassak Formation 99
Mârmorilik Formation 101
Intrusion related mineralisation 103

Preliminary conclusions and recommendations **105**

Acknowledgements **108**

Author contributions **109**

References **110**

Abstract

This report presents the preliminary results of the second field season of a joint project between the Geological Survey of Denmark and Greenland (GEUS) and the Ministry of Mineral Resources of Greenland (MMR) focusing on the Paleoproterozoic Karrat Group. The motivation for the expedition stems from an evaluation of the mineral potential along with understanding the stratigraphic architecture of the Karrat Group and aims to address stratigraphy, structure, and economic geology. Field work extended to northern Karrat Group outcrops, between Upernavik and Kullosuaq, and allowed further studies of the southern Karrat Group outcrops between Svartenhuk and Maarmorilik. The relationship between the Karrat Group and the Prøven Igneous Complex (PIC), emplaced between these two areas, was also assessed. The 2016 field season was aided by oblique aerial photography ("photoflying"), and hyperspectral techniques. Hyperspectral scenes were collected along cliff faces in the areas with the most prospective mineral potential, including Kangerluarsuk Fjord and Maarmorilik. These studies have built on the observations made in 2015, and have led either to the consolidation or to the revision of interpretations suggested after that season.

The exposed Karrat Group extends from ~71° to ~75°N and is composed of five formations: the Qeqertarssuaq (Lower Karrat Group), Qaarsukassak, Mârmorilik, Kangilleq, and Nûkavsak formations (Upper Karrat Group), of which the Qaarsukassak amd Kangilleq formations are informal. The lower and upper Karrat Group are separated by a regional erosional unconformity, which represents a revision to the Karrat stratigraphy established during the 2015 field season. The Karrat Group has not been differentiated north of Upernavik due to the high metamorphic grade and polyphase deformation. Major goals of the field work included delineating contact relationships between units, documenting sedimentary structures that can define depositional environment(s), mapping the lateral extent and nature of extrusive mafic volcanism and volcaniclastic rocks in the upper Karrat Group (Kangilleq Formation), and determining the relative age relationships between units, which is elusive since several units are not in contact with one another. Integrated stratigraphy, sedimentology, volcanology, and ongoing geochronology will lead to a better understanding of the basin tectonic setting(s) in which the Karrat Group was deposited.

The deformation history of the area put forward after the 2015 season has been reviewed, and this succession is suggested: a NW-vergent D1 north of the Prøven Igneous Complex and channel flow in an orogen-scale NW-SE compression; D2 is characterised by E-W extension near Archean orthogneiss at Kangiusap Kuua and distal compression further to the E (previously assigned to D4); D3 is represented by structuring of the Kigarsima nappe overprinting all the other structures on Karrat Island and the peninsula to the SE (formerly described as D2); and, finally, a NW-SE compression, documented in the Maarmorilik area, is now relabeled as D4 (previously assigned to D3).

The time-stratigraphic horizon above and laterally to the Kangilleq Formation volcanism represents a period of VMS-formation on (or just below) the seafloor. Sampling of massive sulfides has yielded anomalous base metal concentrations (typically <0.3% Cu+Pb+Zn). However, because it is known that massive sulfide horizons can display zonations from

low-grade to gold- and/or base metal-rich zones, these horizons potentially constitute targets for future base metal and/or gold exploration in the Karrat region.

A Mississippi-Valley Type (MVT) origin is suggested for the Zn-Pb mineralisation in the Qaarsukassak Formation (RTZ Discovery), which might therefore have formed at the same time as the mineralisation in the Mârmorilik Formation. This is based on proximity of the Qaarsukassak Formation mineralisation to Archean rocks and the association of its distribution with marble and chert horizons. The possible role of evaporites and their diapirism in the mineralising process has been highlighted in the Mârmorilik Formation, by establishing the proximity of the known Lower Mârmorilik Formation showings to what can be interpreted to have been an evaporite horizon (now a “mottled pelite”). From this horizon, evaporites possibly ascended and were emplaced, as diapirs, within the Upper Mârmorilik Formation, underneath the pelites that would have acted as cap rock (where the Black Angel deposit is). Diapirism was likely triggered by deformation, during which evaporites flowed along thrust planes, as has been tentatively documented through the hyperspectral survey.

Possible silicate-silicate liquid immiscibility accompanied by silicate-sulfide immisciblity, occurred in a gabbro complex identified on the eastern side of Nutaarmiut island, to the southeast of Upernavik. The degree of PGE-Au enrichment in the sulfide has not been tested yet, but could potentially be of economic significance.

Background and logistical setup

The KarratZinc is a joint project between the Geological Survey of Denmark and Greenland (GEUS) and the Ministry of Mineral Resources of Greenland (MMR) aiming at the understanding of the architecture and the evaluation of the mineral potential of the Paleoproterozoic Karrat Group (Figure 1). Within this framework, and following a first field season in 2015 described in Rosa et al (2016), a second field season took place in 2016. Between July 14th and August 25th, 2016, a total 13 of geologists conducted field work between Upernavik and Kullorsuaq (first two weeks) and between Svartenhuk and Maarmorilik (last four weeks).

The ship Minna Martek, with a crew of three, was chartered to be used as basecamp, setting anchor in eight different anchorages (Figure 1). At these anchorages, fuel depots where established, and teams were put out on field camps or took off on reccos with an Air Greenland chartered AS 350 B3 helicopter (pilots: Carl Boström replaced by Petter Prydz Johansson on July 26th).

The ship sailed northwards from Upernavik, on July 14th, with gear, provisions, fuel and 7 geologists, to cover the coastline up to Kullorsuaq island, with 5 different anchorages: Anchorage 1, north of Nuussuaq at N 74.298 / W 56.280; Anchorage 2, south of Qullikorsuit island at N73.790, W 56.110; Anchorage 3, at Anarusuk Ø at N 73.441 / W 55.654, Anchorage 4, by Naajat at N 73.140 / W 55.806; and Anchorage 5, in southern Nutaarmiut at N 72.591 / W 55.564.

The ship returned to Upernavik on July 28th, for the replacement of two geologists and subsequently sailed southwards around Svartenhuk, and set anchor in three anchorages: Anchorage 6, in NE Qeqertarssuaq at N 71.6671 / W 52.8115 (same as Anchorage 2 in 2015); Anchorage 7, in Kangerluarsuk at N71.2913 / W 51.7712 (same as Anchorage 1 in 2015); and Anchorage 8, in Maarmorilik at N71.1249 / W 51.2728. Anchorage moves were done on August 10th and August 19th, respectively. On August 11th, 5 geologists were replaced by 4 geologists, who travelled through Qaarsut. At the end of the season and after dropping the 6 remaining expedition participants in Qaarsut on August 25th, the ship sailed with gear, leftover fuel and samples, south to Nuuk, where it arrived on August 27th.
Furthermore, on helicopter pilot rest days, Minna Martek was used to sail along fjords, from which zodiacs were deployed for coastal recco. The weather and snow conditions were good for most of the time, with only occasional morning fog leading to some flying constraints.

In the following sections, the preliminary observations and results of the 2016 fieldwork are reported, which build on those acquired in 2015, organised along different disciplines.

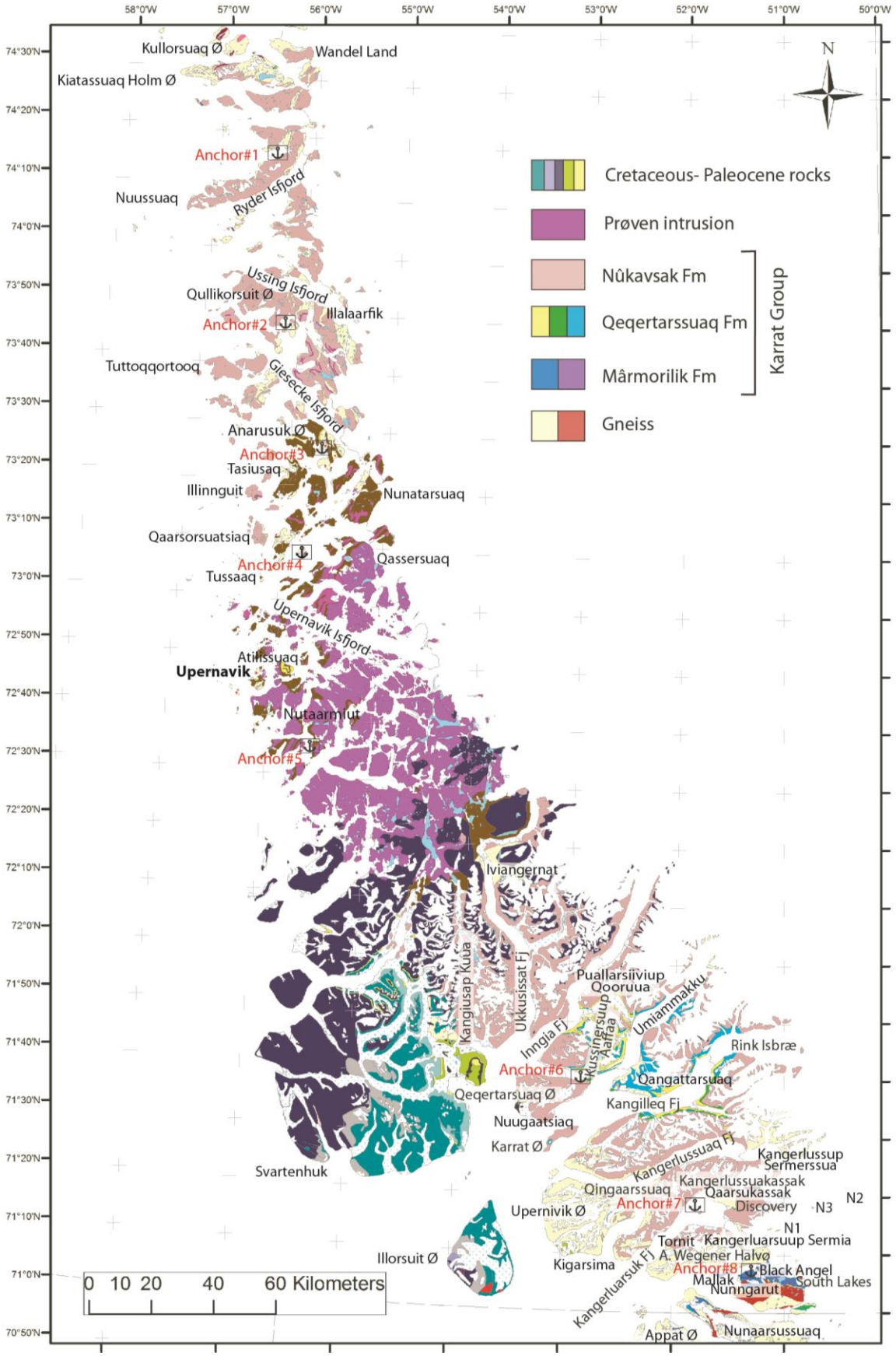

Figure 1. *Geological map of the study area (after Escher, 1980), showing anchorages in red, and highlighting localities discussed in the text.A larger version can be found loose in the report.*

Remote sensing

Oblique aerial photography (Photoflying)

The study area is characterised by steep alpine terrain that in many places is completely inaccessible. This makes field work an extremely difficult task. In 2015, in order to successfully overcome these obstacles a strategy involving acquisition of oblique stereo-images that can be used for 3D-mapping, interpretation purposes and topography extraction was deployed. Similar strategy was followed during the 2016 field work in the northern area. Furthermore, considering the regional scale of the project area, using imagery and remote observations is highly beneficial. In addition, new supplementary imagery was collected from the southern area. By collecting oblique aerial photographs while flying expedition members to their field locations, we are able to bring the field inside the lab in a very effective way, where the images will form the basis for structural mapping, correlation between outcrops and structural restoration. The stereo-images were collected from the helicopter using a calibrated Nikon D800E digital-SLR camera equipped with a 35 mm 1.4L Zeiss lens. A total of around 14000 images were collected from the northern area (Figure 2) while around 6000 images were collected from the southern area (Figure 3).

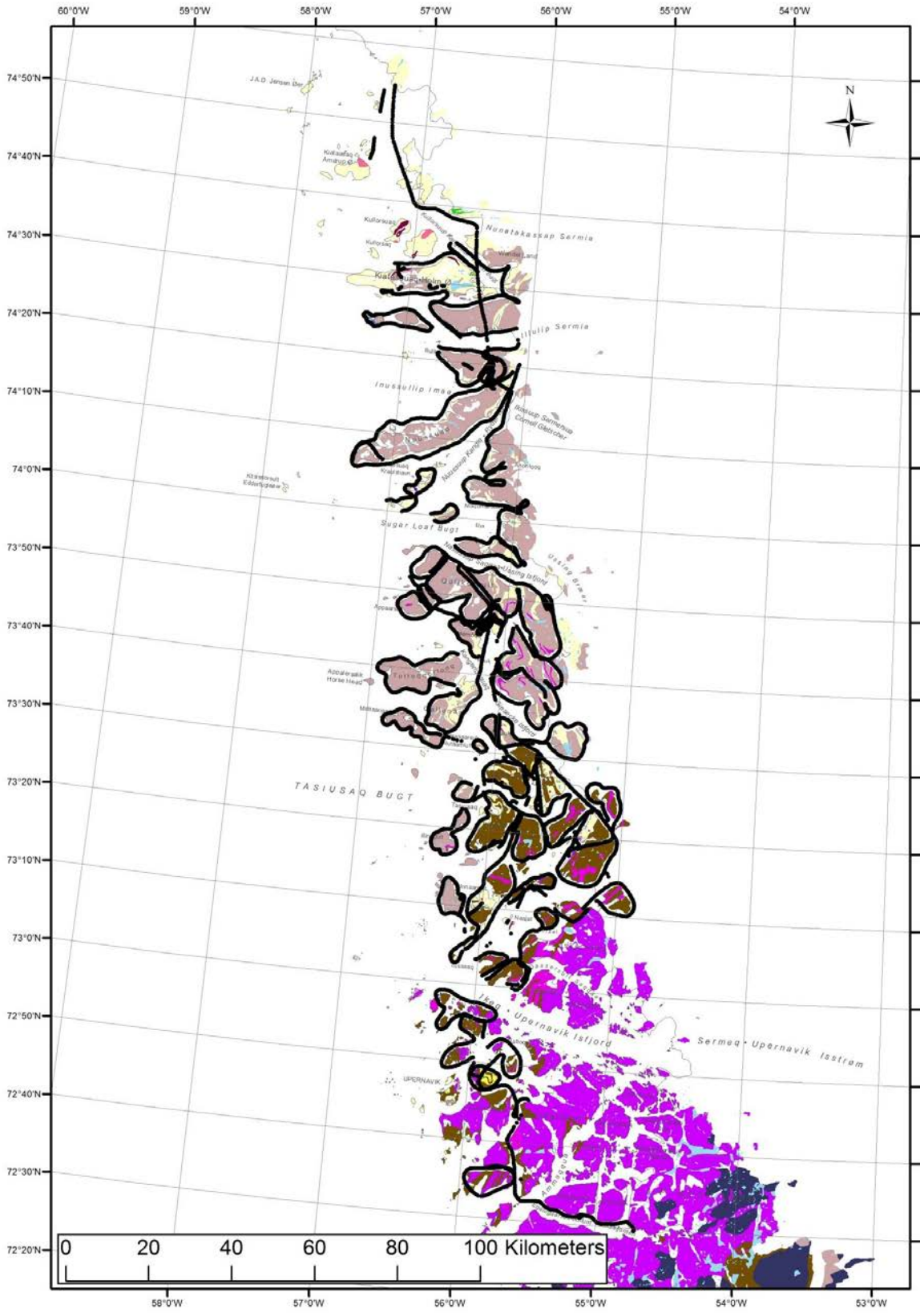

Figure 2. *Locations of collected stereo images (black lines) in northern Karrat, superimposed on geological map after Escher (1980). Same legend as in Figure 1.*

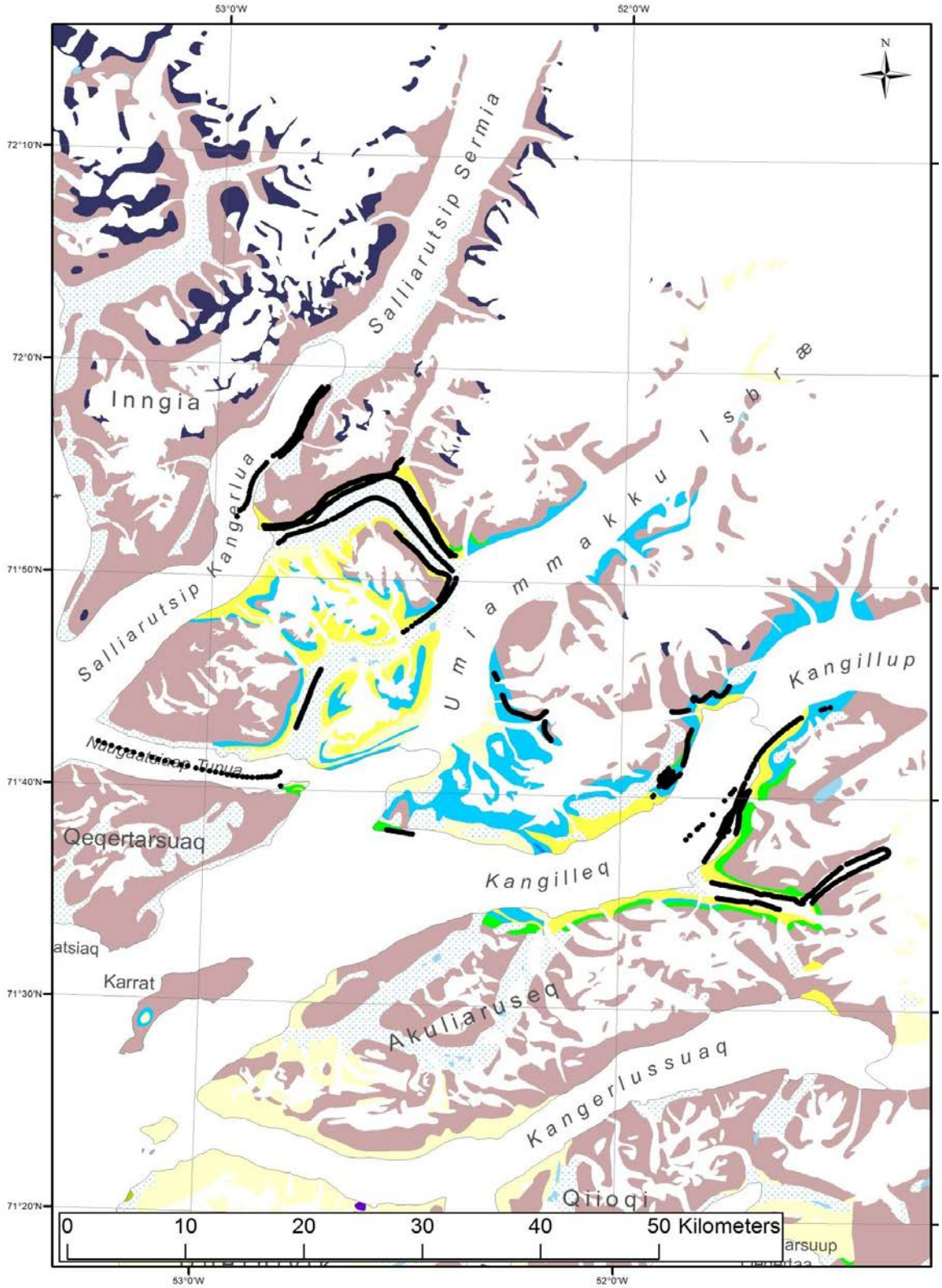

Figure 3. *Locations of collected stereo images (black lines) in northern Karrat, superimposed on geological map after Escher (1980). Same legend as in Figure 1.*

Drone-borne surveys

A drone-borne survey was performed between the Discovery and Discovery South showings (Coppard et al, 1992), in Kangerluarsuk Fjord (Anchorage #7). Separate pre-defined flight plans were applied for each Unmanned Aerial System/camera-combination to meet the requirements in terms of ground resolution, image acquisition time and image overlap. Both systems (see Table 1) store their flight logs internally (flight path and points of image acquisition), so a geo-referencing of the image data is possible afterwards.

Table 1. *Instrument characteristics*

	Flight time	Camera
DJI Phantom 2	25 min	GoPro Hero 4
Aibotix Aibot X6v2	15 min	Nikon Coolpix A RIKOLA Hyperspectral Imager

The Digital Surface Model was computed by using a standard *Structure-from-Motion* (SfM) algorithm implemented in the commercially available software Agisoft Photoscan. SfM is a low-cost, user-friendly photogrammetric technique solving the equations for camera parameters and scene geometry using a highly redundant bundle adjustment. Outputs are high-resolution Digital Elevation Models (DEM) and Orthomosaics.

The hyperspectral data taken with the RIKOLA Hyperspectral Imager were pre-processed following the workflow of Jakob et al. (2017). It includes different steps of geometric, radiometric and topographic corrections (see section Hyperspectral Imaging for details). The scenes were later mosaicked and a principal component analysis (see section Hyperspectral Imaging) was computed.

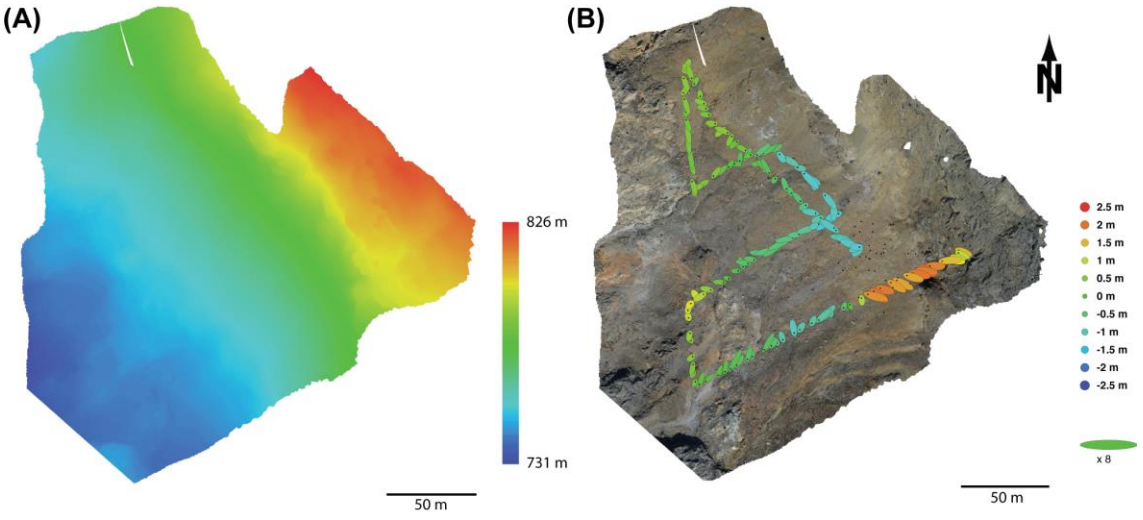

Figure 4. *A) Digital Elevation Model (colour coded according to elevation) of the surveyed Discovery area, B) Orthomosaic and camera position error. X and Y errors are represented by the shape of the ellipse, Z by the colour coding.*

This survey showed that a mafic dyke cutting the Archean rocks is in turn cut by the Qaarsukassak Formation, and was therefore emplaced earlier than the deposition of this formation, and is presumably of pre-Qaarsukassak age.

Hyperspectral Imaging

Hyperspectral imaging was deployed to sense inaccessible areas and to provide information on the spatial extent of alteration mineral assemblages. In combination with photogeological interpretations (Rosa et al., 2016) this spectral information not only helps to evaluate the areas' mineral potential, but also to highlight certain structures (e.g., at Black Angel Mountain) not visible in standard photographs.

Instruments

Two different hyperspectral sensors were utilised to acquire hyperspectral data (Table 2). The Specim AisaFenix was predominately used due to its wider spectral range covering the Visible-to-Near-Infrared (VNIR) and Shortwave Infrared (SWIR) part of the electromagnetic spectrum. Most alteration minerals have dominant absorptions in this wavelength range. In contrast, the RIKOLA Hyperspectral Imager is spectrally limited to the VNIR range, but much smaller and lighter compared to the AisaFenix. Thus, its primary application was drone-based and during photoflying with the helicopter.

Table 2: *Instrument characteristics*

	Sensor type	Wavelength range	Weight (ready for operation)	Spatial Resolution
RIKOLA Hyperspectral Imager	Full Frame	504-900 nm	1 kg	1010 x 1010px
Specim AisaFenix	Push-broom	400-2500 nm	~115 kg	∞ x 384px

Targets and in-field logistics

Several targets were selected on basis of previous photogeological interpretation (see Figure 5 and Table 3 for location). Most scenes were acquired using the Specim AisaFenix Hyperspectral camera due to its higher spectral resolution and range. Regions of interest encompass the contacts of the Archean to overlying Paleoproterozoic meta-sedimentary rocks and associated prospective horizons. Focus around Anchorage #7 in Kangerluarsuk Fjord was the Discovery and other known and indicated Zn-Pb showings. Focus around the Anchorage #8 was the marbles of Mârmorilik Formation at Black Angel Mountain and Nungarut. Hyperspectral images were taken to resolve folding and detect possible fluid-pathways by mapping specific mineral assemblages. Other targets with the RIKOLA hyperspectral imager were the East facing cliffs of Illorsuit Island as well as some parts of Kirgasima.

Table 3: *List of acquired scenes with the Specim AisaFenix Hyperspectral Camera, * X represents the running number of scans from the respective spot.*

Day	Location	Scene-ID	Latitude (N)	Longitude (E)	Scanning Direction (°)
12/08/2016	2016NSC008	GL20160812_Karrat_stop1_X*	71.22085	-51.36382	240
12/08/2016	2016RZI010	GL20160812_Karrat_stop2_X*	71.34270	-51.55241	0
12/08/2016	2016RZI017	GL20160812_Karrat_stop3_X*	71.33825	-51.47569	90
13/08/2016	Kangerluarsuk	GL20160813_Karrat_X*	ship-based		330
14/08/2016	2016RZI018	GL20160814_Karrat_X*	71.38776	-52.11618	340
15/08/2016	2016RZI034	GL20160815_Karrat_Discovery_X*	71.32075	-51.47687	90
18/08/2016	Kirgasima	GL20160818_Karrat_X*	ship-based		330 - 90
21/08/2016	2016RZI102	GL20160821_Karrat_X*	71.11859	-51.27116	70
22/08/2016	2016RZI104	GL20160822_Karrat_stop1_X*	71.11715	-51.20325	290
22/08/2016	2016RZI105	GL20160822_Karrat_stop2_X*	71.08724	-51.06632	0
22/08/2016	2016RZI106	GL20160822_Karrat_stop3_X*	71.07311	-51.21365	340
22/08/2016	2016RZI107	GL20160822_Karrat_stop4_X*	71.09010	-51.20556	30
22/08/2016	2016RZI116	GL20160822_Karrat_stop5_X*	71.15054	-51.23646	170

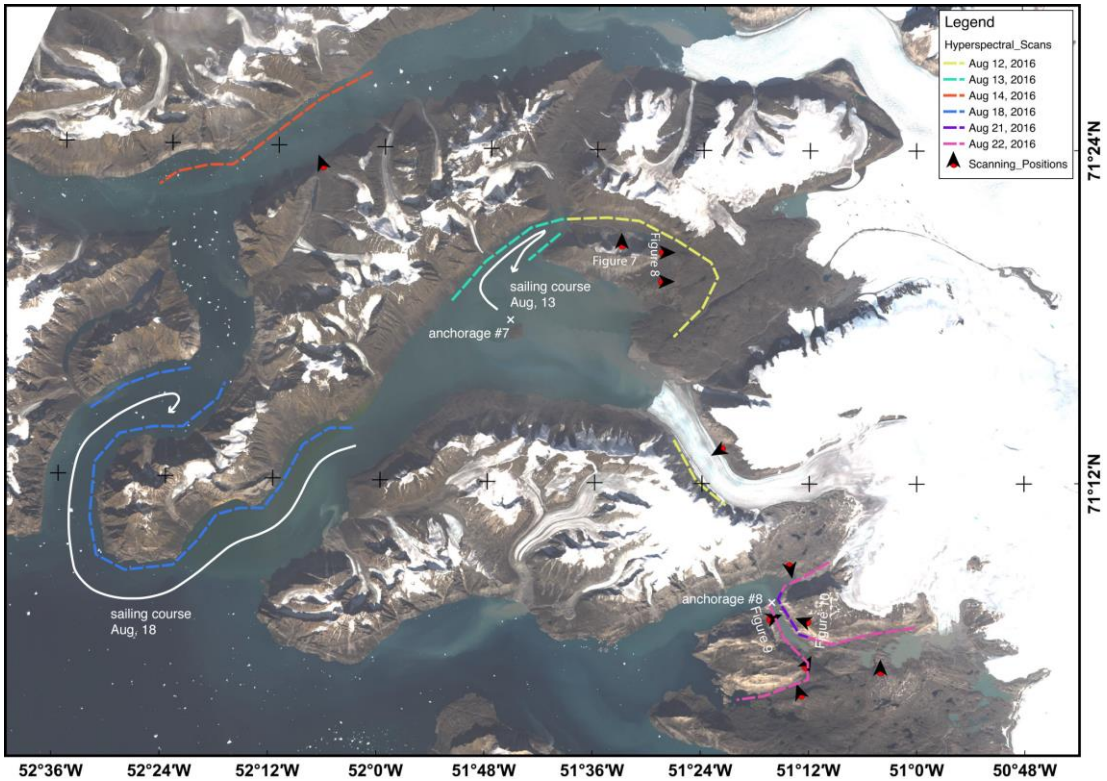

Figure 5: *Cliffs covered by Hyperspectral Images during fieldwork. All scenes are with GEUS as unprocessed data. The scenes are always overlapping to enable later mosaicking and draping on an existing DigitalElevationModel (DEM).*

In-field logistics were challenging as the multiple cases of the Specim AisaFenix, tripod, and generator were shipped and loaded into the helicopter whenever needed. Scanning points had to be close to a suited landing spot for the helicopter as it barely can be transported over long distances due to its high weight (~80 kg + 25 kg generator). A field team of two persons (camera operator + assistant) was necessary to unload, setup and load the instrument. Acquisition of one scene (landing, unpacking, measuring and packing) took about 30 to 60 min.

Processing

All scenes from the Specim AisaFenix were converted to at-sensor radiance (measured signal minus dark current) with Specim's CaliGeoPro software to correct for camera-specific parameters. Selected scenes were further processed to reflectance by empirical line calibration with the SRS-99 white calibration panel. The whole processing workflow (based on Cudahy et al., 2008) can be summarised as:

1. Conversation to radiance (Specim CaliGeoPro)
2. Conversation to reflectance (Empirical Line calibration)
3. Application of a composite mask to mask vegetated and low albedo pixels:
    - 3.1 Green vegetation out: NDVI[1] > 0.25,
    - 3.2 water out: NDWI[2] > 0.1 and
    - 3.3 low albedo out: for reflectance at 1650 nm (band 462) < 5 %.
4. Atmospheric correction using the depth of the 1137nm atmosphere-related absorption
5. Band ratios, absorption wavelength
6. Principal Component analysis (e.g., PCA or MNF[3])
7. Endmember extraction and spectral unmixing

Pre-Processing of the RIKOLA data follows the workflow as proposed by Jakob et al. (2017) with different geometric, radiometric and topographic correction steps. Empirical line correction is used for conversion to reflectance. It then follows the workflow of the Specim beginning with item (3).

1 NDVI = Normalized Differential Vegetation Index. A ratio computed using bands covering the Near-Infrared and Red range

2 NDWI = Normalized Differential Water Index. A ratio computed using bands covering the Near-Infrared and Green range

3 MNF = Minimum Noise Fraction. A double Principal Component Analysis (PCA) often used for noise filtering

Methods

(1) Band ratios and absorption wavelength

Band ratios are used to enhance abundances of specific minerals within a spectral image. They discriminate mineral types by suppressing the proportionally constant values in the bands and enhancing the differences (Zhang et al.; 2007). First, well-known band ratios (Cudahy et al.,2008) were calculated.

Instead of simple band ratios, position and depth of a distinct absorption feature can also be used (e.g., van der Meer, 2003). First the convex hull curve (or Continuum Removal) is calculated for a specific part of the spectra. In the next step, the wavelength of the minimum is extracted using either (1) a moving window or (2) a polynomial interpolation of the spectrum. Absorption wavelength mapping was performed using the HypPy software (Bekker, 2014).

(2) Principal component analysis using Minimum Noise Fraction

Minimum Noise Fraction (MNF) transform is important for dimensionality reduction and filtering of noise from hyperspectral data. It should be preferred over principal component analysis (Canty; 2007) and is widely applied in hyperspectral data analysis.

The transform is a principal component transformation ordering the data based on the signal-to-noise ratio. It computes linear combinations of mutually uncorrelated pixels that have maximum variance. Implemented within ENVI/IDL software is a modified version containing two steps (Canty; 2007): (1) Suppression of the noise contribution to the image with a covariance matrix. This is realised by a diagonalisation of the image. (2) Calculation of an ordinary principal component transformation.

(3) Endmember extraction, mineral mapping and spectral unmixing

Spectral Unmixing describes the procedure of decomposition for a mixed pixel spectra into a set of constituent spectra (endmembers) and their corresponding abundances (fractions), which are indicative of the relative presence of each endmember in the pixel (Keshava and Mustard; 2002). Hereby, an endmember is a distinct surface material with relatively constant spectral properties (Keshava and Mustard; 2002). The performance of spectral-based image endmember extraction algorithms highly depends on the ability to discriminate between pixels based on spectral characteristics. In other words, while endmembers with distinct spectral features (high spectral contrast) are easy to select, those with minimal unique spectral information (low spectral contrast) are more problematic. Spectral contrast, is dependent on the endmember assemblage, such that as the assemblage changes so does the “relative” spectral contrast of each endmember to all other endmembers. It is then possible for an endmember to have low spectral contrast with respect to the full image, but have high spectral contrast within a subset of the image.

Endmember extraction was performed using field spectra and partial unmixing with indicated and inferred endmember from spectral libraries (e.g., USGS spectral library, Clark et al.; 2007).

Multi-range spectral feature fitting (MRSFF; Clark et al., 1990) was used to identify zones enriched in specific alteration and indicator minerals (e.g., gypsum and kaolinite for Discovery showing, calcite, dolomite and gypsum for Mârmorilik Formation). Input spectra from spectral libraries were resampled to fit the original AisaFenix hyperspectral data cube. MRSFF compares the spectral similarity of each pixel spectra to pre-defined segments of a reference spectra and calculates the proportion of the respective minerals contained in the

pixel. It matches the depth and shape of specific absorption features of the continuum removed spectra with the reference spectra using a least-square technique (Clark et al., 1990). The output is a score image and a RMS (Root Mean Squared Error) image with the fitting errors. Pixels with high RMS values were interpreted as false positive. However, MRSFF does not provide information on position and depth of absorption band and thus, an in-depth mineralogical interpretation is not possible.

Another method to derive an image endmember set, is using the spatial–spectral endmember extraction (SSEE) method. This method works by analysing a scene in parts (subsets), such that the spectral contrast of low contrast endmembers increases. This enables the assessment of subtle lithological variability across a given study area (Rogge et al., 2007 and Rogge et al., 2012a).

Endmember extraction approach starts by first dividing the image into equal sized non-overlapping subset regions (subset size = 44 × 44 pixels) where a set of eigenvectors is calculated via singular value decomposition (SVD), i.e., 0.98, to determine the spectral variance within each subset. Next, image data is projected onto the local eigenvectors compiled from all subset regions. Pixels that lie at either extreme of the vectors are retained as possible endmembers. These endmembers are then sorted based on expert knowledge of known spectral features (water, snow, vegetation, lichen, and geological materials) followed by a more detailed sorting within each category into individual classes. Particular attention in the geological materials are subtle SWIR features related to key minerals. The resulting sorted endmember classes are subsequently averaged to produce a final endmember set. A final set of 14 geological endmembers, and 2 endmembers related to vegetation and lichens are deducted from expert based analysis.

Fractional abundances of the endmembers within the scene are determined using an iterative implementation of spectral mixture analysis (ISMA). This algorithm starts with an iterative unconstrained unmixing, which removes one endmember per iteration based on minimum fractional abundance until a single endmember remains. Analysis of the change in the root-mean-square error in each iteration allows the algorithm to locate the critical iteration defining the optimal endmember set. The result is a set of abundance fractions for the optimal endmembers. Resulting fractional abundance maps allow subsequent detailed geologic interpretation. However, in addition it is possible to generate thematic maps showing the distribution of specific geological materials. Thus, each pixel was assigned to the geological endmember with the maximum fractional abundance (>5% confidence threshold). The mapping results are consistent with the existing geological map, but display a higher level of detail.

Spectroscopy

Different samples were measured in the lab to compare the spectra with respective pixel-spectra from the Hyperspectral Images. Lab spectra can be used as validation and comparison for mapping alteration and lithology by hyperspectral imaging and for mineralogical investigations (analysis of clay minerals, carbonate minerals, etc.).

Spectral measurements were acquired using a Spectral Evolution PSR-3500 spectrometer. Spectra were recorded for the VNIR/SWIR part of the electromagnetic spectrum (400 to 2500 nm) with a spectral resolution of 3.5 nm (1.5 nm sampling interval) in VNIR and 7 nm (2.5 nm sampling interval) in the SWIR using a contact probe (8 mm spot size) with internal

light source. Radiance values were converted to reflectance using a Spectralon™ panel (SRS-99 white panel). Each spectral record consists of 10 individual measurements taken consecutively and averaged. Spectra (*n* = 223) were later automatically analysed for distinctive absorption features using an in-house R-script. Absorption wavelength position was later visualised in map view or used for statistical determination if surface mineralogical compositions.

Results

Spectroscopy of carbonate rocks from Discovery area (562003 and 562019) show a dolomite rich composition with minor absorption feature related to tremolite. Dolomite is suggested by both spectroscopy (absorption wavelength ~2320 nm) and pXRF measurements (pXRF ~62% dolomite to 38% calcite). Position of the carbonate absorption in spectroscopy is a direct function of the Mg content (position shifts to shorter wavelength with increasing dolomite content: 2340 nm for calcite to 2320 nm for dolomite; see Gaffey, 1985). In some spectra the dolomite absorption is little shifted to 2315nm caused by the superimposed Mg-OH feature due to tremolite. Rusty surfaces show a wide range of Fe^{2+}/Fe^{3+} absorption minima with two distinct peaks (see Figure 6-A) around 890 nm and 915 nm which can be related to jarosite and goethite respectively (Hunt, 1977). Together with sharp Al-OH and Fe-OH absorption features, a fingerprint for a typical alteration assemblage can be enabled. Based on the results, prospective zones can be better targeted in the hyperspectral images.

The marbles of the Mârmorilik Formation have a variable composition with a prominent carbonate absorption feature (see histogram in Figure 6-B), and minor features to Al-OH and Fe^{2+}/Fe^{3+} (smaller portions of clay and iron minerals). In sample 562048 (tremolite-rich marble) a prominent Mg-OH absorption around 2300 nm superimposes on a dolomitic carbonate feature at 2320 nm. So, the absorption feature shifted towards shorter wavelength (~2315 nm).

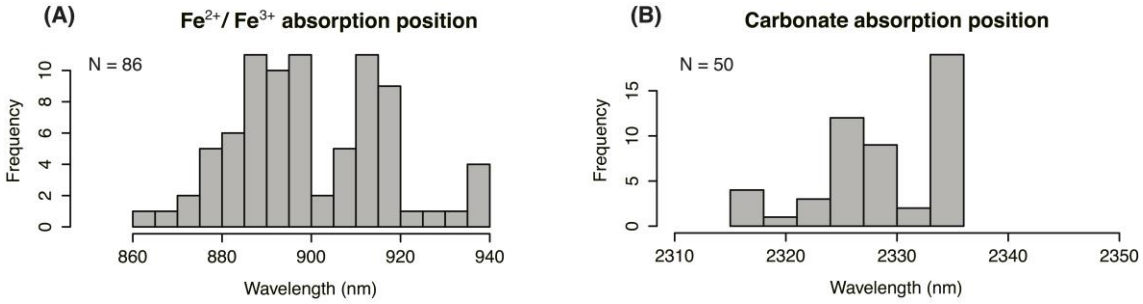

Figure 6. *Histogram of the wavelength range of the hull quotient-corrected absorption features. A) Fe^{2+} / Fe^{3+} absorption of various samples from rusty horizons. Shorter wavelengths indicate jarosite (peak around 890nm), higher goethite (peak around 910nm); B) Carbonate absorption for marbles of Mârmorilik Formation. Marble composition is quite variable with pre-dominant calcite-rich compositions.*

Preliminary results from hyperspectral imaging of the Paleovalleys, north of Qaarsukassak ridge, show prominent Al-OH absorption features that can be related to breakdown of feldspar to clay minerals in Archean rocks (Figure 7-A). Those can be well distinguished from

overlying Paleoproterozoic meta-sedimentary units with a different spectral signature. On top of the Archean rocks, in remnants of the Qaarsukassak Formation, carbonate rocks occur. Stratigraphic descriptions (see Rosa et al., 2016; Guarnieri et al., 2016) and absorption wavelength position between 2310 to 2320 nm suggest these are tremolite-bearing dolomitic marbles (see Figure 7-B and 8-A; see section Spectroscopy). These zones with clay minerals in Archean rocks and marble zones within the Qaarsukassak can be followed the whole way towards the Discovery showing (see Figure 8-A, B, C). The sphalerite occurrence of Discovery showing itself is probably hidden, as scanning position of the camera was too low.

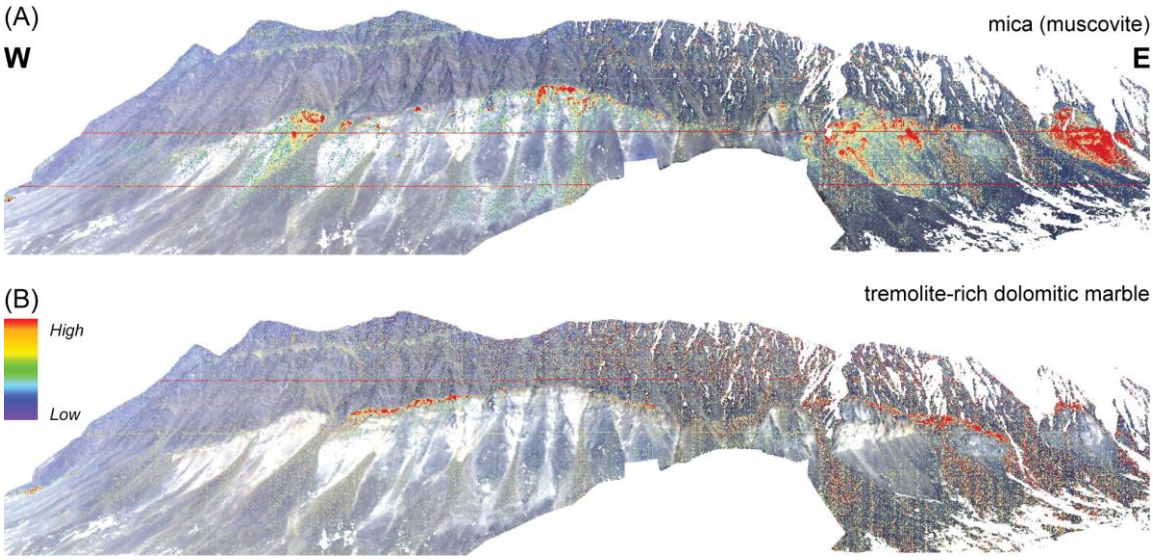

Figure 7. *Paleovalleys, north of Qaarsukassak ridge (looking North). See Figure 5 for scene location. Mineral Mapping results draped on true colour image: A) Relative abundance of clay minerals based on position and depth of the Al-OH absorption feature; B) Relative abundance of tremolite-rich dolomitic marbles based on location and depth of the carbonate absorption feature (see section spectroscopy).*

The MNF image of Discovery (see Figure 8-E) discriminates the major lithologies. Sky blue coloured areas correspond to tremolite-rich dolomitic marble, reddish and yellowish colours to Archean rocks, and dark-blue and greenish to sedimentary units of Nûkavsak Formation. The reason for the highlighted compositional differences in the Archean rocks should be checked during upcoming fieldwork. Brownish colours at Discovery show spectral similarities to gypsum mixed with some probably iron minerals, but needs further investigation. The brownish coloured area can be followed along strike into the Nûkavsak Formation. It is recommended to check those spots (indicated by red arrows in Figure 8-E) next field season.

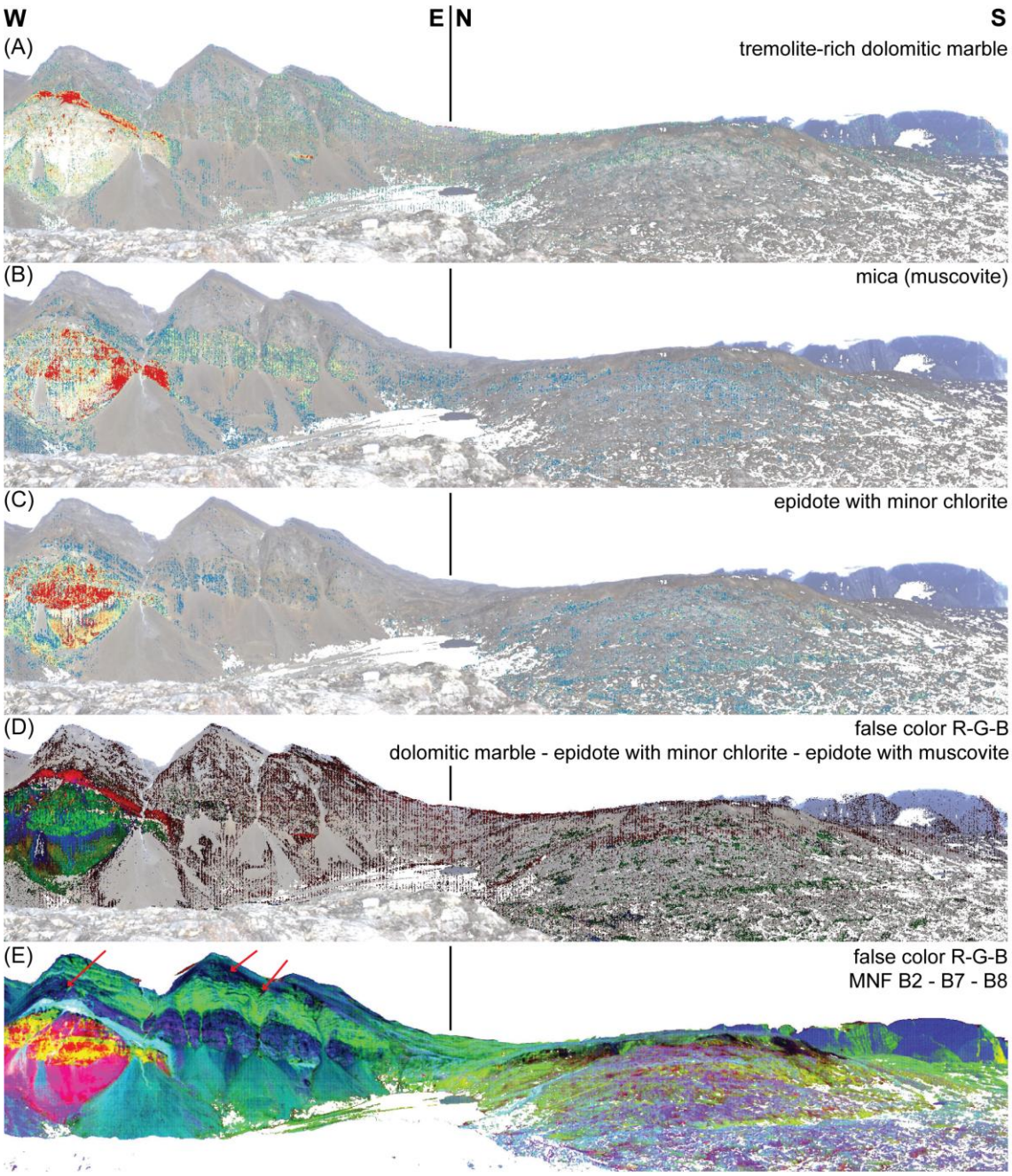

Figure 8. *Discovery area, East of Qaarsukassak ridge (follow-up of Figure 7 to the East). See Figure 5 for scene location. Selected endmember fractional abundance maps generated with the ISMA method: A) tremolite-rich dolomitic marble (dolomite 80% + tremolite 20%); B) mica (muscovite); C) epidote with minor chlorite; D) thematic map with the maximum fractional abundance above 5% for three main geologic endmembers: Red tremolite-rich dolomitic marble; Green: epidote with minor chlorite; Blue: epidote with muscovite; E) MNF false colour image: Red: Band2; Green: Band7; Blue: Band8*

Marbles of Mârmorilik Formation show prominent carbonate absorption features in the hyperspectral images. Different types of marble could be mapped based on the absorption wavelength. In hyperspectral scenes of Black Angel Mountain a fold, which cannot be identified from standard photographs, is visible as interbedded calcitic and dolomitic marbles (see Figure 9-A, B). Also recognised is the thrust mapped by Garde (1978) (Figure 9-C). The weathering of sulfides in meta-pelites that predominate towards the top of the mountain, yield gypsum-rich surfaces and scree (see Figure 9-D). This weathering effect makes it hard to identify gypsum of evaporitic origin. However, higher score values for scapolite-rich marble, interpreted to correspond to an evaporite assemblage, are highlighted above and possibly along the thrust structure (see Figure 9-E).

Hyperspectral scenes covering the East and South facing cliffs of Nunngarut (Figure 10 displays the East facing cliff) show layered, weakly deformed marbles. Some gentle low amplitude folds are visible in the East facing cliff of Nunngarut. Absorption wavelength position images confirm previous observations from Harris (1986) with calcitic marbles on top of dolomitic marbles. Shear zones (as interpreted by Harris, 1986) seem to coincide with dolomite-rich zones.

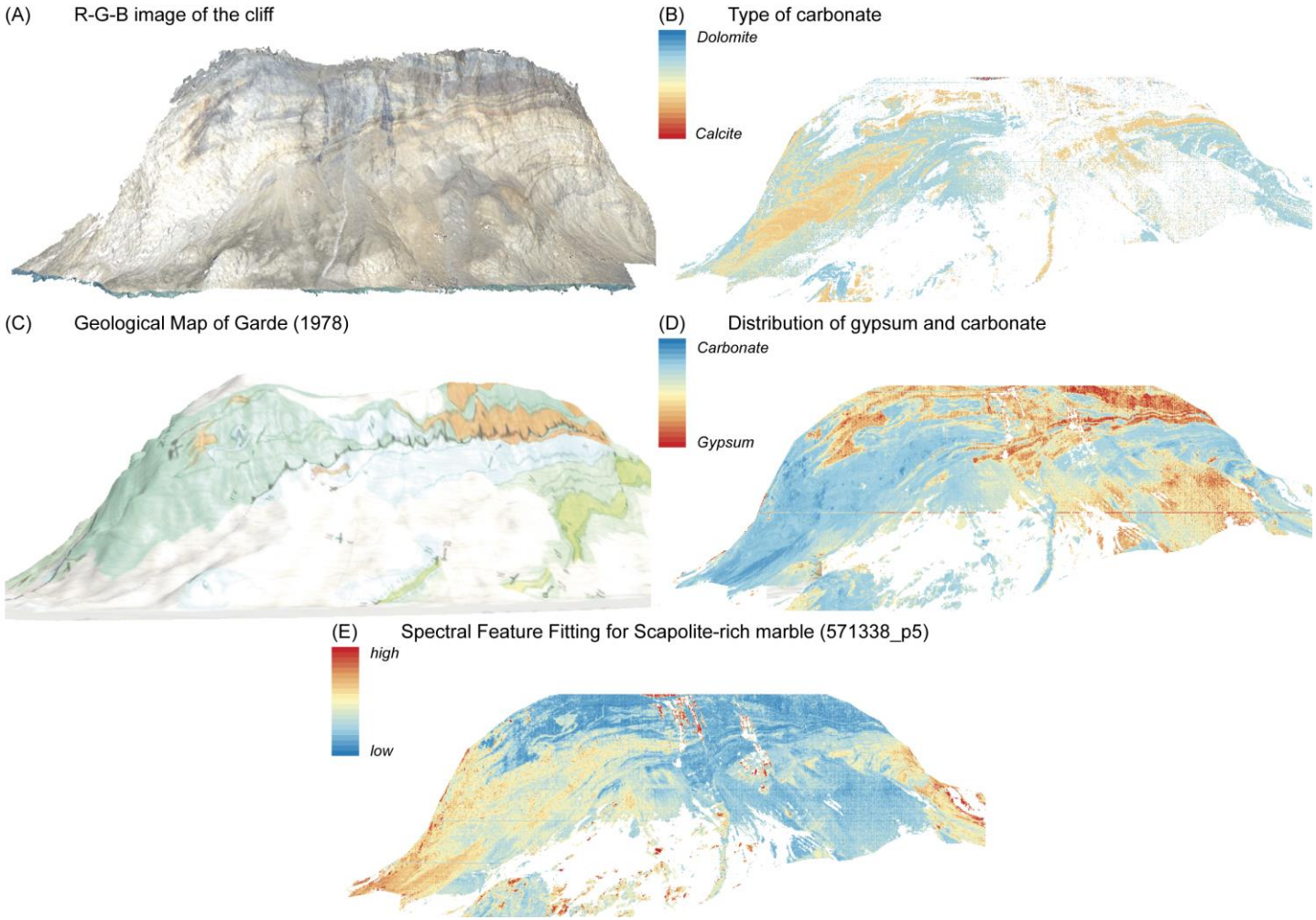

Figure 9. *Black Angel Mountain. See Figure 5 for scene location: A) True-Colour RGB image from oblique photographs; B) Absorption wavelength map highlighting calcite (orange) and dolomite (blueish) compositions; C) Geological map of Garde (1978) for comparison; D) Colour stretch ratio image of Spectral Feature Fitting results for gypsum (orange) and carbonates (blueish); E) Colour stretch of Spectral Feature Fitting result for scapolite-rich marble (571338-p5).*

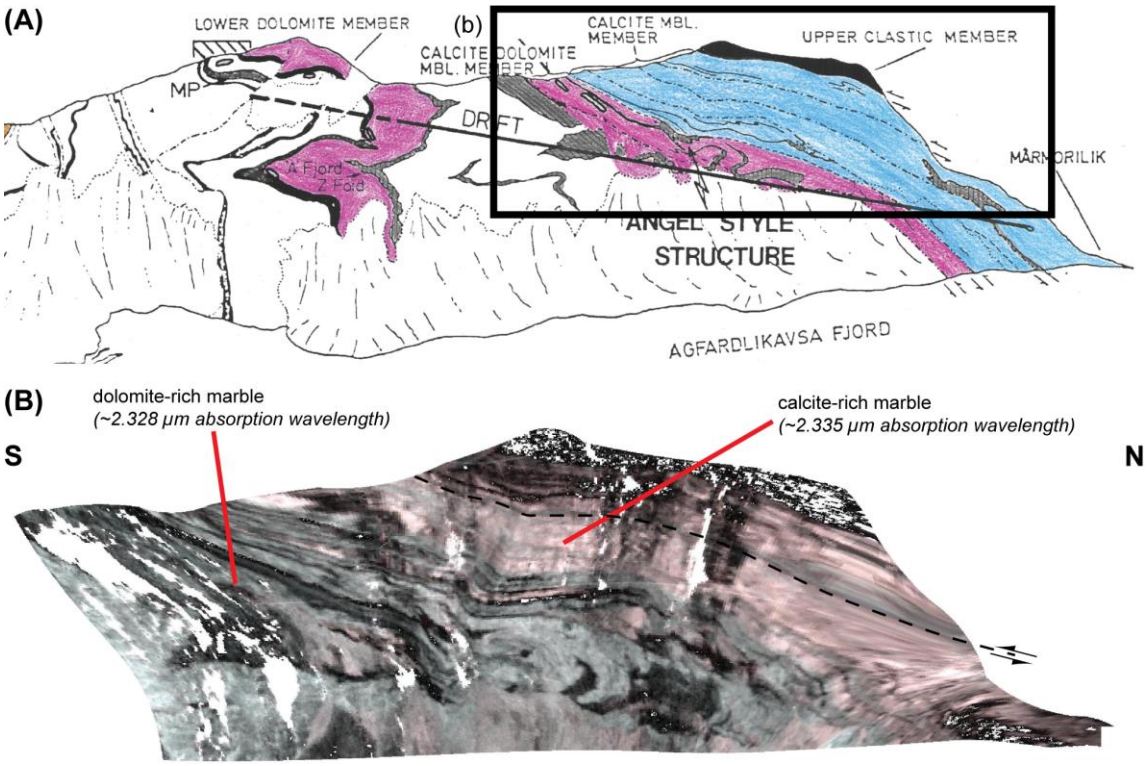

Figure 10. *East-wards facing cliff of Nunngarut. See Figure 5 for scene location: A) Colourised sketch from Harris (1986). Black rectangle corresponds to scene in B; B) Result of mineral mapping (Spectral Feature Fitting; R: Calcite (WS272); G and B: Dolomite (HS102.3B)) suggesting calcite (light grey) and dolomite-rich (darker grey) horizons and in-folded meta-pelites (black). It confirms the observations from A). However, within the calcite-rich marbles thin layers of dolomite-rich marble occur.*

Archean

Throughout the study area, the Karrat Group is underlain by Archean rocks believed to belong to the Rae Craton. In most places, there is a tectonic contact between the Archean rocks and the overlying meta-sedimentary rocks. The tectonic transport distance is unknown so far. The Archean is dominated by orthogneiss. Prior to this study, only very limited age data existed from the Archean. The only previous geochronology is an unpublished U-Pb zircon age of 2710 Ma from Holm Land, carried out by R.T. Pidgeon and referred to by Nutman et al. (2008). South of our study area on Drygalski Halvø, Rb-Sr analyses of tonalite gneiss yield a whole rock isochron age of 3087 ± 139 Ma (Andersen, 1981). During the last two field campaigns, samples of the orthogneiss have been collected throughout the region and U-Pb zircon age determinations are underway.
The Archean in the most northern part of the region, between Lille Renland and Ussing Isfjord, is dominated by banded, medium-grained, leucocratic plagioclase-hornblende-biotite orthogneiss (Figure 11-A). In places, the gneissic banding is not very well defined. Amphibolite dykes and quartz veins crosscut the orthogneiss. At one occurrence in the eastern end of Nuussuaq, a quartz vein contains molybdenite and pyrite. Veins of rose quartz also occur at the same locality. A distinctive sheet of red gneiss, not seen anywhere else in the area, is exposed in the cliff face on the south side of Holm Ø. This sheet is thrust on top of the more common grey orthogneiss and meta-sedimentary rock. North of Holm Land, several larger monzogranite bodies intrude the orthogneiss (Figure 11-B). These granites vary from undeformed to slightly deformed, and their appearance varies from a pink monzogranite dominated by K-feldspar to more plagioclase-biotite dominated composition. The age of the monzogranites is unknown and could be either Archean or Paleoproterozoic.

Figure 11. *A) Archean orthogneiss; B) Archean orthogneiss intruded by monzogranite (east of Kullorsuaq).*

South of Ussing Isfjord and extending as far south as the Prøven Igneous Complex (PIC), the Archean orthogneiss is migmatitic. It is made up of biotite-hornblende ± muscovite-bearing leucosomes, and biotite-bearing meso- and neosomes (Figure 12-A). In the area around Anchorage 3, the orthogneiss is partially melted to form a coarse-grained leucocrat-

ic monzogranite with large mafic xenoliths. The unit locally contains dismembered and boudinaged dykes and xenoliths of varying compositions (Figure 12-B). Peritectic hornblende demonstrates that partial melting of the Archean crust was assisted by fluids.
In the exposures closer to Upernavik, the Archean orthogneiss is leucocratic, coarse-grained and greenish in colour. They contain clinopyroxene ± orthopyroxene indicative of granulite-facies metamorphism in this area. We interpret that at least this area represents a piece of the lower crust that has been exhumed during Paleoproterozoic orogeny.

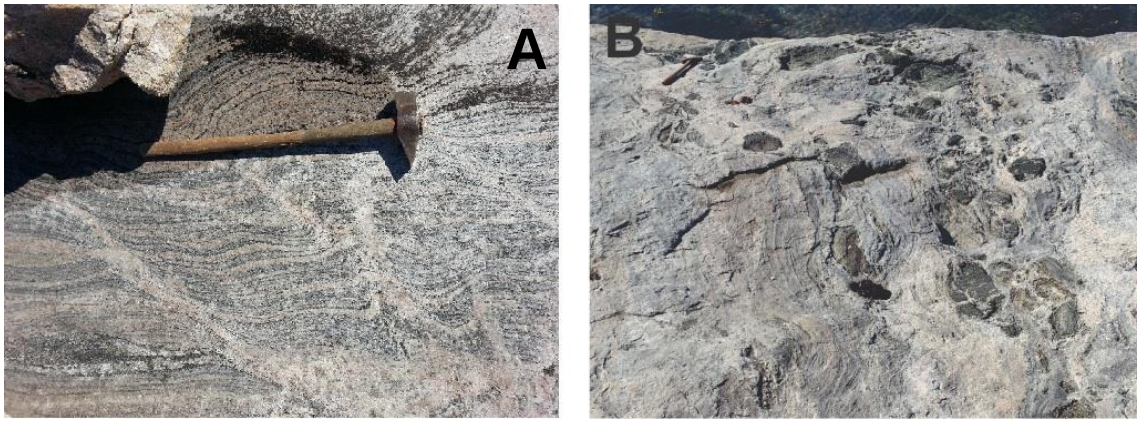

Figure 12. *Archean orthogneiss with S1 and S2 parallel leucosomes. A) Amphibolite-facies migmatite near Anchorage #2; B) Lower crust, granulite-facies orthogneiss near Tasiusaq, containing dismembered dyke*.

South of the PIC, the Archean is dominated by grey, banded, medium-grained, leucocratic, plagioclase-hornblende-biotite orthogneiss. It is deformed and cross cut by monzogranite dykes and pegmatites of several generations, some of which are deformed (Figure 13-A,B). Augen gneisses occur at different places in this area. The largest body of augen gneiss makes up the basement to the Mârmorilik Formation (Figure 13-C). The augen gneiss exposed here is homogeneous, very coarse-grained with large feldspar augen up to 4 cm and quartz augen up to 1 cm.

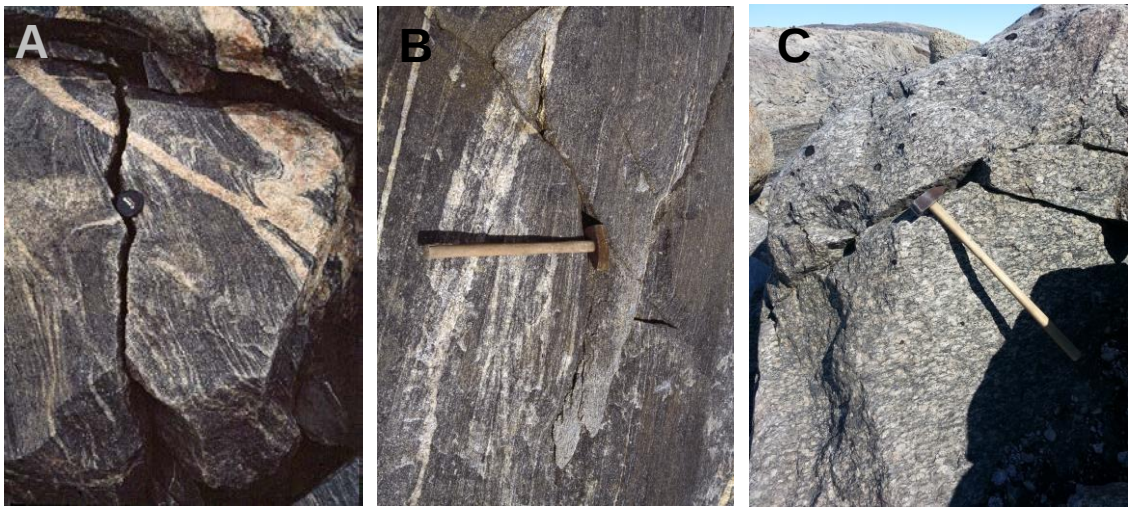

Figure 13. *Archean orthogneiss. A) from the northern end of Ukkusissat Fjord; B) from north of Kangerluarsuk Fjord, western end; C) augen gneiss from Maarmorilik.*

Crystalline rocks in the Discovery area consist dominantly of unfoliated monzogranite (Figure 14), which differs from the typical grey orthogneiss seen elsewhere.

Figure 14. *Unfoliated granite; basement to Qaarsukassak Formation at Discovery area, which differs from the Umanak gneiss seen elsewhere.*

Preliminary U-Pb zircon data show that most of the Archean orthogneiss underlying the Karrat Group is ca. 3000 Ma. However, in the core of the area, both north and south of the PIC, older ages of ca. 3150 Ma are recognised. These old Archean ages seem to be absent in the very northern part of the region, between Holm Ø and up to Kap Walker, where only ca. 2700 Ma ages have been recovered. This suggests that there may be a terrane boundary in the north or that the craton was growing towards the north. Another occurrence of ca. 2700 Ma age rocks is located in the south, namely the augen gneiss forming the basement to the Mârmorilik Formation. The precursor of the augen gneiss is, therefore, interpreted as an intrusion in the surrounding older grey gneisses.

Stratigraphy of the Karrat Group

The Karrat Group is a siliciclastic-carbonate-volcanic succession that was deposited unconformably on Archean crystalline basement rocks. Supracrustal rocks of the Karrat Group extend several degrees of latitude (~71° to ~75°N), spanning several hundred kilometres from north to south along coastal west Greenland. Exposure of the Karrat Group is interrupted by the PIC, which extends about 100 km of this transect, and separates the northern and southern exposures of the Karrat Group. Given the large spatial extent of the Karrat Group, it is unsurprising that the Karrat Group shows marked lateral variations in stratigraphy (Figure 15), which were previously hypothesised to relate to deposition in different subbasins (Grocott and Pulvertaft, 1990).

Reconnaissance mapping over the last two summers revealed that the Karrat Group was deposited in at least two stages, separated by an unconformity (Figure 15). The Karrat Group can be separated into lower and upper formations based on the interpretation of this regional unconformity. The Qeqertarssuaq Formation comprises the lower Karrat Group, whereas the Kangilleq, Mârmorilik, Qaarsukassak, and Nûkavsak formations comprise the upper Karrat Group. This unconformity is documented by variable thicknesses or absence of the Qeqertarssuaq Formation beneath upper Karrat Group a phase of deformation not present in upper Karrat Group rocks, and by the Kangilleq Formation resting on different units of the Qeqertarssuaq Formation (Rosa et al., 2016).

The main goals of the stratigraphic study are to understand the character, thickness, depositional environment(s) and relative ages along with correlation of the various units of the Karrat Group. Sedimentary structures are not ubiquitously preserved, but are present in most units of the upper Karrat Group. Delineating these characteristics leads to a better understanding of the basin tectonic setting(s) in which the Karrat Group was deposited and provides insights into how mineral potential relates to different stratigraphic units in space and time. The intrabasinal correlation of Karrat Group units is challenging since several units are not observed to be in contact with one another (Figure 15), but can be aided with ongoing geochronological studies.

The following is organised by stratigraphic unit within the Karrat Group, starting with the oldest unit, the Qeqertarssuaq Formation. Discussion of undifferentiated Karrat Group rocks north of the area of Prøven precedes these descriptions, since the deformation and metamorphic grade preclude any preliminary assignment of unit within the Karrat Group.

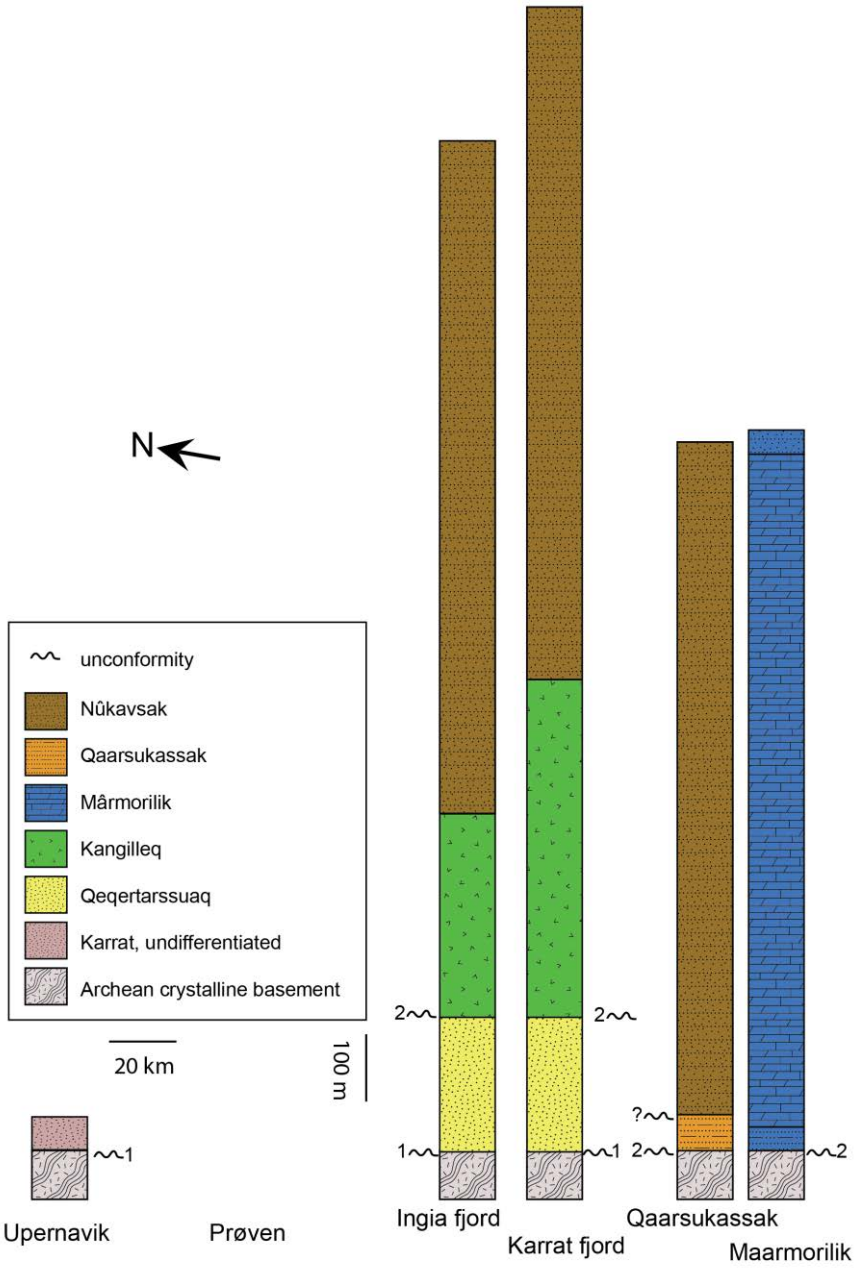

Figure 15. *Schematic stratigraphic columns that show the marked lateral variation in stratigraphy of the Karrat Group from southeast (Maarmorilik) to northwest (Upernavik). Note the differences in lateral and vertical scales. Thicknesses shown for the Nûkavsak Formation are shown as minimum thicknesses only; thickness estimates for the Qeqertarssuaq Formation are tenuous given the degree of deformation of the lower Karrat Group.*

Undifferentiated Karrat Group (north of Upernavik)

North of Upernavik, the Karrat Group comprises dominantly paragneiss that is rusty in colour and easily identifiable (from Archean orthogneiss) in the field. In the north (Lille Renland, north of area in Figure 1) the paragneiss is biotite-sillimanite-garnet bearing with in situ garnet-cordierite-biotite leucosomes (Figure 16-A,B). Toward the South, the leucosomes become increasingly segregated, forming bands of pegmatite within the foliation, ranging from 10 cm to 50 m in width (as discussed in the Intrusive Rocks section). Magmas

coalesced to form hornblende-biotite granodiorite plutons that crosscut the regional planar fabric, demonstrating that melt moved upward through the crust. Garnet is present in the restite. Closer to Upernavik, garnet is not as apparent and thick packages of restite dominate this unit (Figure 16-C). They are typical 'granulites' and are composed of orthopyroxene-biotite-plagioclase-quartz, demonstrating that all melt has migrated from these units, and it is in this area that pegmatite layers are thickest. Rarely, discontinuous thin bands (up to 3 m wide) of marble are found within the paragneiss. The marble is coarse-grained and crumbly, typical of the high grade of metamorphism reached (Figure 16-D).

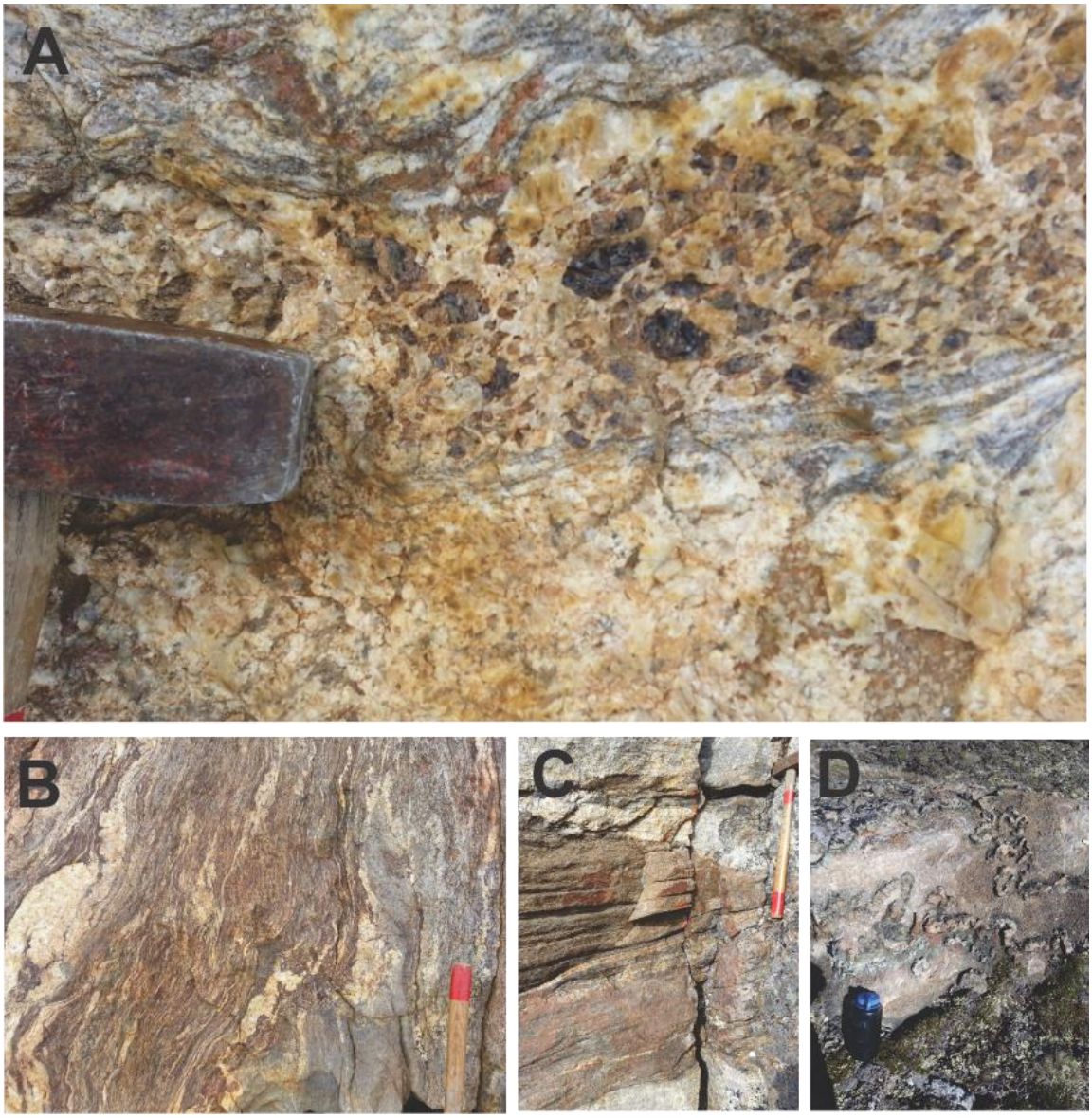

Figure 16. *Paleoproterozoic paragneiss of the Karrat Group between Lille Renland and Upernavik: A) Cordierite-bearing leucosomes in paragneiss, between Nuussuaq and Lille Renland; B) Garnet-biotite-silimanitel-cordierite in the same paragneiss, preserving garnet in both leucosomes and mesosomes. C) paragneiss pyroxene-bearing restite separating leucosomes. D) thin marble band within paragneiss.*

One of the objectives of the work carried out in the northern Karrat was to identify metavolcanic rocks that could be equivalent to those of the Kangilleq Formation (further described in that subsection). However, this is hampered as a result of the higher metamor-

phic grade in the northern area, compared to the grade in the southern area. What has been mapped as amphibolite has a sharp, commonly sheared, seldom migmatised contacts, with both the Archean orthogneiss and Paleoproteozoic paragneiss. Given the metamorphic grade of the rocks in the north, establishing a connection between these amphibolite units and the Kangilleq meta-volcanic rocks to the south will be clarified using whole rock geochemistry.

Only in the following three northern localities were primary volcanic textures or characteristics assumed to be of volcanic origin identified: 1) Northeast Nuussuaq (Anchorage #1); 2) Illalaarfik; 3) Qaarsorsuatsiaq.

At Northeast Nuussuaq primary volcanic textures in the form of white lapilli (10-20vol%, 1-7 mm across) and crude bedding are preserved in fine-grained quartz-amphibolite-biotite-silimanite schist, which hosts massive sulfide mineralisation (Figure 17). In Illalaarfik, an approximately 10 m thick and 400 m long exposure of dark green-black strongly foliated biotite-chlorite schist is located at the contact between the Archean orthogneiss and Paleoproterozoic paragneiss. This unit strongly resembles the unmineralised meta-volcaniclastic rocks at the Northeast Nuussuaq locality. Mafic meta-volcanic rocks on at Qaarsorsuatsiaq Island are in conformable contact with underlying meta-sedimentary rocks of the Karrat Group. The contact is gradational over approximately 5 m and defined by an intercalation of meta-volcanic rock beds with meta-sedimentary rock beds (beds range from 5 – 30 cm; Figure 18). The mafic meta-volcanic rocks range from very fine-grained (<1 mm) and bedded (cm- to dm-scale) to massive and medium-grained (1-3 mm, quartz and pyroxene).

Figure 17. *Mafic lapillistone (between white dashed lines) at contact between Archean orthogneiss (bottom) and Paleoproterozic paragneiss (top).*

Figure 18. *Intercalated mafic tuff beds and quartz-rich (quartzite?) beds at contact between meta-volcanic and underlying meta-sedimentary rocks.*

Black and dark green pods, lenses and boudins occurring directly at or within a few 10's of meters of the contact between the Paleoproterozoic paragneiss and the Archean orthogneiss were sampled in order to determine if they represent tectonically emplaced mantle rocks rather than volcanic rocks, using whole-rock geochemistry. Some occurrences of these dark green and black rocks are amphibolites with interstitial and granular plagioclase. These amphibolites contain green and brown amphibole, plagioclase, pyroxene, biotite (+/- zircon), Fe-oxide, where the plagioclase in the groundmass often occur in a granoblastic fashion with 120° triple joints. The sometimes poikiloblastic amphiboles have inclusions of plagioclase, in which case the latter are anhedral or appear worm-like. Similar, orthopyroxene occasionally contain anhedral inclusions of amphibole and plagioclase. It seems that the samples from localities mapped as Qeqertarssuaq ultramafic rocks contain amphibolites with orthopyroxene, and the undifferentiated amphibolites from bands and pods elsewhere (e.g. orthogneiss) contain mostly clinopyroxene. Zircon inclusions in biotite seem to be restricted for the amphibolites from localities within para- or orthogneiss. Amphibolites from areas mapped as Qeqertarssuaq ultramafic rocks do not display zircon inclusions in biotite.

The ultramafic rocks consist of large cm-sized orthopyroxene grains with multiple inclusions in a groundmass of millimetre-sized clinopyroxene, olivine, amphibole and green spinel. With the exception of sample 572607, the rocks exhibit an- to subhedral fabrics, where the groundmass may contain small interstitial pockets of plagioclase with either well-defined triple junctions with the granular amphibole, or as large interstitial single grains. Sample 572607 consists of the same minerals, but shows euhedral clinopyroxene, growing into orthopyroxene and subhedral amphibole. As such, the ultramafic rocks are classified as pyroxenites, with varying contents of olivine and amphibole, with subordinate amounts of plagioclase and green spinel. The amphibole grains in these pyroxenites are all colourless

and devoid of pleochroism. Furthermore, these amphibole grains reveal no signs of having replaced other minerals, which could suggest they represent a primary magmatic mineral. Green spinel was only present in the ultramafic rocks and shows an spatial affinity towards olivine. By contrast the large orthopyroxene grains contain Fe-oxide inclusions. Some rocks are moderately altered to fine-grained mica, talc, carbonate, and serpentine. The ultramafic rocks found in small boudins wedged in between or close to the contact between the orthogneiss and the paragneiss are texturally remarkably similar in thin section (with the exception of 572607). There is no apparent difference between those occurring in paragneiss or orthogneiss or those occurring as small lenses and regular outcrops.

Several unnamed islands north of and around Upernavik (including Atilissuaq Island) were visited to understand Karrat Group stratigraphy north of exposures dominated by the PIC. Interpretation of meta-sedimentary rocks in these areas present a major challenge due to the overprint by intrusions, multiple deformation events, high metamorphic grade, and probable hydrothermal alteration. The geological maps of these islands appear deceptively simple, but ground control suggests that the distribution of rocks is more complex. As a general observation, exposures are dominated by rocks of igneous protolith rather than sedimentary protoliths. These islands contain only thin exposures (metres to 10s of m) of probable meta-sedimentary rocks; the geology is otherwise dominated by igneous rocks.

On an island south of Upernavik (N72°45.917, W56°08.601), a relatively thin quartzite occurs (10s of m; <50 m overall), followed by less mature semipelitic gneiss. There are no distinguishing features to relate these meta-sedimentary rocks to any specific formations within the Karrat Group. They could permissibly represent either the Qeqertarssuaq Formation or the Nûkavsak Formation or something else. Given the limited stratigraphic thickness of these units, it is very unlikely that both units are present.

In general, where quartzite is mapped, mixed pegmatitic granite and strongly foliated biotite-epidote quartzite is observed. The map unit assigned to the Nûkavsak Formation here contains 20-30vol% euhedral garnet porphyroblasts in a quartz (50-60vol%)-biotite matrix; garnet locally makes up to 50vol% of the rock, suggesting a possible hydrothermal alteration prior to metamorphism. On Atilissuaq Island, rocks mapped as quartzite do not appear to have a sedimentary protolith. Instead, a hornblende-actinolite bearing felsic igneous rock with meta-sedimentary xenoliths was observed (Figure 19). Several intrusive phases are present, including a pegmatitc granite, epidote-bearing granitic gneisses, dolerite (or gabbro) intruded by garnet-bearing granititic gneiss, or a green, feldspar-(microcline)-bearing granite. Some of these granitic gneisses contain xenoliths of meta-sedimentary and metavolcanic rocks, presumably from the Karrat Group. In one exposure, a xenolith-bearing granite forms an L-tectonite. The metasedimentary map unit (Nûkavsak Formation equivalent?) map unit is a very thin (10s of m) rusty meta-sedimentary gneiss. Right-lateral offset of a granitic sill (~WNW/ESE) is observed (Figure 20). Other rusty zones on the island were investigated with the assumption that they would represent meta-sedimentary gneiss, but instead were found to be garnetiferous granitic rocks, which occur along a fault trend. In this area, a float sample with garnet, microcline, and fluorite was found.

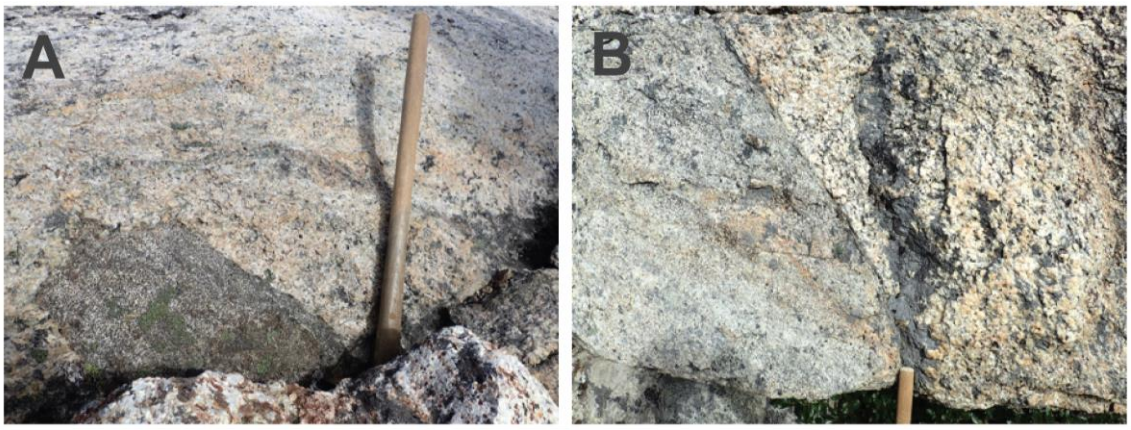

Figure 19. *Atilissuaq Island. A) Hornblende-actinolite bearing felsic igneous rock with meta-sedimentary xenoliths; B) contact between very coarse crystalline pegmatitc granite and coarse crystalline epidote (?) bearing granite.*

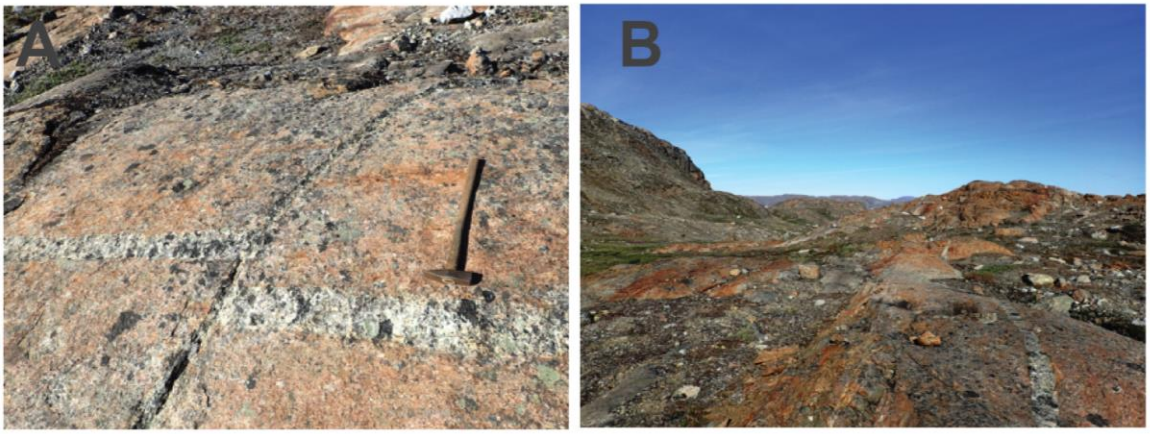

Figure 20. *Atilissuaq Island. A) Right-lateral offset of a granitic sill (~WNW/ESE) in rusty meta-sedimentary gneiss; B) thin exposure (10s of m) of rusty meta-sedimentary gneiss, possibly correlative to the Nûkavsak Formation (?).*

Qeqertarssuaq Formation

The Qeqertarssuaq Formation (lower Karrat Group) poses some challenges in stratigraphic studies since it is deformed, metamorphosed, and always infolded with Archean rocks. Tracking the variation in lithological character is still important in order to understand the early history of this basin. The following is a description of some of the localities visited in 2016 where this unit is relatively well-exposed and accessible. The Qeqertarssuaq Formation is typically overlain by the Kangilleq Formation, but in the absence of volcanic rocks, it is overlain by the Nûkavsak Formation.

The Qeqertarssuaq Formation is relatively well-exposed at Umiammakku Isbrae, and includes quartzite (including a fuchsitic quartzite), mica schist, and garnet amphibolite units (Figure 21) that are characteristic of the Qeqertarssuaq Formation elsewhere. The Qeqertarssuaq Formation is a relatively thick, flat-lying section here, but strata are disconnected by topography (nunataks) and discontinuous outcrop (felsenmeer). This section was previously mapped as Nûkavsak Formation. The Nûkavsak Formation does occur in this

area, but only on the northernmost nunatak on which the Tertiary basalt is found. There, the unconformity between Tertiary basalt and Nûkavsak Formation can be seen.

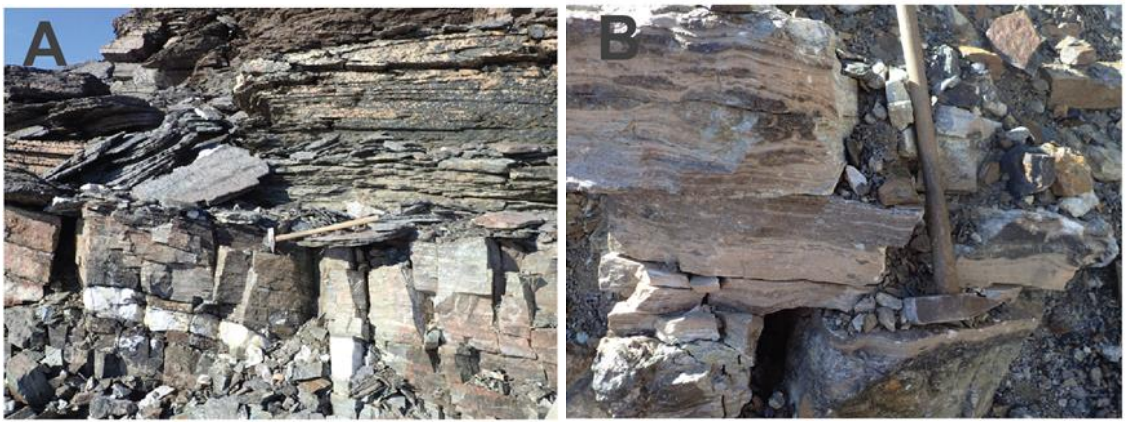

Figure 21. *Umiammakku Isbrae. A) Quartzite overlain by garnet porphyroblastic amphibolite of the Qeqertarssuaq Formation at the nunatak closest to the Umiammakku Isbrae glacial valley; B) calcite marble of the Qeqertarssuaq Formation, at base of cliff below Nûkavsak Formation.*

Though polydeformed, the “type section” of the Qeqertarssuaq Formation occurs on the peninsula on the eastern edge of Qeqertarssuaq Island, which is easily accessible by boat. Overall, this section is not a good representation of the Qeqertarssuaq Formation as observed elsewhere in Kangilleq Fjord. At Qeqertarssuaq Island, an olive green quartzite (Figure 22) can be seen, with ~5vol% muscovite, accessory epidote (0-10vol%), and chlorite that occurs along cleavage planes. Also present is a mica schist with boudinaged fuchsite, quartz nodules and biotite books apparently replacing a staurolite and muscovite matrix. Two amphibolite units occur (protolith unknown) and an augen gneiss (protolith unknown).

Figure 22. *Qeqertarssuaq Island. A) Quartzite of the Qeqertarssuaq Formation; B) mica schist with boudinaged fuchsite and quartz nodules of the Qeqertarssuaq Formation.*

At the head of Kangerluarsuk Fjord near a large waterfall (Figure 23), a thin polydeformed supracrustal succession underlies the Nûkavsak Formation, interpreted to represent an erosional remnant of the Qeqertarssuaq Formation. Archean crystalline rocks are strongly foliated and infolded with the lowermost supracrustal rocks (amphibolite; locally garnetifer-

ous), which is protomylonitic in places. A thin “quartzite” unit (<10 m) occurs above the amphibolite unit, which contains very coarse to granular size particles of feldspar and is therefore described as a feldspathic meta-arenite or meta-subarkose. Above this unit is a chlorite-actinolite schist (<10 m thick), which along strike is chlorite-siderite +talc/muscovite mica schist. A lens of grey-beige tremolite-biotite calcite marble occurs locally. Strongly foliated Nûkavsak Formation occurs above these units, suggesting right way-up.

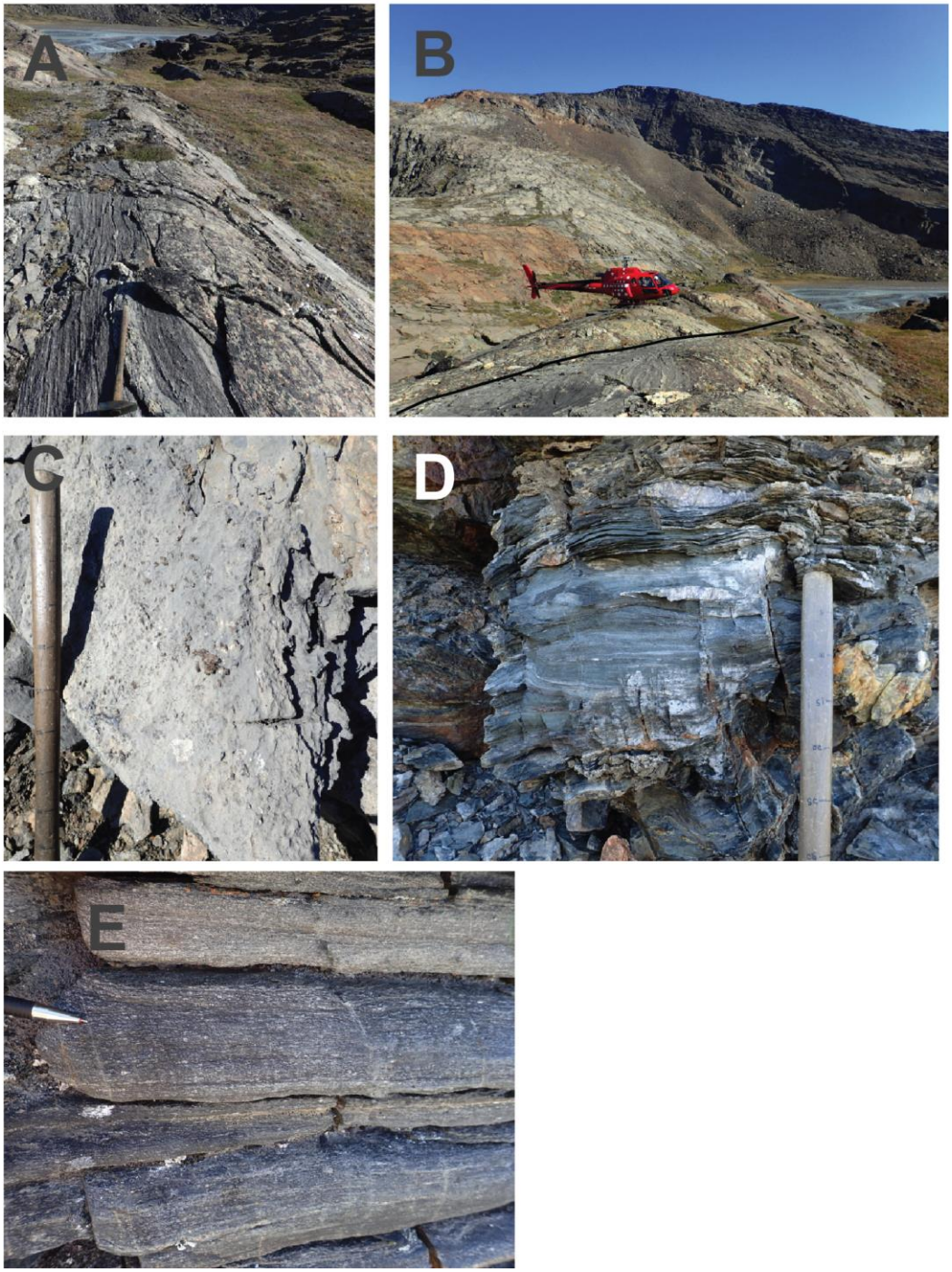

Figure 23. *Waterfall section at the head of Kangerluarsuk Fjord. A, B) Archean-Paleoproterozoic sequence contact; C) lens of tremolite-biotite calcite marble, D) chlorite-actinolite schist; E) protomylonite in lower amphibolite near contact with Archean rocks.*

Similar stratigraphy occurs southwards across the river in the same area, which is also interpreted to represent a thin section (<50 m) of Qeqertarssuaq Formation. The Archean-Qeqertarssuaq Formation contact is covered by scree here. Units in the lower stratigraphy include a chlorite schist (± garnet) with siderite pods and a garnet-bearing amphibolite. The chlorite schist is overlain by a very coarse-grained meta-subarkose (as on other side of river) (Figure 24). The Nûkavsak Formation here is a massive to thickly bedded fine to medium- to coarse-grained meta-sandstone with minor (deformed) quartz veins and is in contact with isoclinally folded garnet-chlorite mica schist.

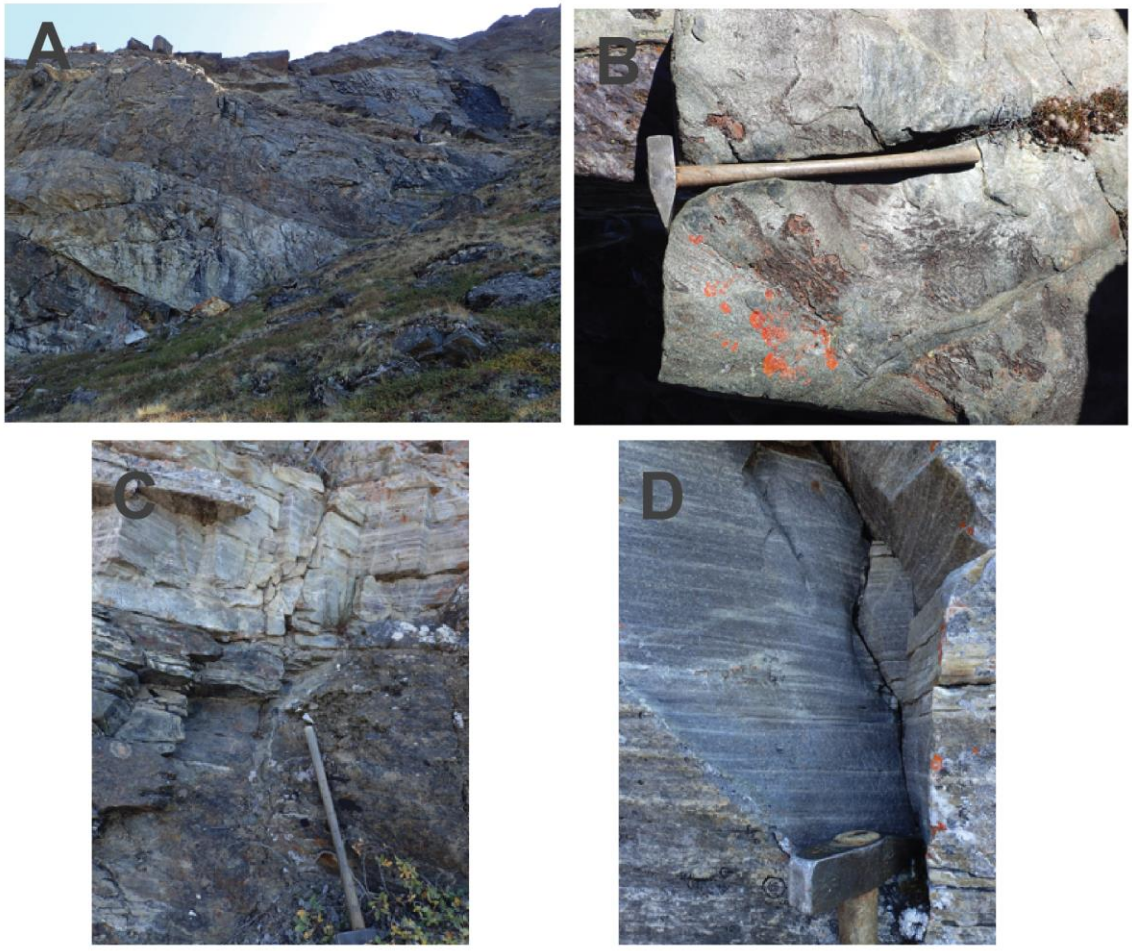

Figure 24. *Chlorite-siderite (± garnet) schist, subarkose units of the Qeqertarssuaq Formation at the head of Kangerluarsuk Fjord.*

Near Tornit in Kangerluarsuk Fjord, glacially polished outcrops of several units of unknown age and stratigraphic affinity occur in a wide valley. These units include a dark grey feldspar banded gneiss that is in contact with a dark green to rusty-weathering amphibolite, neither of which contain primary structures. Though the deformation makes determination of relative age relationships unclear, it appears that the gneiss protolith intrudes the amphibolite, since xenoliths of the latter occur in the gneiss. Both units are intruded by syn- to post-kinematic pegmatitic monzogranite dykes. A rusty-weathering sandy tremolite-calcite marble occurs above the amphibolite, which is infolded with quartz veins and pegmatite dykes (Figure 25). Given that amphibolite and calcite-tremolite marble have been observed elsewhere as part of the Qeqertarssuaq Formation, these rocks are tentatively assigned to this unit.

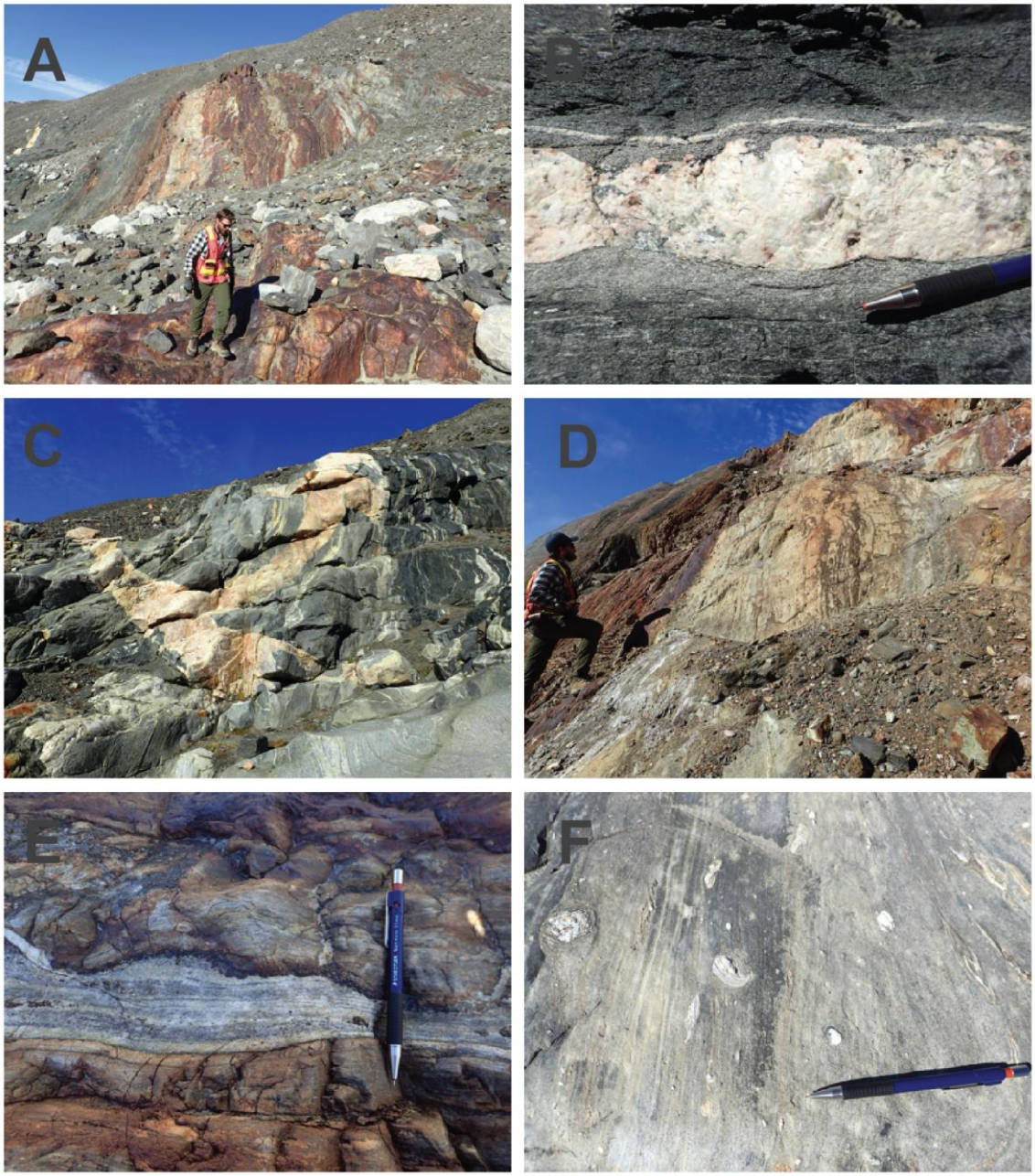

Figure 25. *Tornit. A, B, C) Rusty to dark green amphibolite intruded by syn- to post-kinematic pegmatitic monzogranite dykes; D,E,F) A deformed and in some places brecciated calcite-tremolite marble, which occurs above the amphibolite.*

The Qeqertarssuaq Formation in southwest Kangilleq Fjord (across from Karrat Island) is represented by quartz-garnet amphibolite schist and quartzite rocks above, towards the east, and a quartz augen gneiss, towards the west (Figure 26).

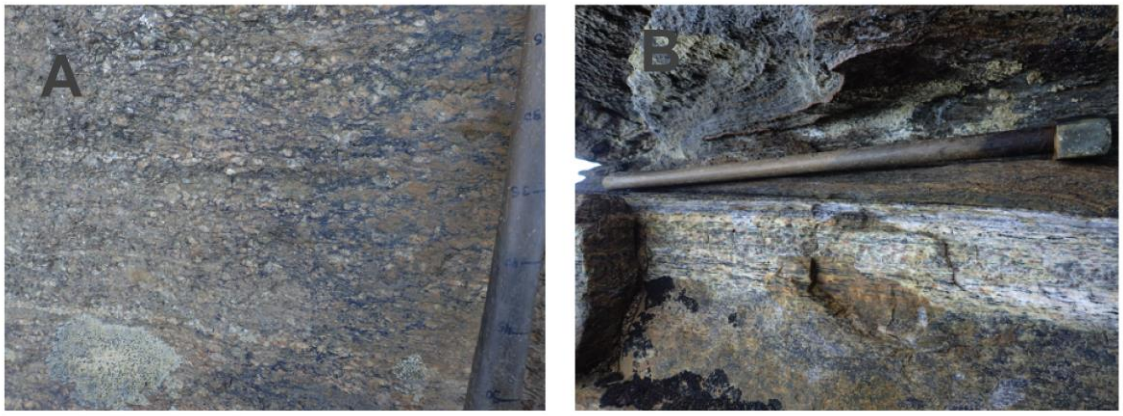

Figure 26. *Quartz-garnet amphibolite schist (A); quartz augen gneiss (B); Qeqertarssuaq Formation.*

Qaarsukassak Formation

The Qaarsukassak Formation hosts the Zn-Pb mineralisation described by Coppard et al. (1992). While it has some similarities to the Mârmorilik Formation with regards to the presence of mineralisation, a basal quartzite unit and the presence of carbonate rocks, the overall stratigraphy is quite different. The unit is thin (2 to <50 m) compared to the Mârmorilik Formation (<2 km). The Qaarsukassak Formation (Guarnieri et al., 2016) was investigated laterally along the length of the Discovery area, above the paleovalleys, and the KGS East locality of Coppard et al (1992). The Qaarsukassak Formation appears to be spatially restricted to Kangerluarsuk Fjord.

The Qaarsukassak Formation was investigated along the length of the Discovery area (northern extension of Discovery ("North"), Discovery, the area between Discovery and Discovery South ("Central"), and Discovery South). Stratigraphic thickness and character are variable along exposure, showing lateral variations in the first several metres at the base of the formation. Additionally, some upper stratigraphy is missing along strike, for example at North, where only ~2 m of section occurs. Though this pinchout could be structural or stratigraphic/erosional, the erosional interpretation is most consistent with the paleotopography of the Archean rocks beneath the Qaarsukassak Formation in that areas of higher paleotopography show lesser stratigraphic thickness. Primary sedimentary structures can be observed in the lowermost Qaarsukassak Formation nearest to the contact with Archean rocks at Discovery and Discovery central, but not elsewhere.
The Archean-Qaarsukassak Formation contact is a well-preserved sedimentary contact that demonstrates erosion prior to deposition of the Qaarsukassak Formation. The undulatory/erosional surface preserved on Archean rocks can be followed along strike, showing ~5 m of relief over ~25 m. New evidence from the 2016 field season indicates that the paleoenvironment for at least the earliest Qaarsukassak Formation was likely fluvial, which is consistent with subaerial erosion and paleovalley development prior to Qaarsukassak deposition.

A poorly-sorted meta-conglomerate, preserved as a <5-10 cm veneer on Archean rocks, occurs locally at the base of the Qaarsukassak Formation (Figure 27) at both Discovery central and at the KGS East showing of Coppard et al (1992). The meta-conglomerate con-

tains imbricated angular to subrounded pebbles to cobble size clasts in very coarse to granular sized matrix. Clasts are composed mostly of quartz pebbles, in addition to a graphitic non-calcareous meta-siltstone, and one granitic gneiss clast (possibly derived from Archean orthogneiss). The meta-conglomerate is thin, channelised, and laterally discontinuous, making it a highly local feature. Along strike, a very immature lithic meta-arkose occurs in channel deposits above Archean rocks that is also possibly of fluvial origin. Finally, asymmetrical ripple marks in fine-grained meta-sandstone in the lower Qaarsukassak Formation are consistent with a fluvial origin.

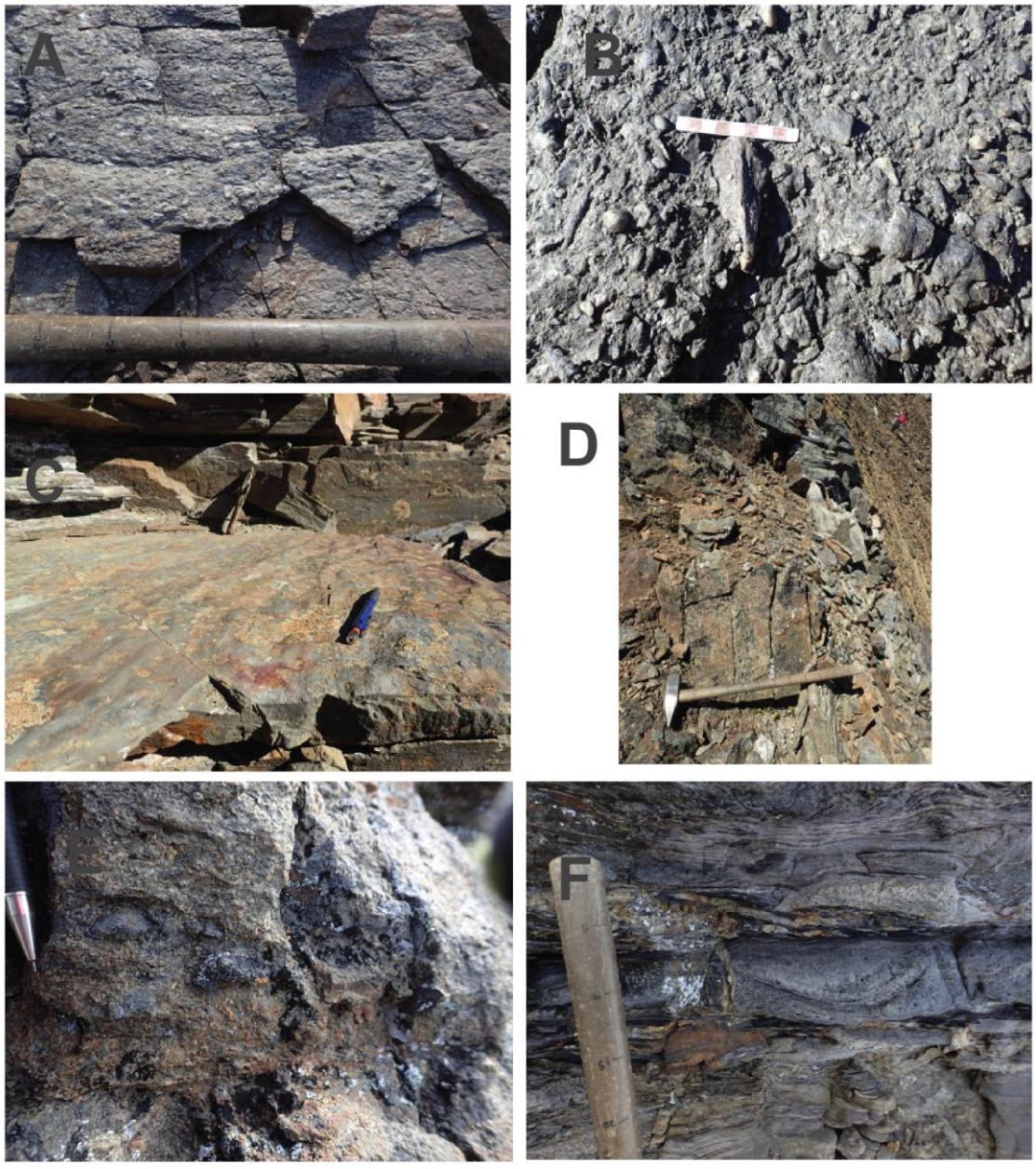

Figure 27. *A) Quartz-pebble meta-conglomerate, lower Qaarsukassak Formation, KGS East showing; B) Discovery central; C) Asymmetrical ripples at Discovery central; D) basal Qaarsukassak at paleovalleys; E, F) Lowermost (0-5m) of the Qaarsukassak Formation at the Discovery area, which includes medium-grained calcareous meta-sandstone and meta-lithic (feldspathic) wackes.*

The uppermost Qaarsukassak Formation in Discovery proper is composed of ~3 m thick chlorite schist, followed by 1-5 m of black siltstone/shale (Figure 28). Followed along strike, these units are either complexly folded, structurally cut or slumped. A similar situation occurs at KGS East (Figure 29). Other than the basal 1- 20 m, it is difficult to delineate the upper stratigraphy of the Qaarsukassak Formation due to the deformation.
The Qaarsukassak Formation-Nûkavsak Formation contact is typically sheared (top to the NNE); it usually occurs above a fissile black shale unit, which acted as a weak layer for the development of a décollement. It is unclear whether or not this was originally a depositional contact. When followed along strike, the Qaarsukassak Formation shows a gradual, but dramatic pinch-out towards the northern extension of Discovery down to 2 m. While it is possible that this could represent 'cut-out' stratigraphy from the thrust panel above, it more likely represents erosional pinch-out.

Figure 28. *Examples of the Middle-upper Qaarsukassak Formation that crop out at the Discovery area.*

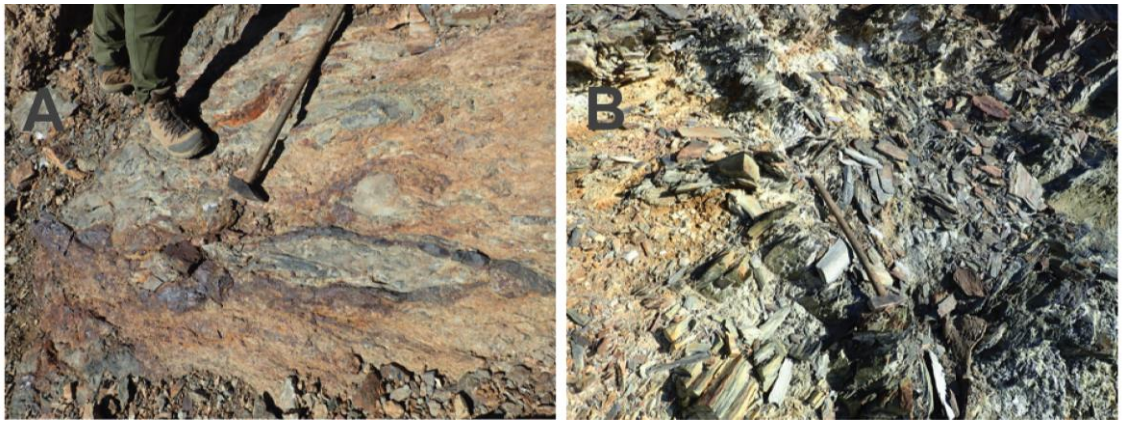

Figure 29. *Middle-upper Qaarsukassak Formation at KGS East showing, southeastern Kangerluarsuk Fjord.*

At Kangerluarsuup Sermia, Archean rocks are thrust on top of supracrustal rocks suggested to belong to the Qaarsukassak Formation (Guarnieri et al., 2016). Archean rocks are thrust directly on top of a marble-black chert unit (Figure 30). The units below are comprised of shale, possible meta-rhyolite, chlorite-siderite schist, thin lense of altered tremolite-calcite marble, amphibolite and a strongly foliated light purple grey to green chloritic meta-sandstone at the base of exposure. Sulfides (pyrite, pyrrhotite) are hosted in a shear zone of chlorite schist, calcite marble and amphibolite. A possible meta-rhyolite (?) with

flow banding and disseminated pyrite occurs here. The shale near the top of the exposure is rusty to white altered sulfidic black shale.

Figure 30. *A) lowermost meta-sedimentary unit at Kangerluarsuup Sermia; B) sulfide-bearing unit.*

At Nunatak 1, the Archean is represented by undeformed felsic igneous rock at the base of the section. Supracrustal rocks above show a rusty weathering veneer and were investigated. The Nûkavsak Formation does not occur as mapped, instead a heterolithic breccia with dominantly dark grey calcitic marble clasts and subordinate quartzite clasts occurs (Figure 31). Rock fragments are dominantly angular to subangular, though some are subrounded, in a medium to very coarse sand matrix, suggesting reworking of fragments by sedimentary processes. Clasts are not imbricated. The unit is very poorly sorted, with particles ranging in size from gravel to cobble to boulder size (m- to dm-scale). Locally, mm- to cm-sized quartz-phyric, subrounded to rounded pebbles occur along with metre-size quartzite boulders. The breccia contains inclusions of sulfide-bearing cobbles in marble; sulfides also cross-cut or partially replace other cobbles or occur in veins (Figure 32). The nature of the matrix changes from siliciclastic to what might be volcaniclastic (tuff or felsic volcanic). A pyrite-bearing shale unit occurs across a fault (Figure 33), which appears to be stratigraphically above the heterolithic breccia.

A grey calcitic marble-black chert rock looks similar to rocks observed in Kangerluarsuup Sermia. The genetic origin of the deposit is not clear, but appears to represent a reworked gravity flow (mass wasting event), possibly associated with fault/seismic activity or volcanic activity. This unit is interpreted to contain reworked (lithified) fragments of Qaarsukassak Formation, therefore it is younger than the Qaarsukassak Formation and possibly coeval with Kangilleq volcanism.

Figure 31. *Nunatak 1. Heterolithic breccia with variable clast types and matrix; C, might represent a breccia with a felsic volcanic matrix.*

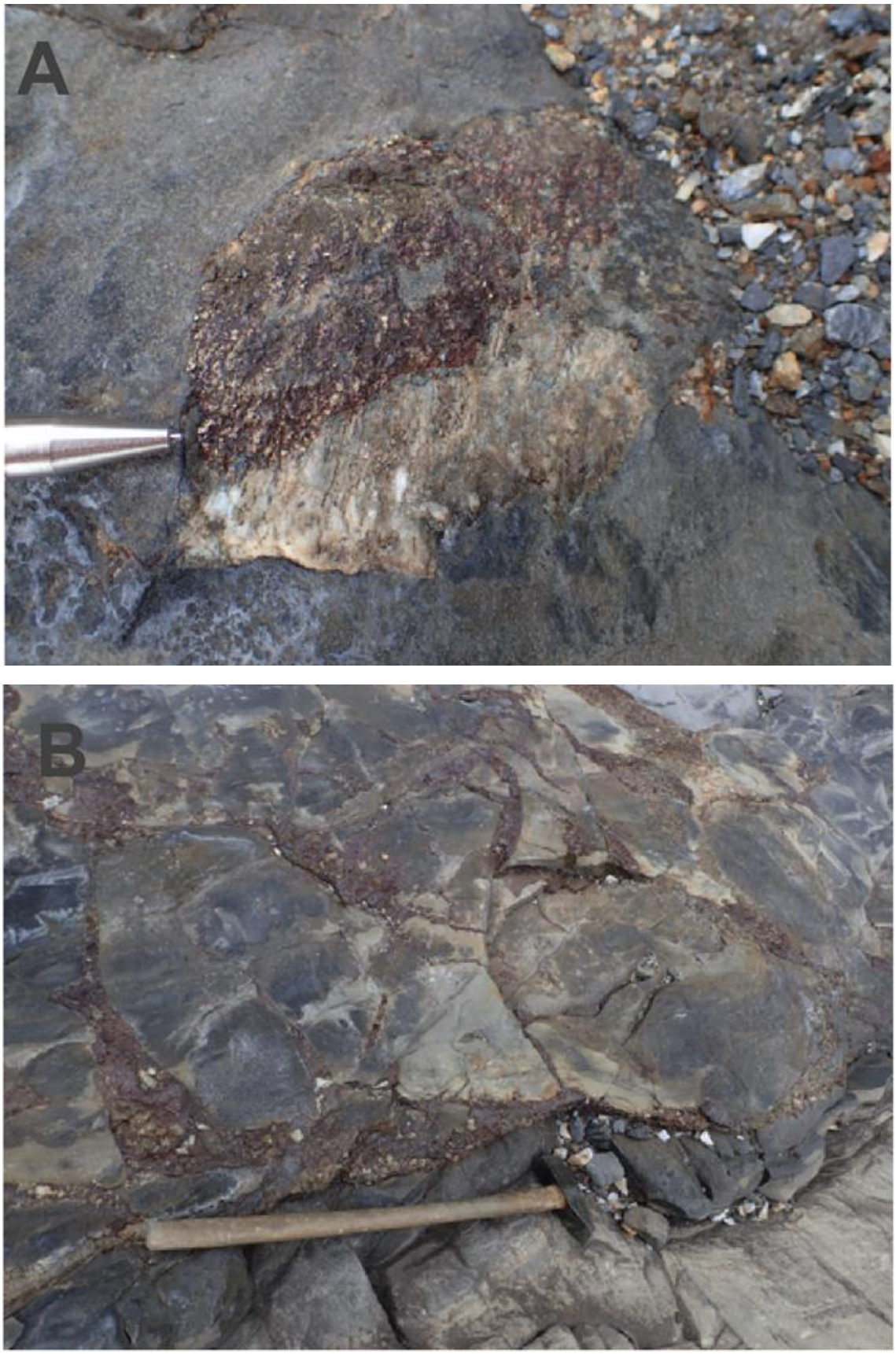

Figure 32. *Nunatak 1. A) partial replacement of a carbonate clast by sulfides; B) sulfide veins throughout a carbonate layer.*

Figure 33. *Nunatak 1. A) black chert in marble, very similar to Kangerluarsuup Sermia; B) quartz-phyric basement to the breccia unit.*

Mârmorilik Formation

The Mârmorilik Formation is an important member in the stratigraphy of the Karrat Group since it hosts a world class mineral deposit. Intrabasinal stratigraphic correlation of the Mârmorilik Formation is challenging since it is not observed in contact with other units of the Karrat Group that occur north of Maarmorilik. Its relativey isolated position led Grocott and Pulvertaft (1990) to suggest this unit was deposited in a sub-basin separated by a topographic high. This interpretation might be complicated by the involvement of Archean rocks in the thick-skinned fold-and-thrust belt in which the Mârmorilik Formation occurs. In other words, it is unclear if the basement high that separates the Mârmorilik Formation from the rest of the Karrat Group is structural or if it represents paleotopography. An argument can be made for paleotopography and deposition in a separated sub-basin, since units in the Mârmorilik Formation are not contiguous or repeated north of Maarmorilik. Due to this lack of continuity in the southernmost stratigraphy of the Karrat Group, stratigraphic correlation must rely on depositional environment, tectonic setting and geochronology.

One outstanding stratigraphic question is whether or not the semipelite unit above the Mârmorilik Formation is correlative to the Nûkavsak Formation. Therefore, investigations of semipelite outcrops were made. These occur at high elevations on the Black Angel plateau, close to the edge of the inland ice, and are often covered by thick glacial debris. No sedimentary structures were observed in the semipelite unit that could aid in understanding the depositional environment. Discontinuous outcrop (interrupted by glacial debris and inland ice), in addition to polyphase deformation and a lack of marker beds, precluded accurate thickness estimates of the semipelite unit. The best exposed section was found to be directly north of Lake 480 (Big South Lake), where calcareous pelites and medium-grained non-calcareous meta-sandstones occur. These rock types are similar to other Nûkavsak Formation rocks elsewhere, so therefore are probable, but not definitively, part of the Nûkavsak Formation. Coarser-grained beds within the semipelite unit were collected for detrital zircon geochronology. On-going research will compare the detrital zircon profiles of Nûkavsak Formation to the north with the semipelite unit of the Mârmorilik Formation to test their age and correlation.

The lower Mârmorilik Formation stratigraphy is quite remarkable, and unlike the uppermost Mârmorilik Formation, does preserve some sedimentary structures. In the South Lakes area, siliciclastic units preserve a depositional contact with Archean rocks that include gravel to cobble meta-conglomerates with relatively undeformed clasts. This lowermost siliciclastic unit is just tens of metres below a regional thrust fault that truncates the dolomitic marble. At Mallak peninsula near Maarmorilik, the contact of the Mârmorilik Formation with Archean rocks is also exposed. A thin (15-20 cm) basal quartzite unit occurs with depositional contact directly to Archean gneiss. No primary structures were observed in units at this locality, though the stratigraphy appears to be right way-up. A relatively pure dolomite marble (no tremolite) occurs above the thin quartzite unit. Disseminated pyrite and sphalerite occur in the cream- to buff-coloured dolomitic marble.

In the area south of South Lakes, a dolerite dyke intrudes the lowermost dolomite marble of the Mârmorilik Formation (Figure 34). The dyke appears to be folded, therefore could pre-

date the deformation. The basal siliciclastic unit is cut out in some areas, likely by thrust faults that cut the lowermost dolomite marble. Where present (only ~2m of exposure), the basal quartzite unit is a dark grey/brown massively bedded quartzite interlayered with tremolite-chlorite marble with no preserved sedimentary structures. In the basement a meta-basite unit occurs. This local unit is comprised of some meta-sedimentary units and a plagioclase and hornblende-bearing chloritised gabbro-monzogabbro (?) (Figure 34). This unit is infolded with the augen gneissic basement rocks, suggesting that this unit is not likely part of the Mârmorilik Formation. The possible meta-sedimentary rocks have large pseudomorphs (now actinolite) in a quartz-biotite matrix. The actinolite-pseudomorph rock is intercalated with quartzite here.

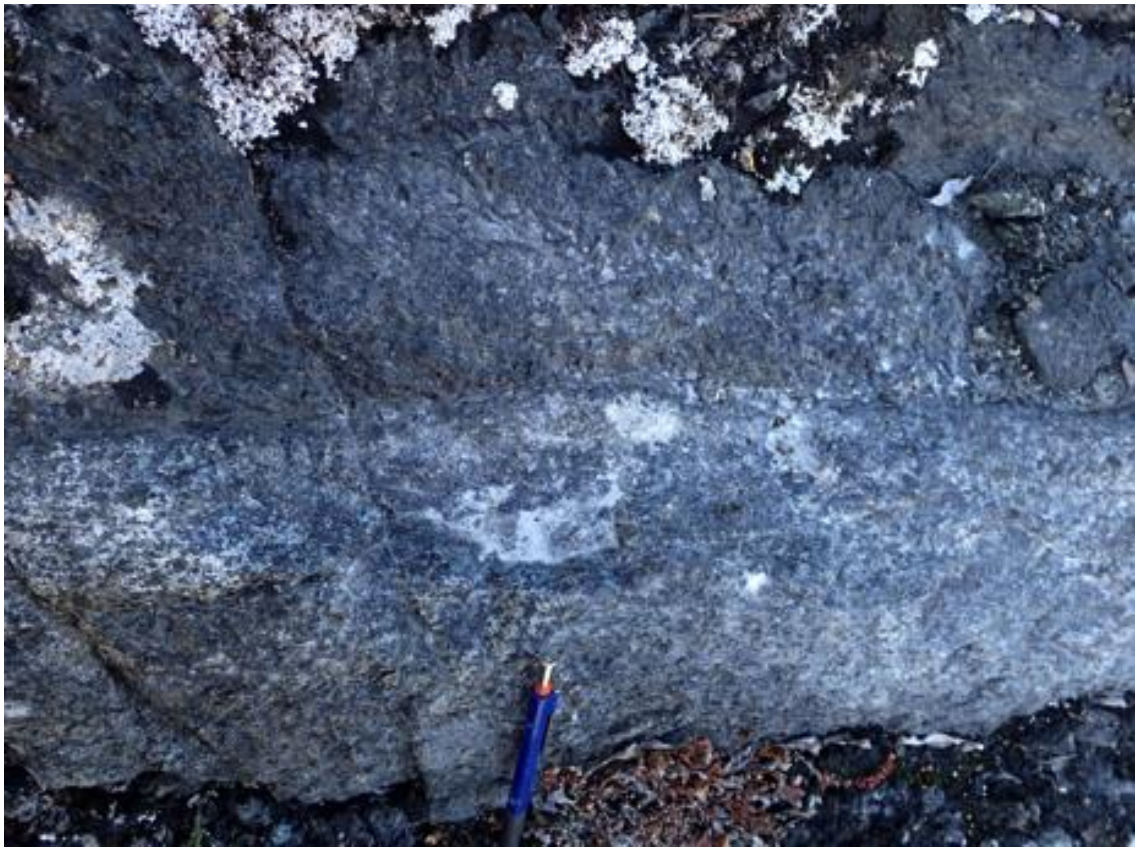

Figure 34. *Gabbro of the meta-basite map unit.*

To the west of the 746 Lake, a heterolithic, poorly sorted meta-conglomerate and a quartz pebble gravel meta-conglomerate occur with a depositional contact to Archean rocks (Figure 35). The meta-conglomerate contains subangular to subrounded clasts in a coarse to very coarse angular quartz sand matrix. Clasts do not appear to be stretched or elongated. Many of the clasts appear to be composed of quartzite; rare actinolite-amphibolite clasts also occur. The quartz pebble gravel meta-conglomerate contains angular to subrounded rock fragments. Above these units, a purple-green tremolite rock with angular quartz pebbles occurs, which looks similar to the top of siliciclastic succession at Nuungarut (described below).

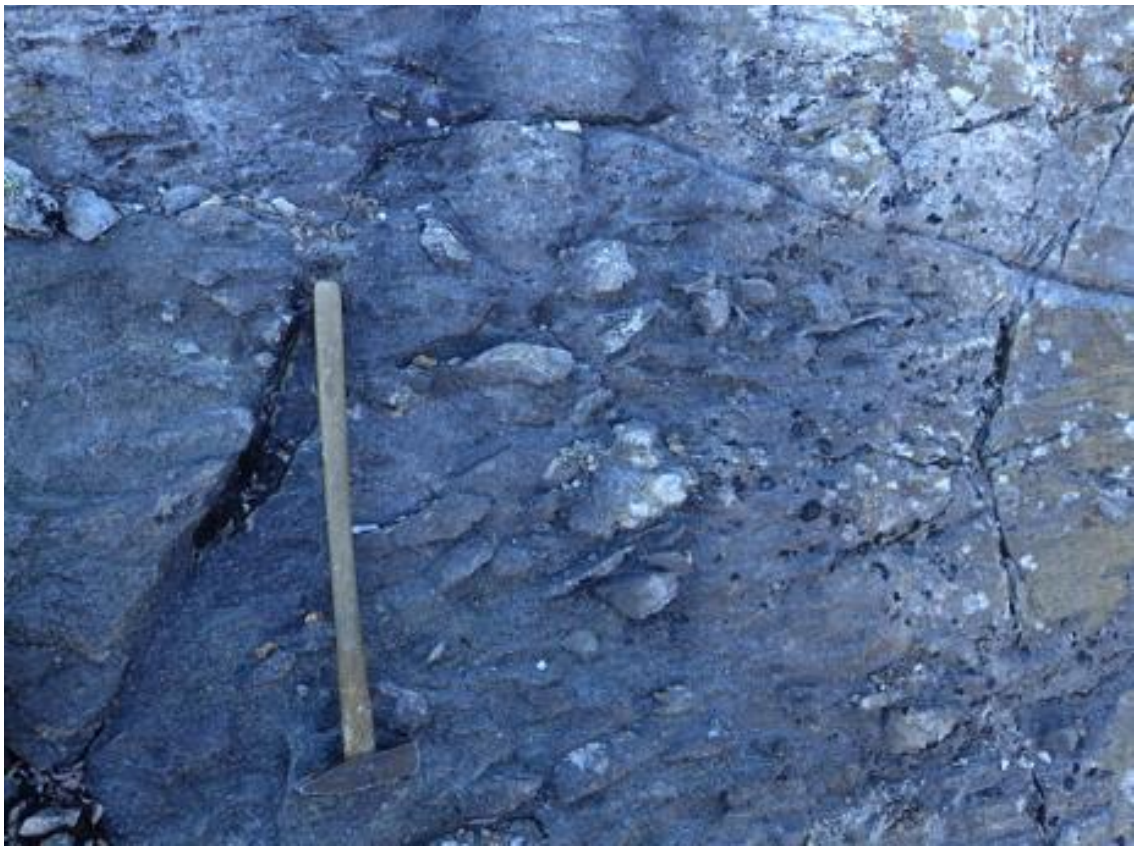

Figure 35. *Base of Mârmorilik Formation west of 746 Lake: Poorly sorted heterolithic meta-conglomerate.*

The lower Mârmorilik Formation west of the South Lakes area consists of white to green quartzite with tremolite-actinolite layers, mica ± actinolite schist, a black magnetite-bearing quartzite, calcite marble, and a grey fine-grained K-spar-bearing meta-sandstone (Figure 36). The contact of the quartzite with Archean rocks is sheared, but ~10 cm above the contact the rock is well-bedded recrystallised coarse-grained quartzite. Nearby, at another basement-quartzite contact, symmetrical ripples are preserved. Thickness of the lower succession beneath the dolomite marble is variable, from only a few metres to tens of metres.

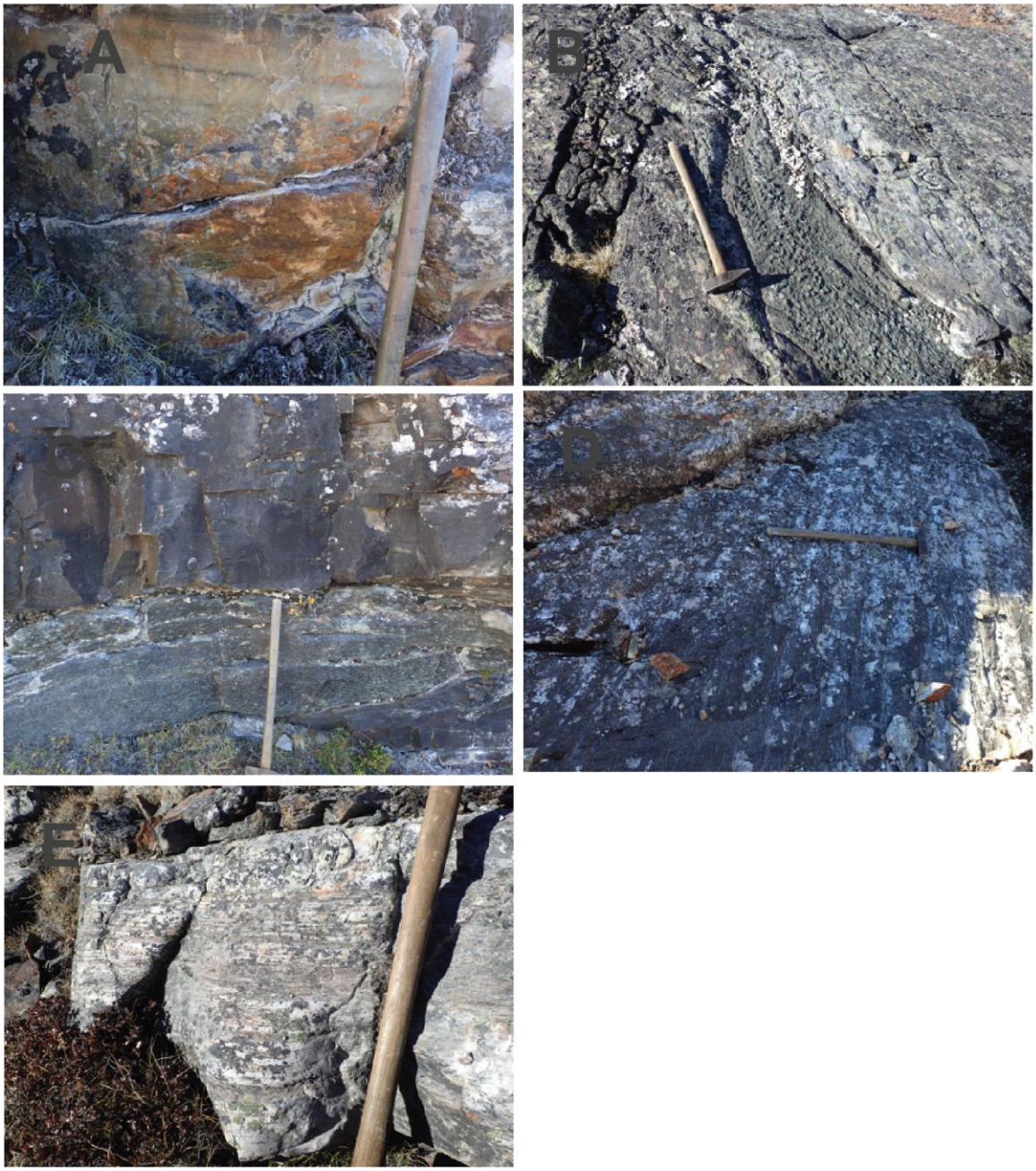

Figure 36. *A, B) lower quartzite of the Mârmorilik Formation with tremolite-actonolite layers; C, magnetite quartzite in contact with green quartzite; D, E) ripple marks in lower quartzite above basement contact and calcareous meta-sandstone above.*

The basal siliciclastic rocks of the Mârmorilik Formation were also investigated at Nunngarut, where a relatively thick (~35 m) and well-preserved section occurs below the dolomitic marble (Figure 37). Basal meta-sedimentary rocks are dominantly calc-silicate rocks (calcite + quartz + biotite + epidote), quartzites, magnetite-bearing quartzites, and continued siliciclastic or possibly volcaniclastic rocks at the top of the section (Figure 38). The quartz-pebble meta-conglomerate at the base of Mârmorilik Formation seen elsewhere is absent at Nunngarut.

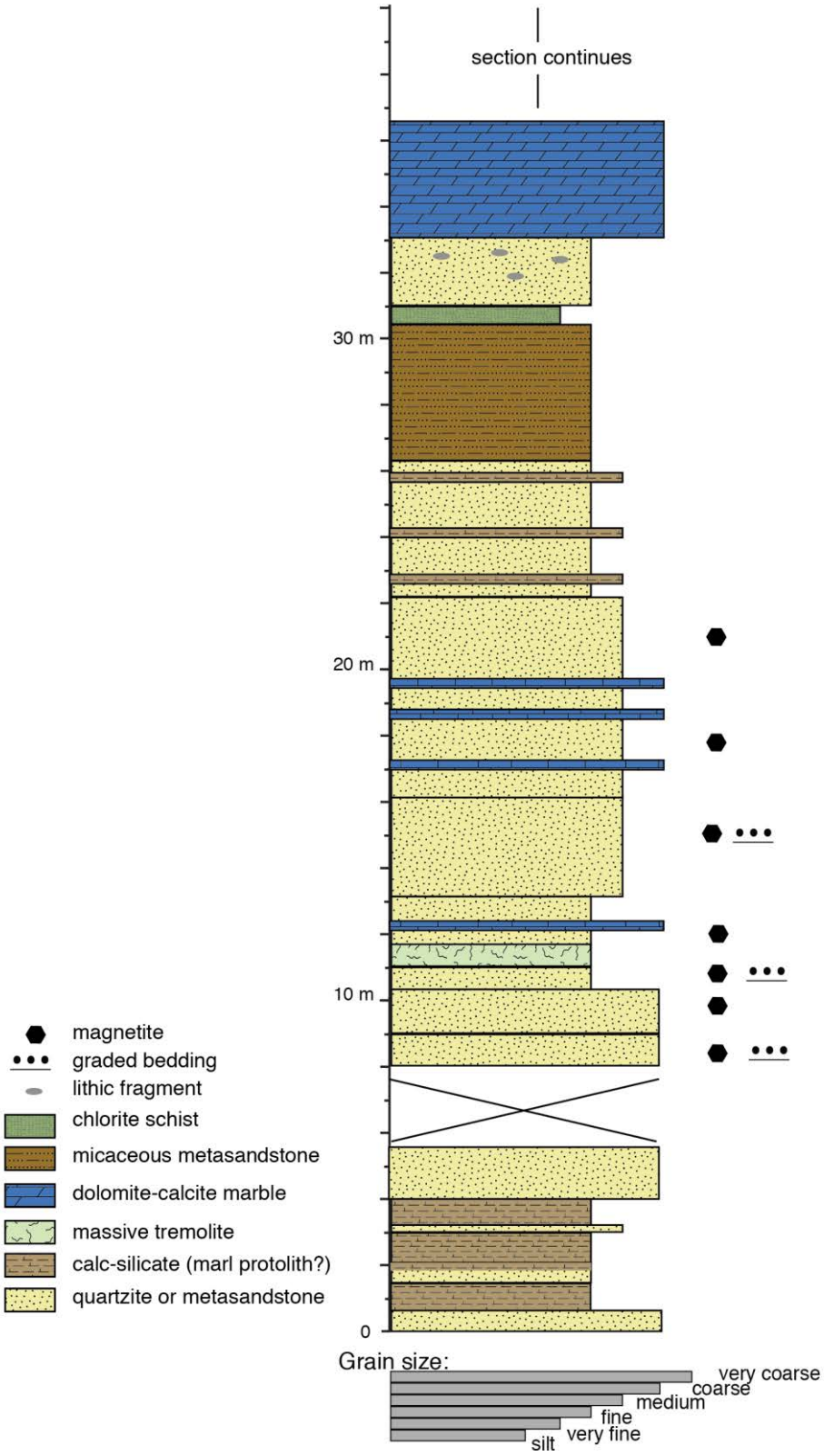

Figure 37. *Measured stratigraphic section of the lower Mârmorilik Formation (below the dolomitic marble) at Nunngarut.*

Figure 38. *Nunngarut. A) Lowermost quartzite and calc-silicate of the Mârmorilik Formation; B) Lower Mârmorilik Formation siliciclastic (volcaniclastic?) rocks.*

The semipelite unit in the uppermost Mârmorilik stratigraphy was investigated to understand similarities/differences between this unit and Nûkavsak Formation to test their possible correlation. Due to the degree of deformation in exposures on Black Angel Mountain, it is not possible to measure stratigraphic thicknesses or track lateral variations in stratigraphy. This unit is a mixture of calcareous pelite and non-calcareous meta-sandstone (Figure 39). A recrystallised calcite light grey marble (no tremolite or other accessory minerals) is intercalated with the semipelite unit. In another area, a ~2 m thick rusty black shale occurs in centre of syncline. The unit overall is relatively thin (estimated <50 m). No sedimentary structures were observed.

Figure 39. *Top of Black Angel Mountain: Medium-grained non-calcareous meta-sandstones of the semipelite unit of the Mârmorilik Formation.*

The semipelite unit also occurs on top of the Nunngarut peninsula, where it is a dark grey strongly foliated and isoclinally folded medium grained meta-sandstone with no primary structures (Figure 40). A flattened quartz-biotite inclusion ~15cm long appears to occur as a clast in the semipelite unit. As with the Black Angel locality, a dirty calcite marble occurs beneath the semipelite. Thin (10 cm) tan to grey chert layers occur within the calcite marble. A grey dolomite marble occurs stratigraphically below calcite-chert marble.

Figure 40. *Top of Nunngarut: semipelite unit of the Mârmorilik.*

Kangilleq Formation

Meta-volcanic rocks of the Kangilleq Formation are found throughout the southern Karrat region and are dominantly in the greenschist facies (Rosa et al., 2016). They are dominated by chlorite with variable proportions of amphibole, carbonate, quartz, feldspar, titanite, rutile, Fe-oxides +- biotite and classified as alkali basalts based on the revised Zr/Ti-Nb/Y Wincherster-Floyd diagram of Pearce (1996). Observations from 2015 included the discovery of a thick sequence (≤ 850 m) of meta-volcanic rocks at Qangattarsuaq where the contact between the Kangilleq and Qeqertarssuaq formations is unconformable (Rosa et al., 2016). Primary volcanic textures at Qangattarsuaq include pillow lavas, pillow breccias and hyaloclastite, indicative of eruption in a subaqueous environment, to more massive, sheet-like flows. Such textures were also observed in other localities throughout the area.

The contact between the Kangilleq Formation and the underlying Qeqertarssuaq Fomration has been described as unconformable (Rosa et al. 2016). However, a note was made to check localities where remote observations could be interpreted in a conflicting manner. The discrepancy in the contact relationship led to more investigation into the nature of this contact at the Qangartarssuaq locality in Kangilleq Fjord. At this locality, meta-volcaniclastic rocks of the Kangilleq Formation overlie a garnet-mica schist underlain by a thick grey massive quartzite typical of the Qeqertarssuaq Formation. Locally the meta-volcaniclastic rocks directly overlie the quartzite and the contact is sheared. Overall the contact is undulatory and sharp with local shearing (Figure 41). The change from amphibolite facies, within the lower meta-sedimentary rocks, to greenschist facies, within the overlying meta-volcanic

rocks, together with the nature of the contact suggests an erosional unconformity below the Kangilleq Formation confirming the original conclusions from Rosa et al. 2016.

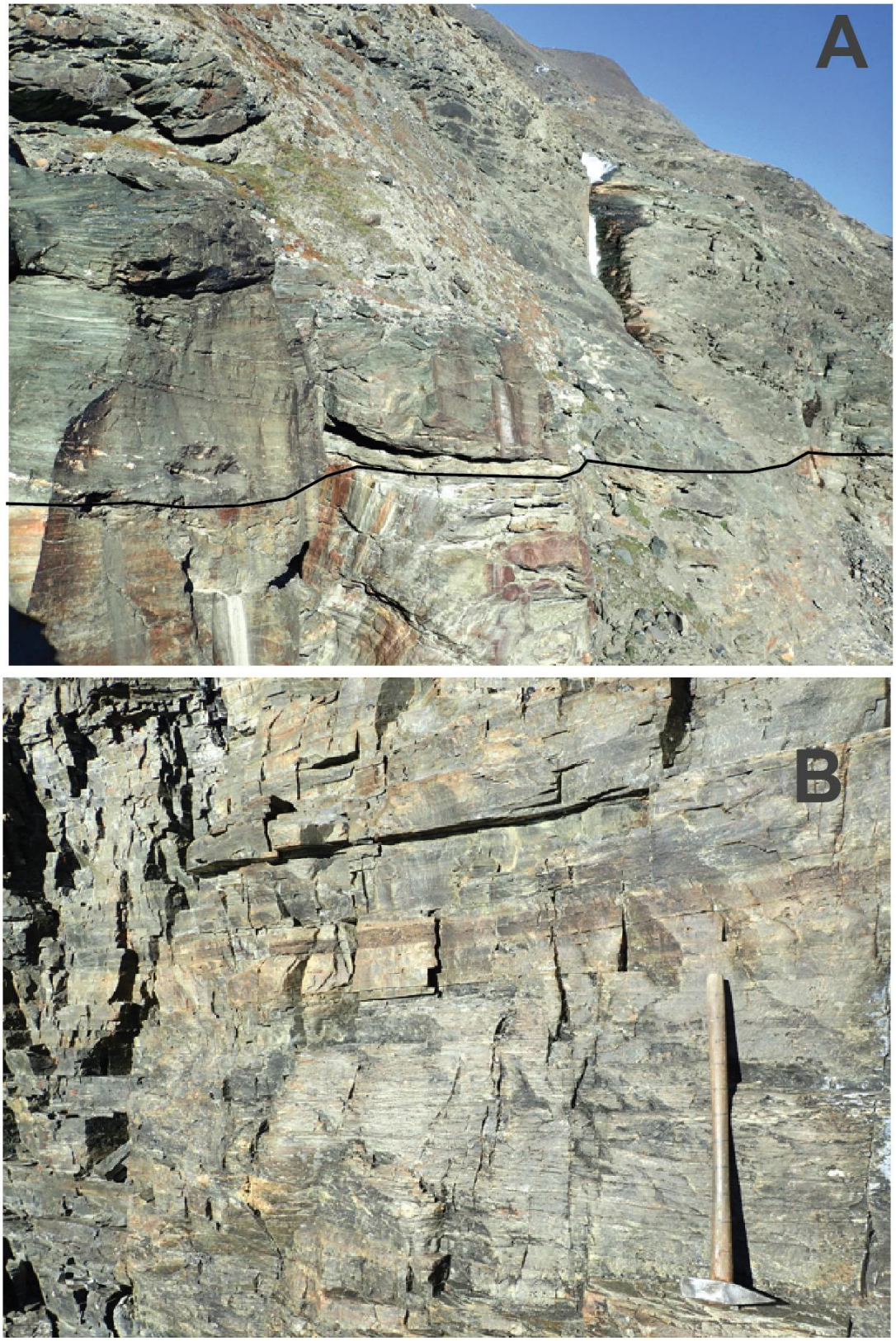

Figure 41. *Qangatarssuaq, Kangilleq Fjord . A) Contact between Qeqertarssuaq Formation and Kangilleq Formation; B) Detail of the quartzite of the Qeqertarssuaq Formation.*

New observations were made about the relationship between meta-sedimentary rocks of the Nûkavsak Formation and meta-volcanic rocks of the Kangilleq Formation in different locations. Most notable is the south facing cliff in Puallarsiiviup Qooruua Valley where excellent exposures of the near vertical cliffs testify to how meta-volcanic rocks of the Kangilleq Formation are interleaved with meta-sedimentary rocks of the Nûkavsak Formation. This is illustrated in Figure 42 where meta-sedimentary rocks of the Nûkavsak Formation are seen intercalated with meta-volcanic rocks of the Kangilleq Formation along a couple of kilometres of strike.

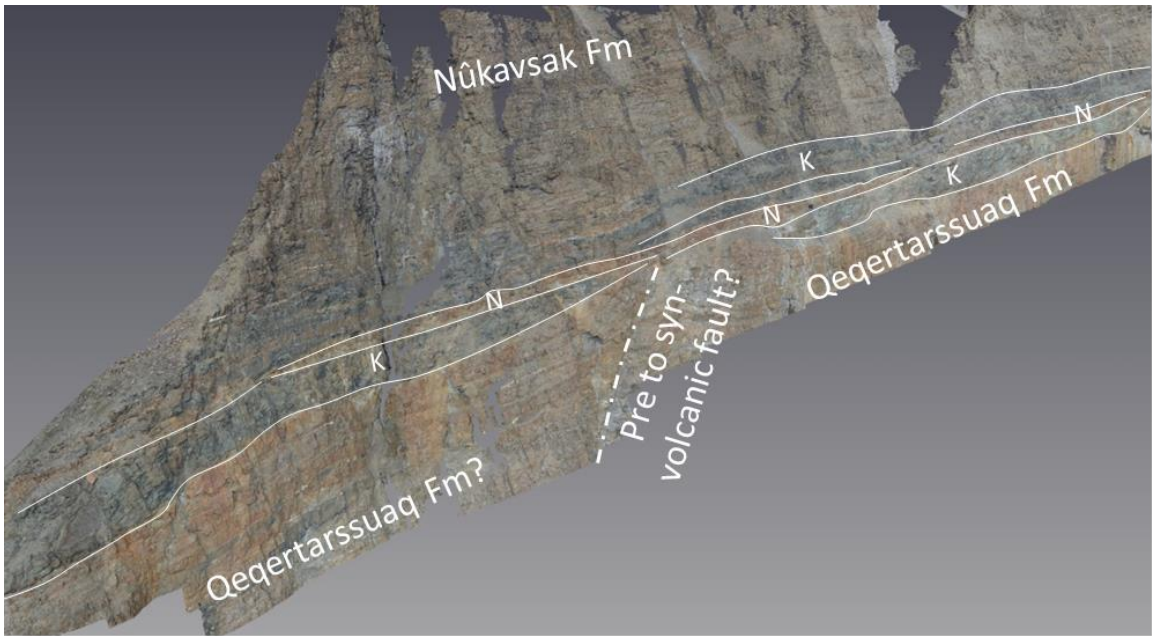

Figure 42. *Perspective view of the steep south facing cliff in the Puallarsiiviup Qooruua Valley illustrating how the Kangilleq and Nûkavsak Formations are intercalated. Field of view is approximately 1 km. Letters K and N denote Kangilleq and Nûkavsak Formations respectively.*

Similarly, detailed re-examination of some of the close-up images from the Qangátarssuaq area confirms the intercalation of meta-sedimentary rocks of the Nûkavsak Formation with meta-volcanic rocks of the Kangilleq Formation, suggesting concomitant deposition of Kangilleq Formation meta-volcanic and Nûkavsak Formation meta-sedimentary rocks.

The transitional contact between the Kangilleq Formation and Nûkavsak Formation as seen in the inner parts of Inngia Fjord was visited again by boat in 2016. In particular, an outcrop was visited that contains a monolithic pebble wacke, originally thought to be at base of transition between the two units. Revisiting the outcrop revised this interpretation, suggesting that these meta-sedimentary strata are actually within the uppermost Kangilleq Formation, not the lower Nûkavsak Formation.

The excellent exposures in the vertical cliffs of Puallarsiiviup Qooruua valley also reveal important new evidence to the nature of the volcanic environment (Fig. 43 and 44). Preliminary interpretation shows packages of what is interpreted to be pillow lavas and massive lava flows of variable thickness conforming to the paleo-seafloor. A sharp contact with an overlying package of darker coloured meta-volcanic rocks and the truncation of pillows by the overlying volcaniclastic rocks suggests an erosional contact. Initial interpretation of the

overlying package is that it comprises mafic volcaniclastic rocks, massive lava flows or a combination of the two. Considerable lateral facies variation exists in pillow dominated facies as well as in the upper darker coloured part of the volcanic sequence. Systematic mapping out the different facies along the more than 20 km long profile would provide a much better constraint to the nature of the Kangilleq Formation.

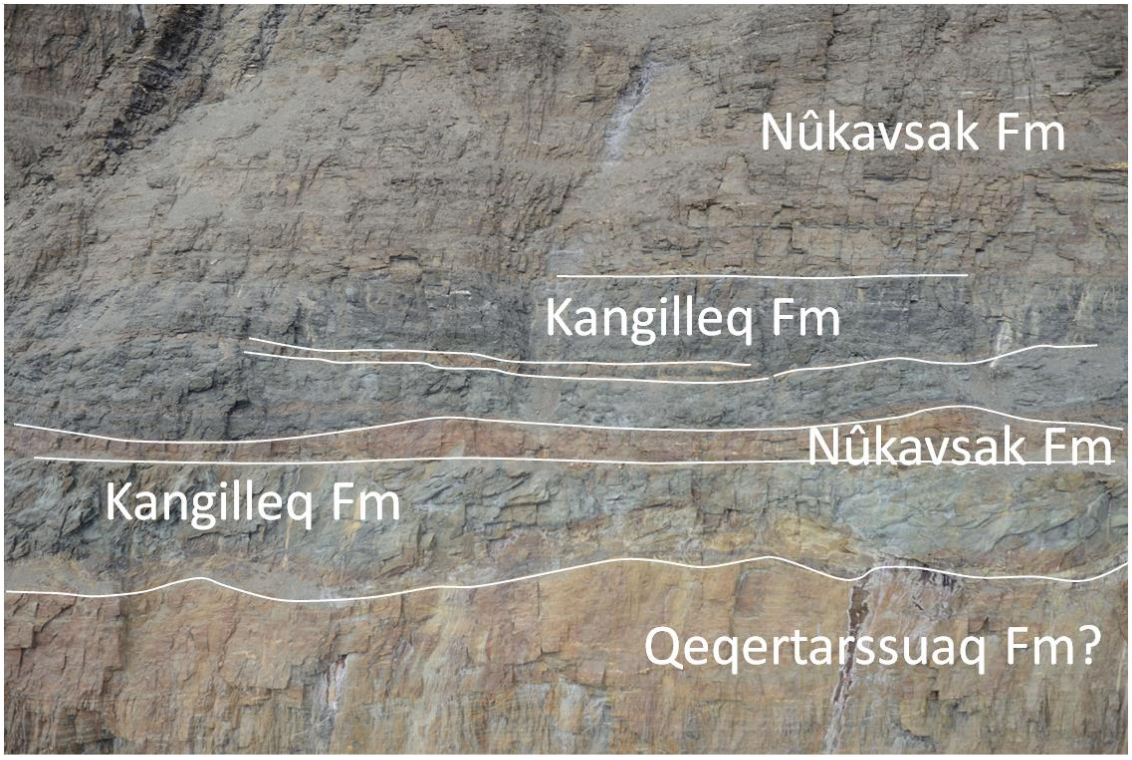

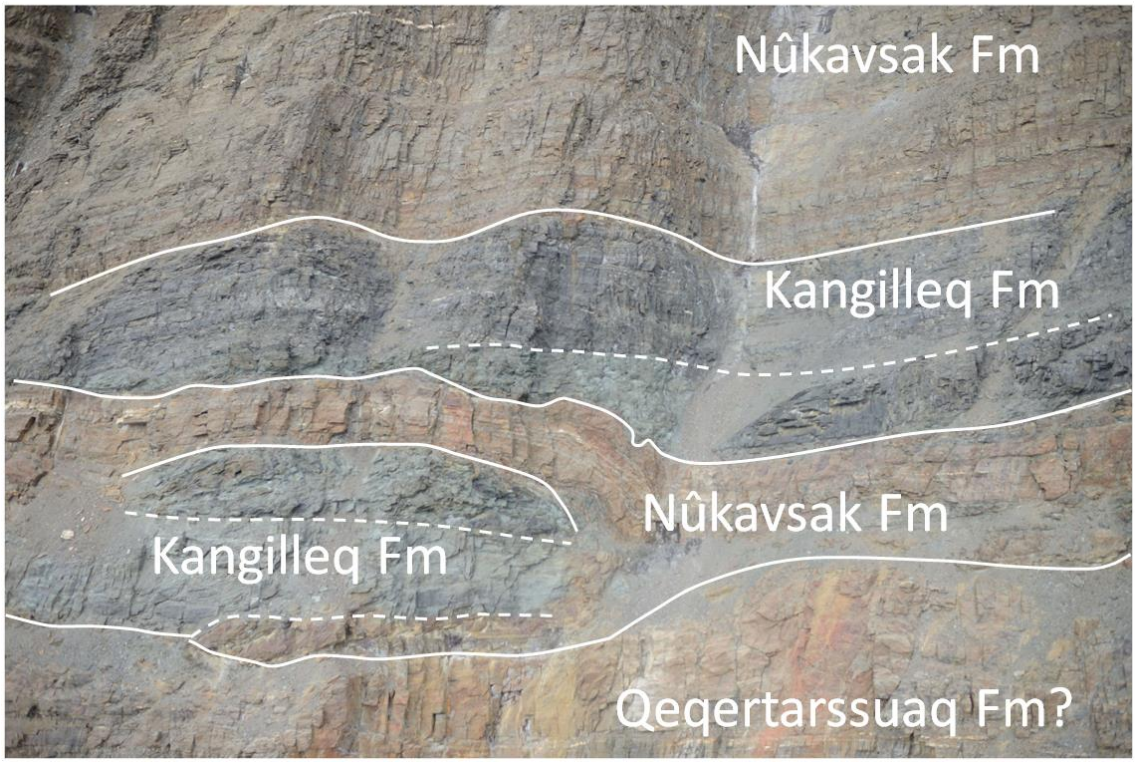

Figure 43. *Close-up images of the Kangilleq-Nûkavsak transition in Puallarsiiviup Qooruua valley. Field of view is approximately 200 m.*

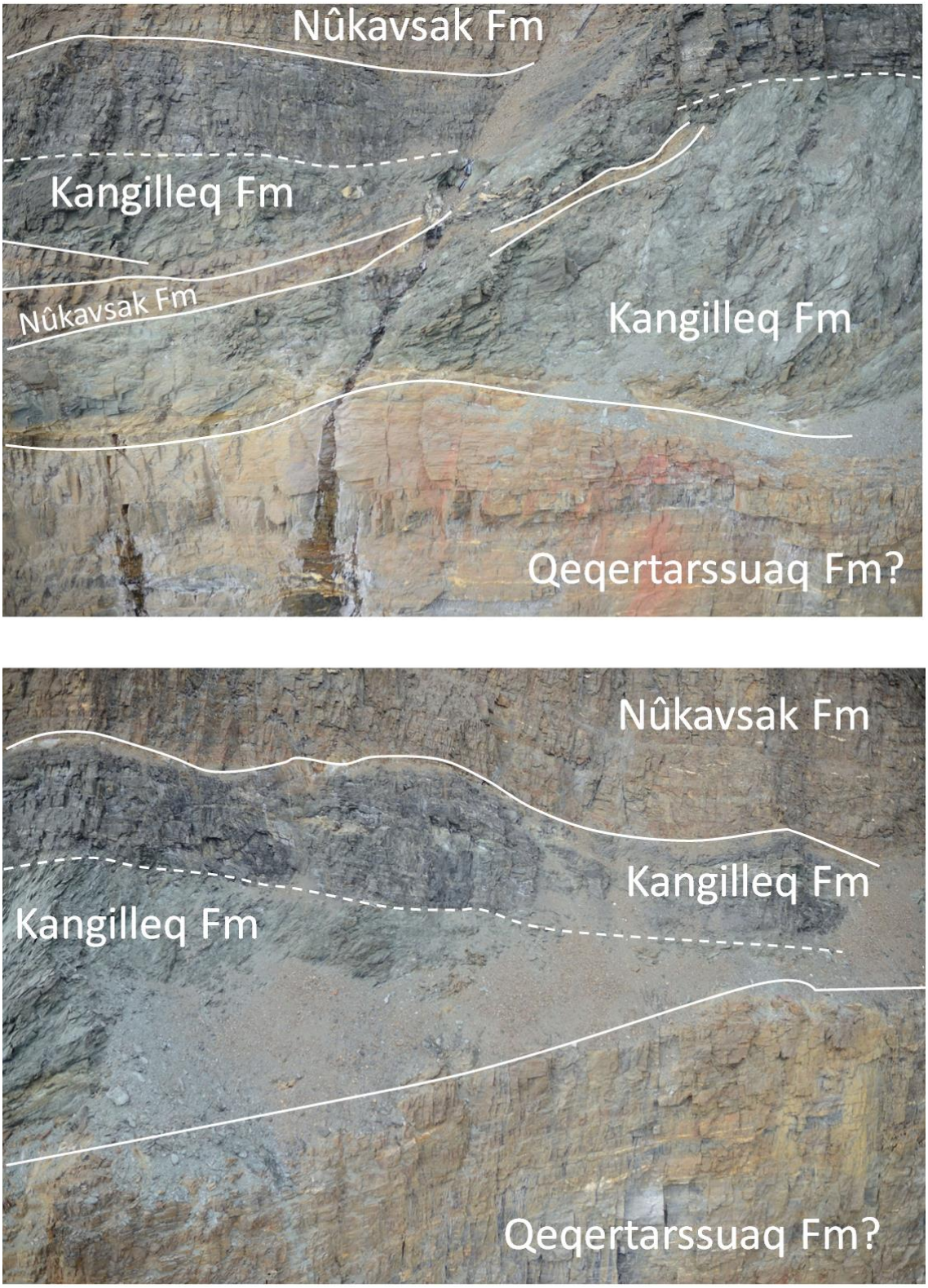

***Figure 44**. Puallarsiiviup Qooruua valley: Close-up images of facies variation within the Kangilleq Formation. A sharp contact (dashed lines) delineates the truncation of a lower package of predominantly pillow lavas and a darker upper package of what is interpreted (preliminary) to be volcaniclastic rocks, massive lavas or a combination of the two. Field of view is approximately 200 m.*

The volcanic environment was also studied at Central Kangiusap Kuua. In the locality, rocks of the Kangilleq Formation area are dominantly mafic in composition, but varying from mainly pillow basalt at the base of the exposure to dominantly mafic meta-volcaniclastic rocks at the top of the exposed section of meta-volcanic rocks (Figure 45). The meta-volcaniclastic rocks in the area are dominated by mafic tuff breccia beds and the bedforms present (normal to reverse grading, massive to crudely bedded, and channel/scour structures) suggest emplacement by mass debris flows. The possible recognition of a felsic breccia near the top of the meta-volcanic package of rocks, and hosting the sulfide mineralisation (see Economic Geology section), suggests bi-modal volcanism in an area that was previously thought to contain only evidence of mafic volcanism (Figure 46). The silicified unit at the top of the meta-volcanic package of rocks may represent a chert, or silicified tuff bed, which may have capped the hydrothermal system responsible for the mineralisation. Changes in facing direction in this area suggest the meta-volcanic rocks, including the sulfide mineralisation and silicified cap rock, are repeated through folding. Future work in this area needs to concentrate on reconstructing the volcanic environment by unfolding or removing the structural deformation of the rocks to recreate a paleoseafloor at the time of volcanism/hydrothermal alteration, and whole rock geochemistry from samples collected in 2015 (data available) and 2016 (data not yet available) must be used to better understand the petrogenesis of the volcanic rocks in this area and to compare them to volcanic rocks of the Kangilleq Formation elsewhere to see if they have the similar geochemical signature(s).

Figure 45. *Central Kangiusap Kuua: Mafic tuff breccia unit, which shows normal grading (fining to the right).*

Figure 46. *Felsic breccia unit, which hosts sulfide mineralisation at Central Kangiusap Kuua.*

Excellent exposure of the Kangilleq Formation in the Qangattarsuaq area (Figure 47) resulted in the mapping of 4 stratigraphic sections (1:200 scale). This covers 790 m of stratigraphy, in order to better understand the distribution of lithofacies within the meta-volcanic rocks with the goal of reconstructing the volcanic environment of formation. The lower contact of the meta-volcanic rocks of the Kangilleq Formation is exposed in three locations in the Qangattarsuaq area and can be described as variably faulted/sheared, or sharp and undulatory (see above section), with underlying garnet-mica schist or quartzite typical of the Qeqertarssuaq Formation.

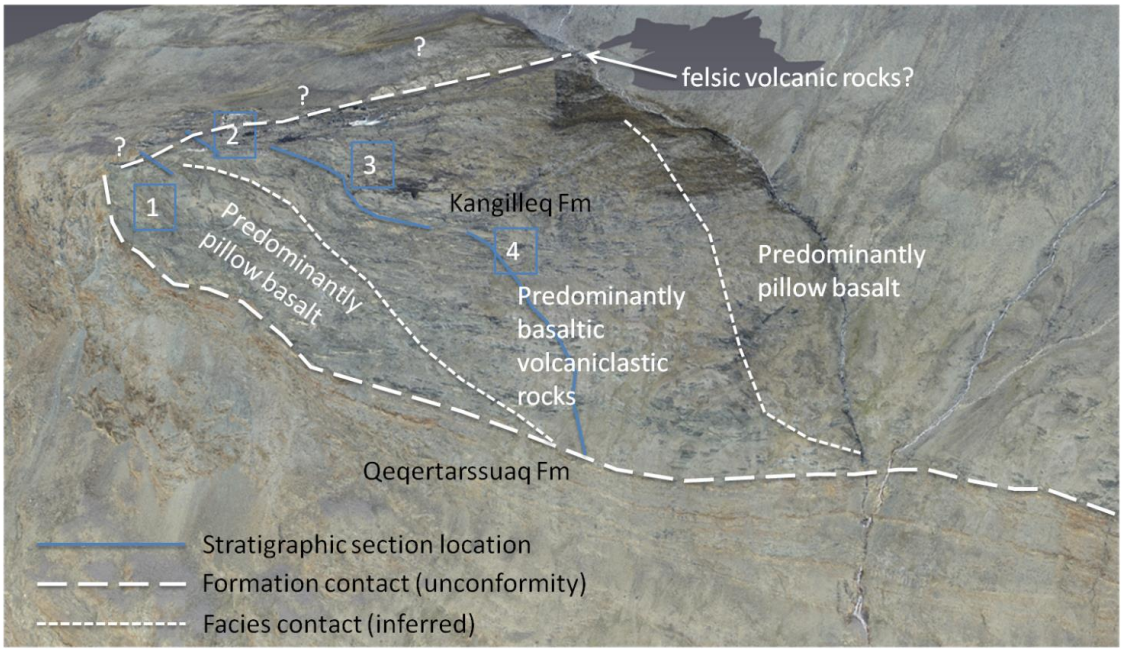

Figure 47. *Overview figure of the Qangattarsuaq area.*

Rocks of the Kangilleq Formation in this area vary along strike from dominantly pillowed basalt flows to dominantly mafic volcaniclastic rocks. Near the top of the exposed volcanic sequence are what appear to be massive rhyolite flows and intercalated felsic to intermediate tuffs. The sequence of predominantly mafic volcaniclastic rocks are dominated by mafic tuff breccia units ranging 6 – 35 m in thickness and characterised by block- and lapilli-size scoria clasts, with lesser amounts of mafic tuff and mafic lapilli-tuff beds. These mafic volcaniclastic beds are commonly separated by 15 – 30 m thick pillow basalt flows and seldom by massive, aphyric basalt flows.

Only a few hundred metres along strike to the northeast the Kangilleq Formation is dominated by pillow basalt where it comprises ~ 50 m of mafic volcaniclastic rocks, similar to those along strike, overlain by >200 m of pillow basalt (Figure 48) with individual flows ranging from 10 to 100 m. Massive facies, hyaloclastite, and varioles locally occur within the dominantly pillowed flows. Overlying the pillow basalts is a massive to flow banded, aphyric to weakly quartz and plagioclase (<5%, <1 mm) porphyritic felsic rock. The felsic body has a minimum thickness of 45 m and its upper and lower contacts are not exposed. Stratigraphically above the felsic rocks is a sequence (~15-30 m) of plane bedded felsic tuff (± mafic tuff beds; Figure 49).

Figure 48. *Massive basalt flow (below white, dashed line) with pillowed top, Kangilleq Formation.*

Figure 49. *Bedded felsic to intermediate tuff, Kangilleq Formation.*

Rocks of the Kangilleq Formation in the Qangattarsuaq area, unconformably overly metasedimentary rocks of the Qeqetarssuaq Formation and are dominantly mafic in composition, but vary along strike from dominantly pillow basalt in the northeast to dominantly mafic

volcaniclastic rocks only several hundred metres to the southwest. The mafic volcaniclastic rocks (> 300 m total thickness) in the area form a sequence of tuff to tuff breccia beds whose bedforms (normal to reverse grading, massive to crudely bedded, and channel/scour structures) suggest emplacement by mass debris flows. The thickness of the volcaniclastic sequence and the abrupt nature of the lateral facies change from pillow basalts to volcaniclastic rocks suggest the presence of a synvolcanic fault, which would delineate the northeast side of a synvolcanic subsidence structure in which the volcaniclastic material was deposited. The possible recognition of felsic volcaniclastic rocks and rhyolite in the Qangattarsuaq area suggests bi-modal volcanism in an area that was previously thought to contain only evidence of mafic volcanism. Future work in this area needs to concentrate on reconstruction of the volcanic environment of formation of the Kangilleq Formation using the stratigraphic sections measured this summer, future mapping using stereo-images taken in 2015-16, and whole rock geochemistry from samples collected in 2015 and 2016.

Nûkavsak Formation

The youngest sedimentary unit in the Karrat Group is the Nûkavsak Formation, which is dominated by sandy lithologies. This thick unit (previously estimated with a structural thickness up to 5 km; Grocott and Pulvertaft, 1990) occurs in transitional contact with the Kangileq Formation (Rosa et al., 2016). Depending on the location within the Karrat basin, the Nûkavsak Formation overlies the Qeqertarssuaq, Qaarsukassak, or Kangileq formations, or directly overlies Archean crystalline rocks. As discussed in the Mârmorilik Formation section, siliciclastic rocks of the uppermost Mârmorilik Formation possibly correlate with the Nûkavsak Formation. The quality of outcrops for stratigraphic or sedimentologic study is variable; examples of some of the best outcrops that preserve sedimentary structures are described below, starting with an anomalous local facies.

On the SE side of Kangilleq Fjord, across from Qangatarssuaq, a local heterolithic meta-conglomerate unit was observed in an exposure just above sea level. The stratigraphic position of this meta-conglomerate is unclear, but likely belongs to the lowermost Nûkavsak Formation. The outcrop exposed in the sea cliff is variably covered by large boulders, providing a challenge to follow subunits both laterally and vertically. The base of the outcrop is dominated by dark purple to light green quartzites (with no sedimentary structures), which passes upward into a flattened heterolithic meta-conglomerate that has not been observed elsewhere. The flattened heterolithic meta-conglomerate contains only about 10-20% matrix, which is fine-sand sized and grey in colour (Figure 50). Clast types include (Table 4): 1. relatively fresh-looking basalt pillows, 2. sub-rounded dark grey very fine-grained meta-sandstone, 3. rounded to subrounded light grey quartzite, 4. subrounded unfoliated granodiorite-tonalite, and 5. rounded to subrounded unfoliated rhyolite (?). The relative abundance and size of each clast type was measured in a ~60x60 cm exposure (summarised in Table 4).

Table 4: *Clast types, relative abundance, and size in the flattened heterolithic meta-conglomerate in E. Kangilleq Fjord.*

Clast type	Relative abundance (vol%)	Typical size range
1 - fresh-looking basalt pillows	5%	27-30 cm
2 - very fine-grained meta-sandstone	10-20%	1-5 cm
3 - light grey quartzite	5-10%	2-4 cm
4 - unfoliated granodiorite-tonalite	40%	4-20 cm
5 - unfoliated rhyolite (?)	5%	2-5 cm

Three meta-conglomerate horizons of different thicknesses (1 to 3 m) were found at this locality. In another exposure, a very elongate garnet-chlorite clast (~27 cm x 0.5 cm) was observed. Above the first meta-conglomerate exposure is a ~3 m thick pale green micaceous horizon with <1% pebbles and <10% quartz sand layers, which could possibly represent a reworked tuff. This is followed by a ~1 m meta-conglomerate horizon with similar clast composition. A third meta-conglomerate horizon (before a vertical cliff) contains up to 50 cm long pillows and vesicular basalt boulders and one large (~120 cm) granodiorite/tonalite block.

The meta-conglomerate horizons were deposited in a high energy, tectonic active environment. They represent a local facies not observed elsewhere. Presumably some of the clasts were derived from the Karrat Group, especially the basalt pillows, which occur in Kangilleq Fjord. This provides an important age relationship: the meta-conglomerate is either syn-volcanic or younger than meta-volcanics since pillowed basalt clasts are found in the conglomerate. This unit can be attributed to either the uppermost Kangilleq Formation or lowermost Nûkavsak Formation. These rocks occur stratigraphically above a thick section of Kangilleq Formation that continues on the southwest side of the Fjord.

Figure 50. *A) Flattened heterolithic meta-conglomerate in E Kangilleq Fjord, see Table 4 and text for description of clasts; B) Resedimented pillow in flattened meta-conglomerate*

S. Qeqertarssuaq Island (NE of the town of Nuugaatsiaq) offers excellent exposures of sedimentological features in the upper Nûkavsak Formation. It appears to be a relatively intact section, where right way-up could be confirmed in several places. The dominant lithofacies here are fine to medium-grained meta-sandstone (with or without lithic fragments) and medium to very coarse meta-sandstone (probably subarkose) with dispersed clasts of meta-volcanic origin. Finer grained deposits, including sporadic dark grey to black very fine-grained to silty horizons, are only laterally continuous for 1-3 m, and probably represent channel-edge suspension deposits.

Bedding thickness is variable (few cm to dm). Graded bedding is not commonly observed, but where present is either tabular or swaley to festoon cross-bedding (Figure 51). Mud rip-

up clasts seldom occur at the base of graded beds. Scour structures are common (medium to coarse sand cutting fine sand). Some evidence of soft-sediment deformation (including flame structures and dish structures) suggests that at times deposition was relatively rapid. The dispersed clasts tend to occur in the medium to coarse sand flows but are not sorted (Figure 52). The clast horizons are typically laterally continuous for several metres; the clast size tends to decrease towards the south. Overall this section of Nûkavsak Formation is poorly sorted, from cobble to silt sized particles. Cobbles of volcanic origin occur at several stratigraphic levels of the Nûkavsak Formation (Rosa et al., 2016). This detritus is most likely from the Kangilleq volcanics, which continued to shed into the basin throughout the deposition of the Nûkavsak Formation.

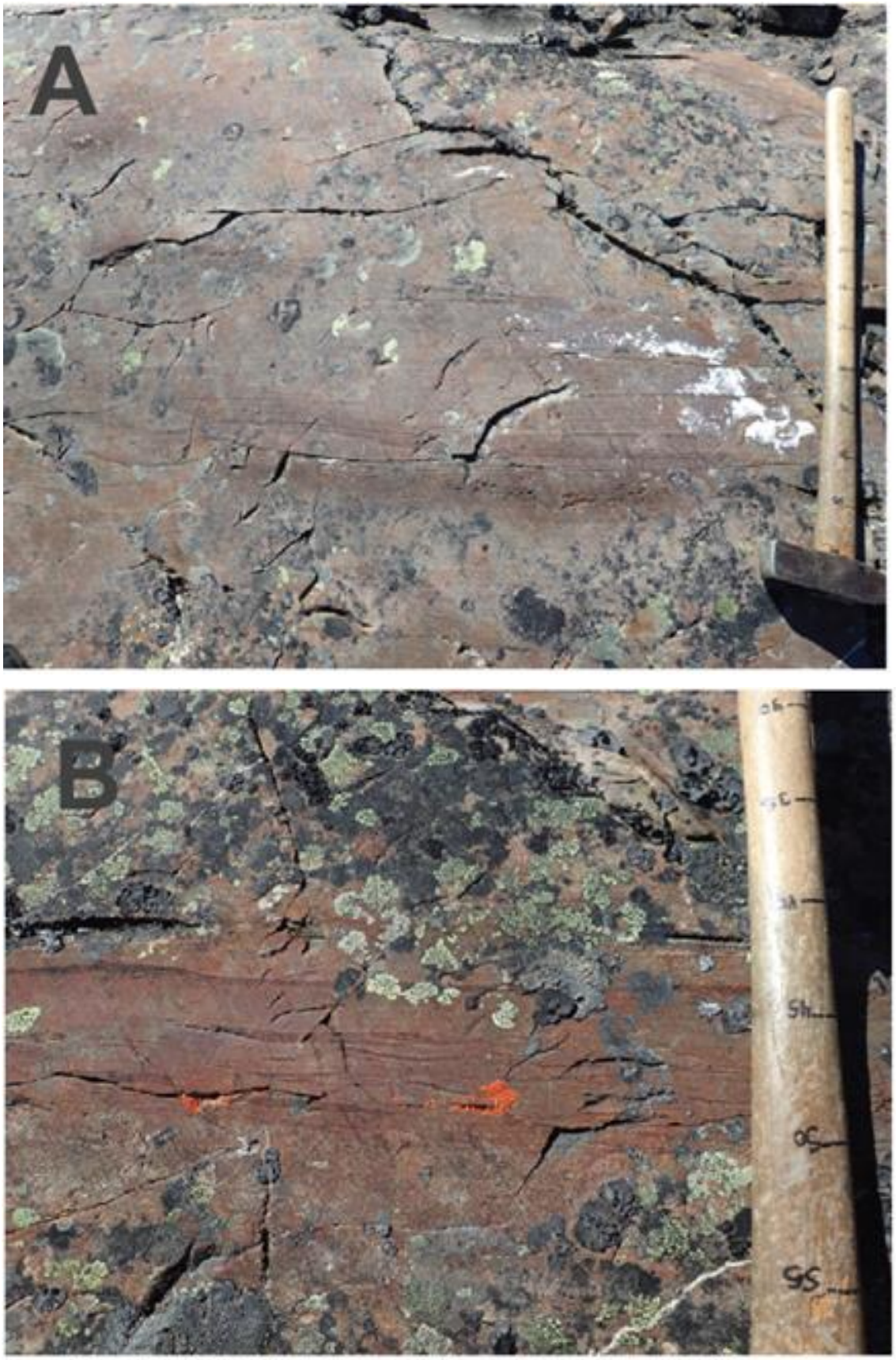

Figure 51. *Nûkavsak Formation in S. Qeqertarssuaq Island. A) Swaley and tabular cross bedding; B) dish structures (soft sediment deformation).*

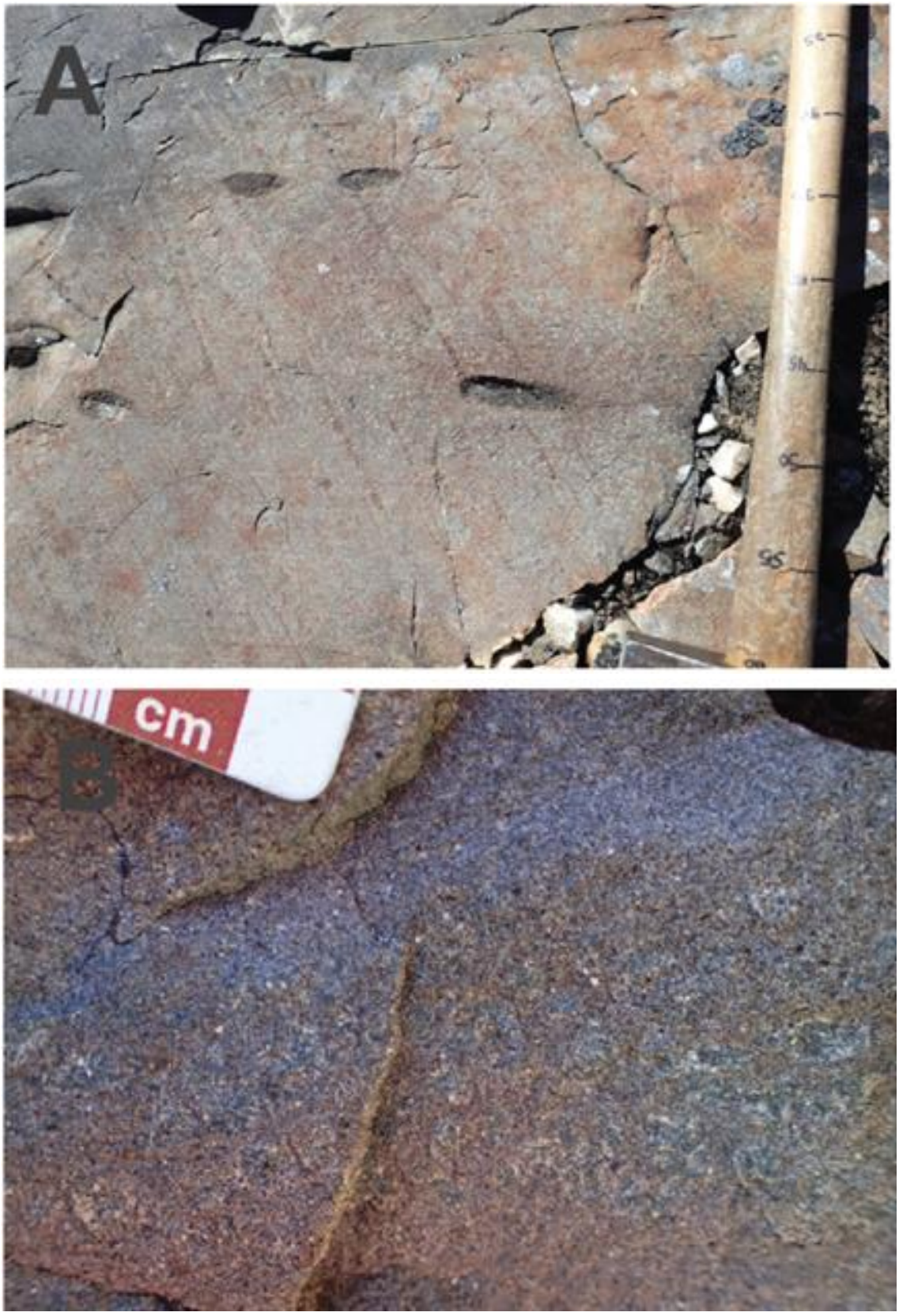

Figure 52. *Nûkavsak Formation in S. Qeqertarssuaq Island. A, B) Mafic volcanic pebbles and lithic fragments in very coarse arkosic meta-sandstone.*

The Nûkavsak Formation at Umiammakku Isbrae is relatively flat-lying (dipping <10°), and unconformably overlain by Tertiary basalts (Figure 53). The Nûkavsak Formation is not easily accessible here due to the vertical cliffs on either side of the nunatak. The Nûkavsak Formation is a fine- to medium-grained meta-sandstone with biotite as the only metamorphic grade indicator.

In northern Kangiussap Kuua, a quartzite/chert unit occurs above meta-volcanic rocks of the Kangileq Formation, similar to Central Kangiussap Kuua, and is cut by a hydrothermally-altered molybdenite bearing intrusion (Rosa et al., 2016). This intrusion, however, does not cut the Nûkavsak Formation. An undeformed granitic intrusion cuts all units present at this locality, including the Nûkavsak Formation.

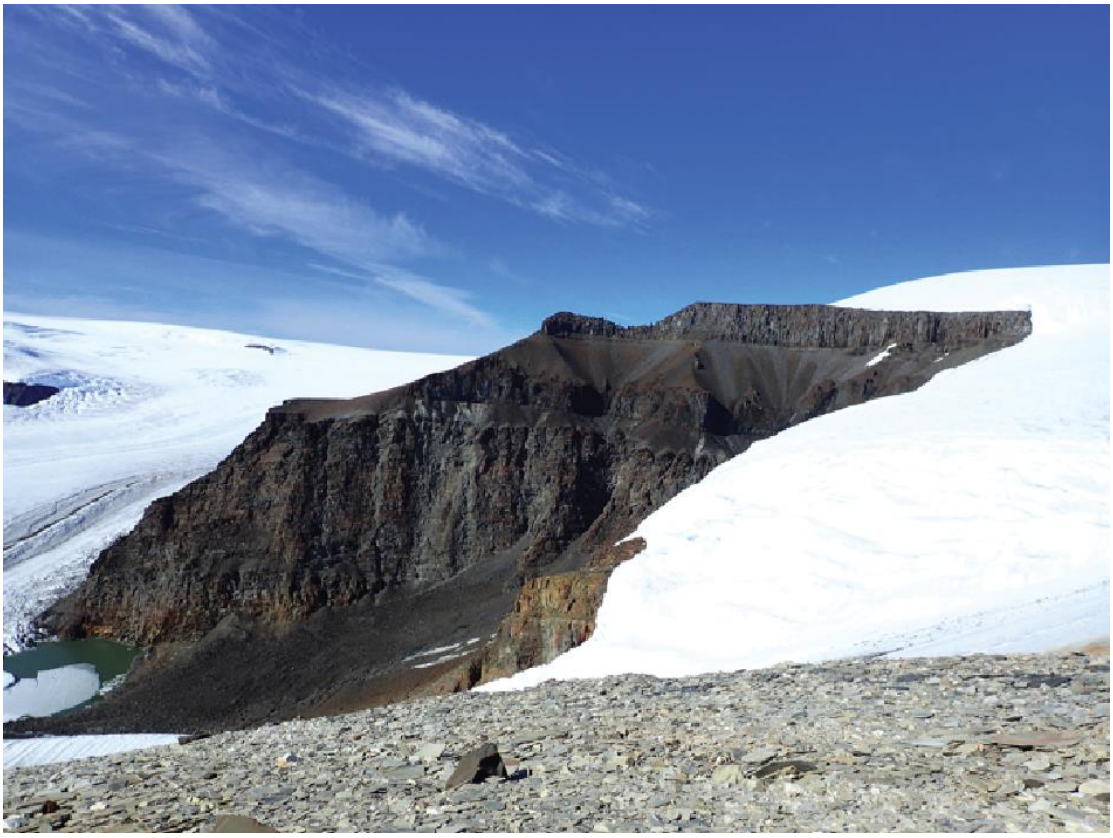

Figure 53. *Umiammakku isbræ: Nûkavsak overlain by Tertiary volcanics (contact at slope break).*

The Nûkavsak Formation at Central Kangiussap Kuua is largely similar to that observed on S. Qeqertarssuaq Island (NE of Nuugaatsiaq). The dominant lithofacies is very fine-grained meta-sandstone with <10% silt/mud with dispersed monolithic cobbles. Overall, this unit is poorly sorted with silt to medium sand to cobble sized particles. Rare tabular (+swaley) cross-bedding, scour structures, and wispy rip-up clasts are also present (Figure 54).

Figure 54. *Nûkavsak Formation at central Kangiussap Kuua. A) Sedimentary structures in the scour structure; B) mafic volcanic clasts; C, D) cross-bedding and dish structures.*

A locality in Rinks Isbrae south was visited to investigate the Nûkavsak Formation. The area is structurally complex and lacks contacts and consistent stratigraphic-up indicators. The Nûkavsak Formation is a medium-grained calcite-cemented massive meta-sandstone with some very coarse-grained feldspar-bearing beds. Locally, mud rip-up clasts occur above very coarse sand cutting into medium-grained sand (as a scour structure) with <5% mud, with ~15-20 cm bed thicknesses. Concretions (calcareous) are present, with elongate concretions up to 1 to 1.5 m. One block of cherty material (rhyolite?) occurs in between rusty chlorite and pyrite rich zones (Figure 55).

Figure 55. *Rinks Isbrae south. A) Calcareous concretion in Nûkavsak Formation; B) rhyolite(?) clast in Nûkavsak Formation.*

The Archean basement-Nûkavsak Formation contact can be observed at Kangerlussup Sermerssua, northeast of Kangerluarsuk Fjord. At this locality, the Archean basement is well-foliated, potassium-feldspar megacrystic granitic gneiss with some pyrite. The Nûkavsak Formation above is also foliated, and contains boudins of mafic material. A ~1 m thick amphibolite layer occurs in the lowermost Nûkavsak Formation near the basement contact. In between Archean gneisses and Nûkavsak Formation, a thin layer of foliated micaceous (~10%) quartzite occurs. The micaceous quartzite is interpreted to represent an erosional remnant of the Qaarsukassak Formation (Figure 56).

Figure 56. Kangerlussup Sermerssua. A) Lower Nûkavsak Formation; B) thin veneer of micaceous quartzite (erosional remnant of Qaarsukasak Fm.?) above Archean rocks.

Intrusive Rocks

Prøven Intrusive Complex (PIC)

The PIC is a medium-grained charnockite containing biotite-plagioclase-k-feldspar-quartz-orthopyroxen±garnet. It is homogeneous, weakly foliated and cross cut by younger granites with garnets and pegmatite dykes. In places xenoliths of the Karrat Group were observed within the PIC.
Intrusive relationships between what has originally been mapped as the PIC and the Karrat Group were observed in two localities: on the northern point of Qassersuaq (northern point of main intrusion) and the west side of Nunatarsuaq. The Karrat Group at both localities has previously been mapped as Nûkavsak Formation.
At Qassersuaq, the PIC can be difficult to recognise in the field due to the beige weathering which gives it an appearance similar to the later pegmatites and granites. On fresh surfaces, however, it has the distinct waxy-green lustre, which is characteristic of charnockites. While the field relations are rather diffuse it appears that the PIC is locally intruding the meta-sedimentary rocks if the Karrat Group.
At Nunatarsuaq, the PIC also outcrops. An intrusive phase clearly cross-cuts the foliation, peak metamorphic mineral assemblages and leucosomes of the Karrat Group (Figure 57-A). In the field the intrusive phase was assumed to be represent the PIC, however, it has a biotite-plagioclase-k-feldspar-quartz assemblage, and it is still a question whether it contains orthopyroxene, and it may instead represent a younger granite, as described in the following subsection.

Crustal melting, melt migration, and S-type pluton formation

In the area between Holm Ø and Ussing Isfjord, melt forms sheets of 'pegmatite' or wide leucosomes separated by meso- and melanosomes (Figure 57-B). We interpret these structures to indicate that melt was extracted during deformation. These sheets become increasingly prominent from the northernmost exposure visited of Karrat Group (Holm Ø) moving south. South of Ussing Isfjord, the Karrat Group becomes more heavily intruded by granitic pegmatites and larger granitic bodies. North of the northern outlet of the Giesecke Bræ, small and large granitic dykes and bodies cut the regional fabric (Figure 57-C,D), and a large (>500 m wide) granitic intrusion is present (Figure 57-E). It is a massive to weakly foliated, medium-grained biotite-granodiorite. The pluton is clearly intruding into the meta-sedimentary rocks and the pluton also contains large rafts of these (Figure 57-E), formerly mapped as the Nûkavsak Formation. The intrusion is interpreted as a S-type granite, formed by melting of the meta-sedimentary rocks of the Karrat Group, and includes assemblages typical of having intruded the middle crust. Associated with this pluton are muscovite-biotite pegmatite dykes that also cut the regional fabric.
We interpret these features to indicate that melt segregated from meta-pelitic gneiss as leucosomes, during burial and deformation, and migrated through the crust during rapid decompression. This process is interpreted to post-date the timing of peak metamorphism, and exhumation of the lower crust. However, further geochronology will aid in understanding these observed field relationships.

Post-kinematic pegmatite dykes

South of Giesecke IsFjord, post-kinematic pegmatite dykes crosscut all other lithologies and the regional fabric (Figure 57-F). Post-kinematic pegmatite dykes are up to 3 m wide and very coarse-grained, composed dominantly of biotite, K-feldspar and quartz with large magnetite grains (up to 2 cm wide).

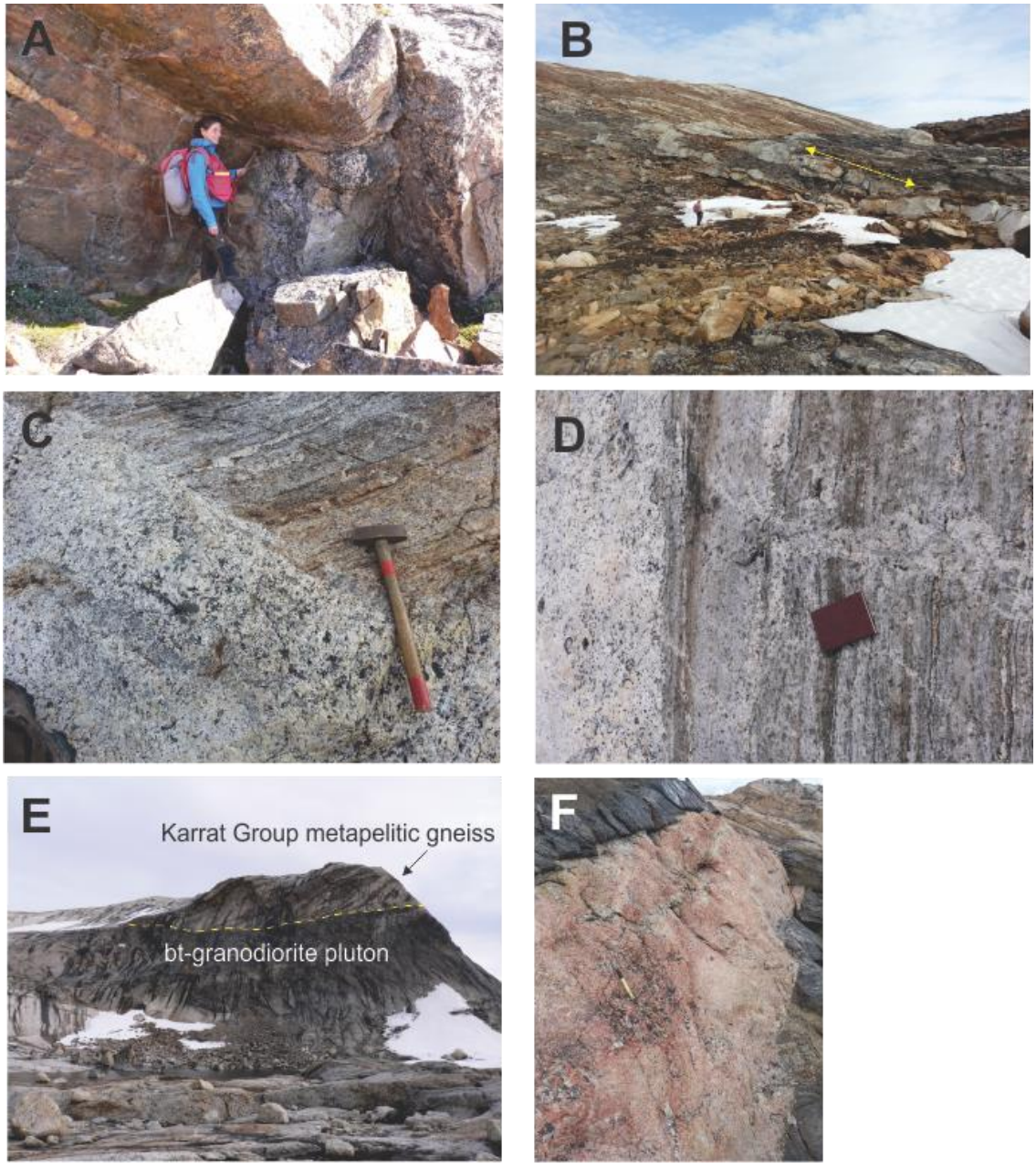

Figure 57. A) *Intrusive relationship between what is mapped as PIC and the Karrat Group paragneiss; B) Leucosome and restite banding within paragneiss of the Karrat Group, in the direction of the regional penetrative fabric. Leucosome bands can be up to 10 m wide; C,D) Granitic veins and dykes cross cut the fabric of the paragneiss of the Karrat Group, just north of the northern outlet of the Giesecke Bræ.; E) At the same locality as C and D, a large (>500 m wide) biotite granodiorite pluton intrudes the surrounding Karrat Group at top of hill; F) Post-kinematic biotite-magnetite pegmatite dyke cutting across all other lithologies and fabrics.*

Nutaarmiut gabbro complex

On the east side of Nutaarmiut, a location known for malachite staining was revisited. Thomassen et al. (1999) briefly studied the location and reported anomalous Cu, Au and As values from geochemical analyses. They interpreted the outcrop as showing granite sheets that intruded meta-sedimentary rocks in the contact zone of the PIC. We identified, however, a new intrusive unit that was not previously mapped or recognised in the area. The rocks are gabbro, monzogranite or syenite and a hybrid rock of both endmember compositions that intruded quartzite of the Karrat Group (Figure 58-A). Interestingly, this large (> 500 m wide) intrusion is undeformed and preserves igneous layering and other primary igneous structures. The structure of the intrusive body is characterised by medium- to coarse-grained, green and pink sheets that are inter-layered on the 30 m-scale (Figure 58-B).

Felsic layers are dominantly composed of syenite or monzogranite, with K-feldspar, plagioclase and quartz. These layers have diffuse, undeformed boundaries (Figure 58-C). Green layers consist of randomly oriented mafic mineral grains, plagioclase and quartz and thus gabbroic in composition (Figure 58-D). All rocks are metamorphosed to greenschist facies and have a chlorite-epidote-calcite assemblage. The darker gabbro shows patches, veins and dykes of more felsic composition (Figure 58-C,D). The patches, locally, have a salt-and-pepper structure. The veins and dykes are connected and open out into the larger-scale felsic sheets. These magmatic structures were, in the field, interpreted as representing unmixing of granophyre melt from a gabbro host intrusion.

All lithologies from this intrusive unit will be investigated to complete detailed petrography. A sample has been submitted for SHRIMP geochronology. Samples of each lithology have also been submitted for major and trace element geochronology and assay.

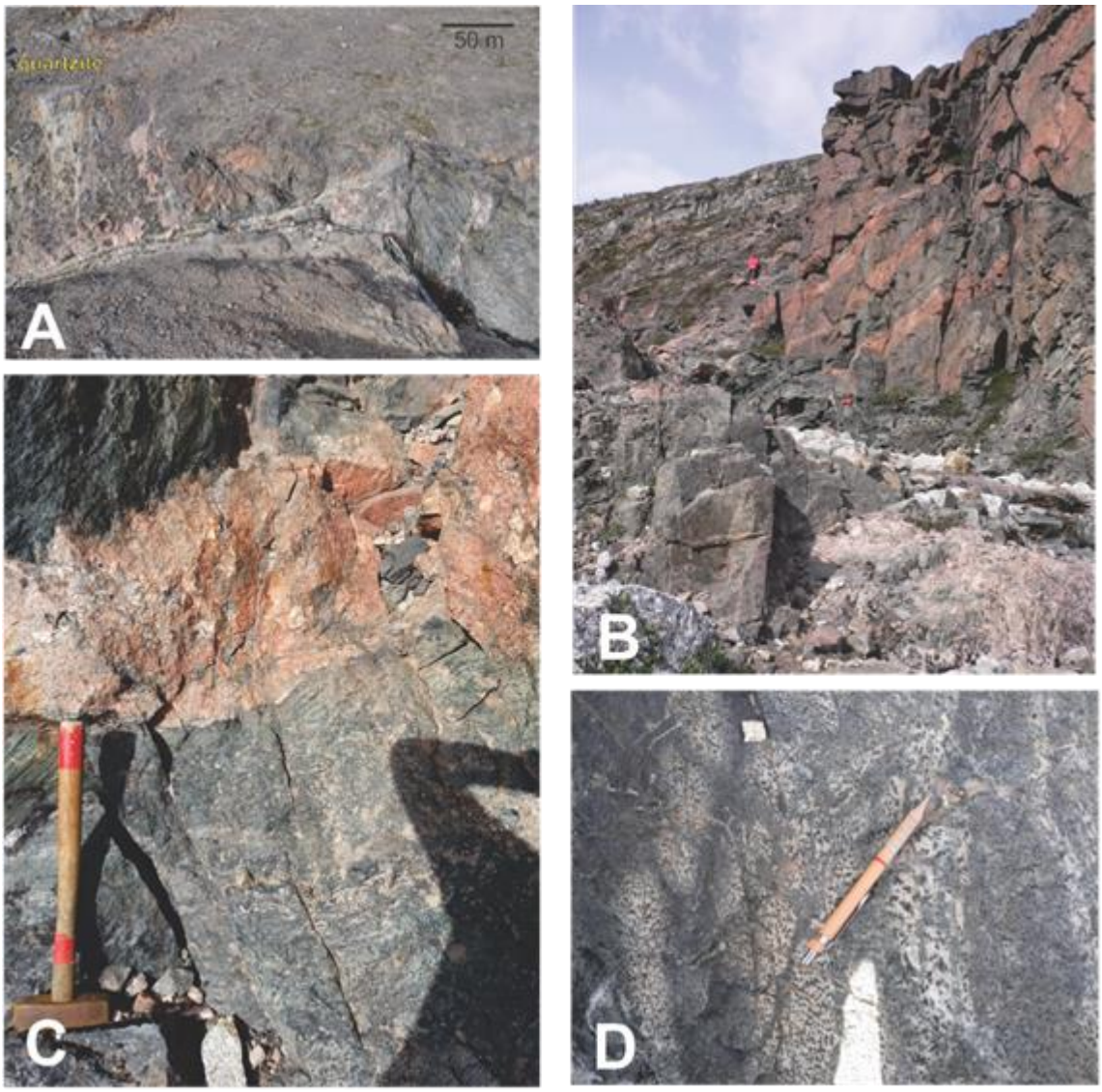

Figure 58. *A) Helicopter view of the Nutaarmiut gabbro complex. Pluton extends to the ocean. It is interpreted to have intruded the Karrat Group quartzites exposed in the left of this picture. The contact was not observed, but "skarn-like" garnet + clinopyroxene assemblages were observed in the quartzite. B) Green-pink layering in intrusion. C) Relationship between green and pink layers in intrusion. Contacts are diffuse and undeformed. D) Randomly oriented mafic minerals within feldspar matrix of green layers.*

Structural Geology

The Paleoproterozoic meta-sedimentary rocks of the Karrat Group extend for more than 500 km from Lat. 71ºN to Lat. 75ºN in West Greenland. The region is separated into two blocks by the Prøven Intrusive Complex (**PIC**) (Thrane et al. 2005). Based on the different types of rocks and metamorphic grade, meta-sedimentary rock covers, structures and basement-cover relationship, the region is subdivided from north to south into six structural domains (Figure 59):

- Northern Domain
- Prøven Domain
- Kangiusap Kuua-Ukkusissat Fjord Domain
- Umiammakku-Inngia Fjord Domain
- Alfred Wegeners Halvø-Kangerlussuaq Fjord Domain
- Nunaarsussuaq-Maarmorilik Domain

The northern contact between the PIC and the Paleoproterozoic gneiss is intrusive (see Intrusive Rocks section) but often obscured by near-vertical structures while the southern contact is sheared and the PIC thrust onto Paleoproterozoic meta-sedimentary rocks of the Karrat Group (Rosa et al. 2016).

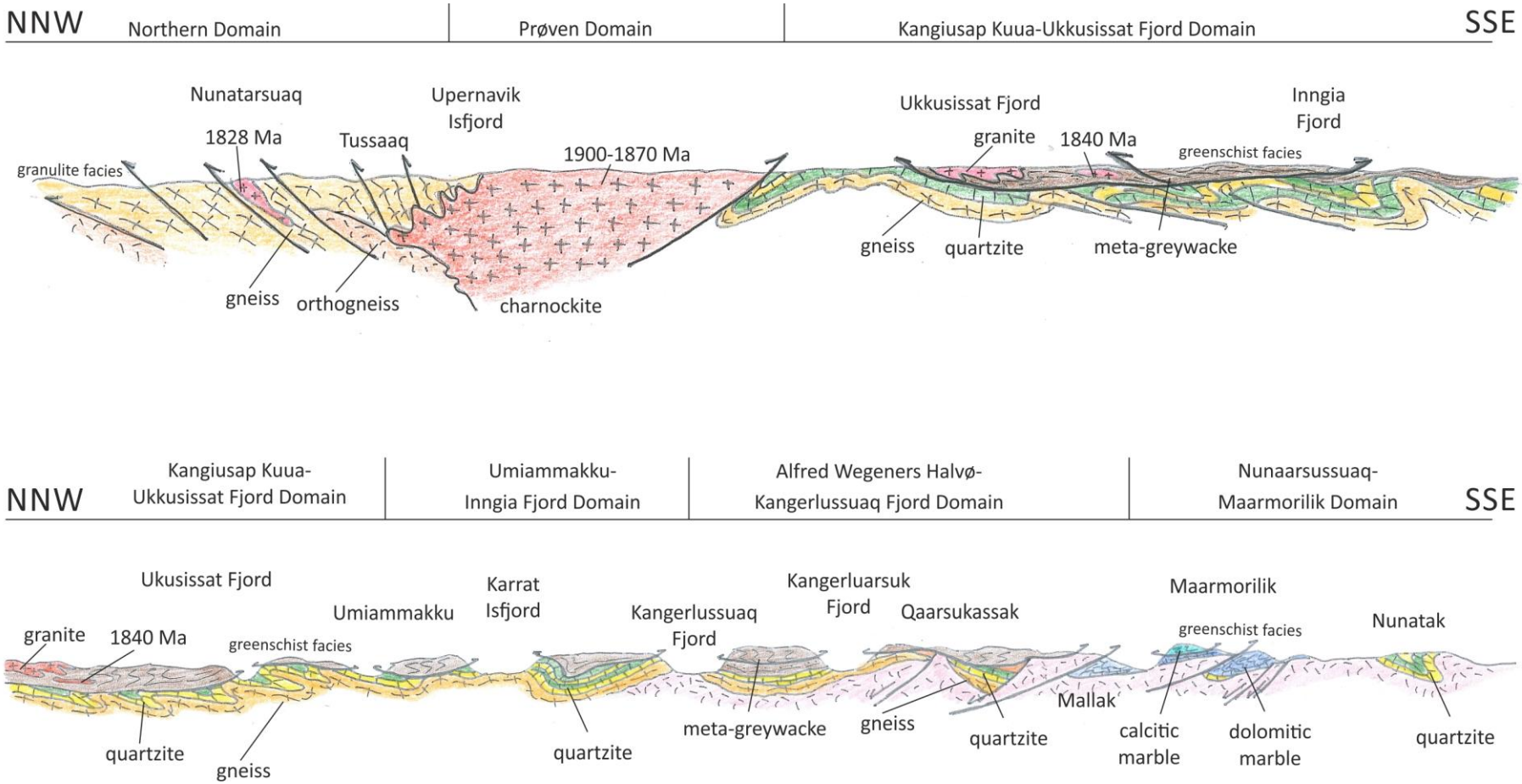

Figure 59. *NNW-SSE schematic geologic cross-section (not to scale) of the Karrat area showing the tectonic relationships between structural Domains and major structures.*

The new observations and data collected during the 2016 field campaign indicate that the E-W extensional tectonics and related fold structures (recognised in the Kangiusap Kuua-Ukkusissat Fjord Domain and described in Rosa et al. 2016 as D4) are post-dated by structures belonging to the Kigarsima Stage. For this reason the relative chronology of deformation stages is updated as follows (Figure 60):

- D1 = compressional tectonics, Qeqertarssuaq Stage
- D2 = extensional tectonics
- D3 = compressional tectonics, Kigarsima Stage (ex D2)
- D4 = compressional tectonics, Maarmorilik Stage (ex D3)

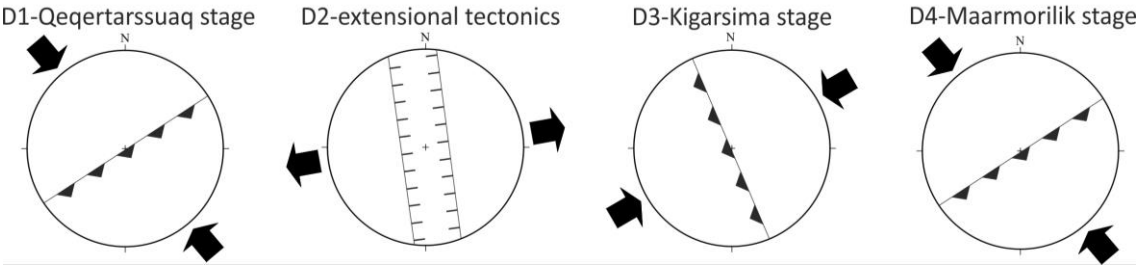

Figure 60. *Scheme of suggested evolution of deformation stages.*

Northern Domain

The area between Lille Renland and Upernavik is mainly underlain by Archean orthogneiss and Paleoproterozoic paragneiss at granulite-facies (Figure 59). The rocks have mainly just one penetrative S1 foliation that is folded into open to close folds at various scales. The S1 foliation is defined by the alignment of biotite, amphibole, aluminosilicates, compositional banding in paragneiss and, locally, leucosomes at higher strain (Figure 61). In low strain areas, leucosomes are at a low angle to the main S1 foliation and preserved F1a fold structures, which are transposed into S1 at higher strain, forming rootless intrafolial isoclinal folds (Figures 61-A,B,C). Increased shear strain is nearly always developed at the contact between orthogneiss and paragneiss. The S1 foliation dips shallowly to moderately NNE-SE and the mineral stretching lineation plunges NE-S, due to later folding. The S1 foliation is laid into regional-scale, recumbent, NW-vergent F1b fold structures with abundant parasitic folds at smaller scales (Figures 62, 64-C). The F1b fold axes plunge shallowly to moderately SW or NE, perpendicular to the L1 stretching lineation on the S1 foliation.
High strain zones are characterised by a closely-spaced S1 foliation and an overall shear sense to the NW (Figure 62). These low-angle shear zones are commonly developed at the contact between Archean orthogneiss and Paleoproterozoic paragneiss and form together with the F1b folds regional-scale nappe structures. Multiple traverses across the two units demonstrate that the relationship between the Archean orthogneiss and the overlying Paleoproterozoic paragneiss is tectonic. The large-scale relationship between the two units is presented in Figure 63-A, and at the outcrop-scale, it is apparent that orthogneiss and paragneiss are tectonically interleaved at tens of metre-scale, where strain is most intense (Figure 63-B). The contact between these two units preserves thin 2-3 m wide mylonite zones (Figure 63-C), with both units becoming increasingly strained toward the contact. Overall, this tectonic contact is a 50 m wide shear zone in which both units (Archean or-

thogneiss and Paleoproterozoic paragneiss) are completely strung out (i.e., the migmatitic banding becomes thin, Figure 63-D). Interestingly, within the shear zone contact area, many lithologies can be observed that are not commonly observed elsewhere and include marble lenses, calc-silicate rock, and silicified layers resembling altered meta-volcanic rock. Additionally mafic to ultramafic lenses at the decimetre to tens of metre-scale occur within this contact zone (Figure 63-E).

Notably, the fabrics vary between the different shear zones, although the kinematic indicators are constantly indicating overall NW-vergent deformation. Feldspar augen in mylonite indicate shearing in the amphibolite facies, whereas alternating feldspar and quartz bands as well as stretched leucosomes indicate deformation in the upper amphibolite facies (Figure 62). Even higher metamorphic conditions may be indicated by brittle rock fragments in a S1-foliated leucosome matrix. The various shear zones juxtapose similar rocks of similar metamorphic grade with a general increase of leucosome and leuco-granite to the SE (Figure 61-A-F). Retrograde metamorphic overprint at amphibolite facies grades is restricted to the D1 shear zones, where rocks outside the high-strain zones preserve their peak granulite facies assemblages. Corona textures of biotite-quartz-plagioclase rimmed by garnet and in turn rimmed by plagioclase indicate prograde crustal thickening followed by decompression during D1. The D1 shear zones are interpreted as major thrusts, based on the high strain deformation and the interleaving of different rock types in the structure that are preserved as lenses. The fact that the shear zone contact between Archean orthogneiss and Paleoproterozoic paragneiss documents different PT conditions in the same kind of deformation regime indicates that they were active during exhumation of rocks from the lower crust (or even upper mantle) to upper crustal levels during NW-SE compressional deformation. This can be explained by channel-flow of lower crust during continent collision.

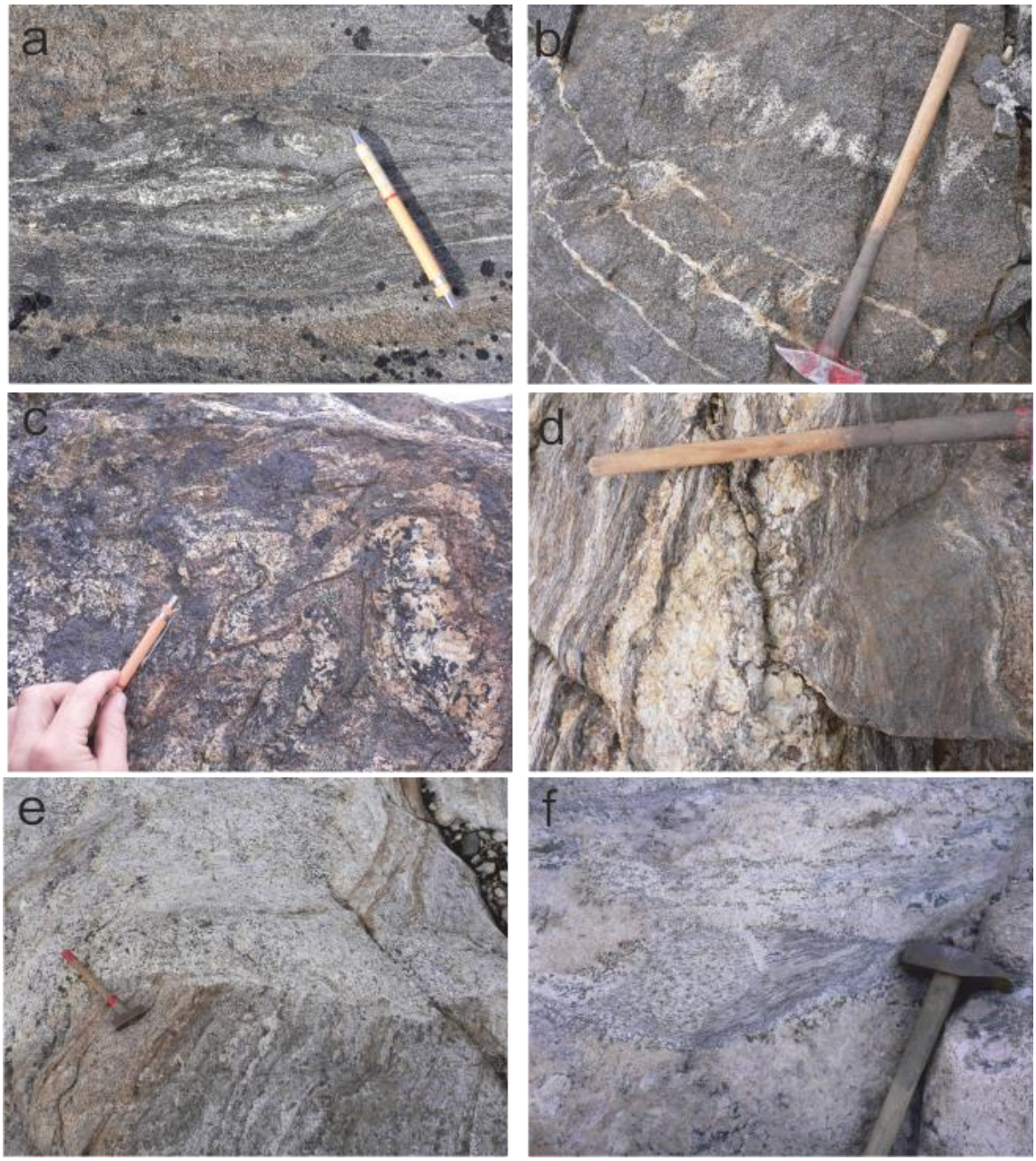

Figure 61. *Field photographs of various types of migmatite from central West Greenland between Lille Renland and Upernavik: A) mafic granulite with plagioclase-quartz-clinopyroxene leucosome; B) mafic granulite with leucosome veins and patches, indicating in situ partial melting and transport of the anatectic melt into vein systems; C) fold interference pattern (F1a and F3) of quartz-plagioclase leucosome in paragneiss; D) foliation-parallel leucosome and larger leuco-granite veins in paragneiss; E) foliation-parallel leucosome bands in paragneiss that open out into a leuco-granite, indicating melt migration into larger systems and formation of leuco-granite by partial melting; F) nebulitic restite in leuco-granite indicating anatectic origin of the leuco-granite.*

Figure 62. *Field photographs of D1 shear zones from central West Greenland between Lille Renland and Upernavik: A) closely-spaced S1 foliation in an upper amphibolite facies shear zone; B) shear zone involving leucosome with brittle deformation of large clinopyroxene; C) mid- to lower amphibolite facies shear zone with plagioclase porphyroclasts and locally brittle deformation of feldspar.*

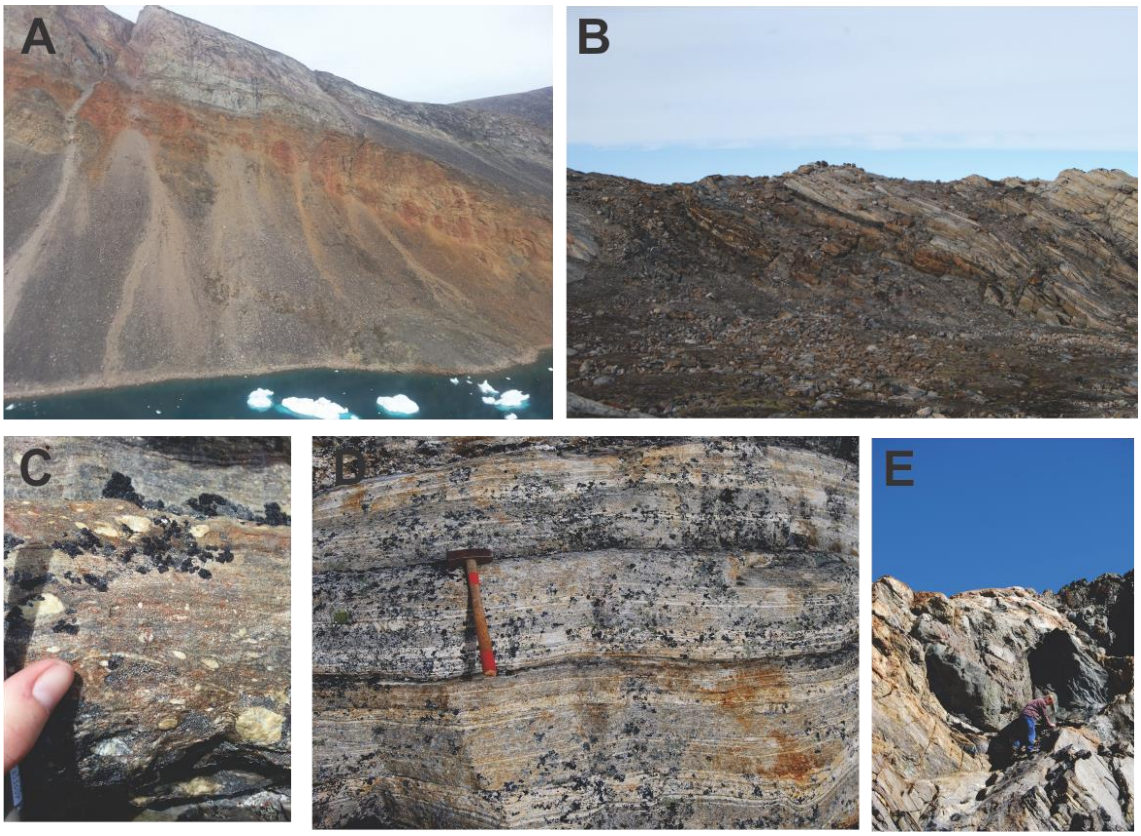

Figure 63: *Tectonic relationship between the Archean orthogneisses and Paleoproterozoic meta-pelitic gneisses of the Karrat Group. A) Archean grey orthogneiss overlying rusty meta-pelitic gneiss; B) Tectonic contact demonstrating interfingering of orthogneiss and meta-pelitic gneiss due to thrust imbrication and/or late parasitic folding. High strain; C) Thin mylonitic layers within shear zone contact between orthogneiss and meta-pelitic gneiss; D) Elongation of leucosomes, neosomes in orthogneiss as approaching contact with meta-pelitic gneiss (becoming a "straight gneiss"); E) Large ultramafic boudin within tectonic contact between orthogneiss and meta-pelitic gneiss.*

The D1 fabrics are only locally deformed by decimetre-scale extensional D2 shear zones that form a conjugate set (Figures 64-A,B). The shear zones are refolded subsequently, but indicate overall NE-SW extension. Locally, leucosomes are developed parallel to these shear zones, indicating high-grade metamorphic conditions and possibly formation at the same time as D1 fabrics (Figure 62-B). The structures are interpreted as extension features related to crustal overthickening and local relaxation. All D1 and D2 structures are refolded into upright open to close F3 folds with mainly SE-plunging fold axis during renewed NE-SW compression (Figure 64-D).

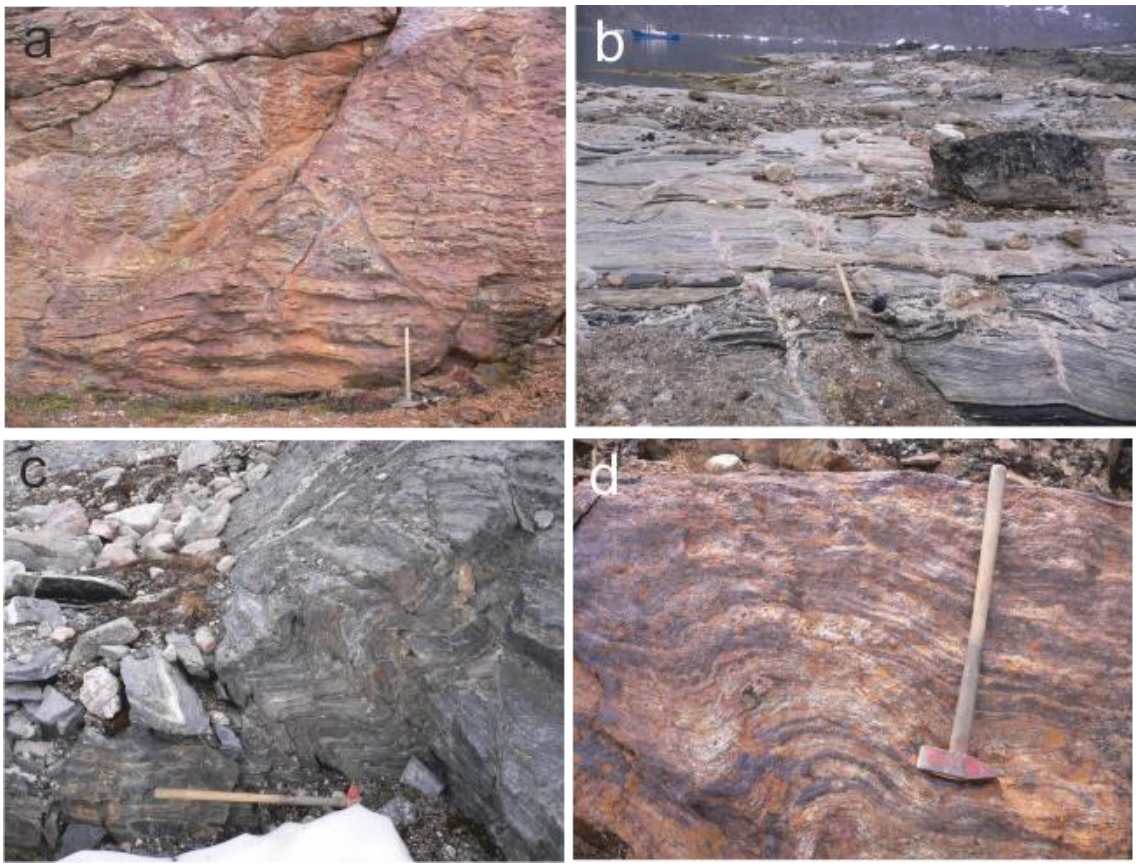

Figure 64. A*) Outcrop-scale normal D2 shear zone; B) Extensional shear zones in Archean orthogneiss. These 20 cm-scale structures are parallel to the structure shown in A) and show the same kinematics; C) Parasitic F1b fold structure in mafic granulite; D) F3 fold structure in paragneiss.*

Prøven Domain

The main fabric steepens to the north of the PIC, where a major shear zone (Tussaaq straight belt) is developed that has been active as NW-vergent reverse, sinistral strike-slip, and SE-vergent normal shear zone in amphibolite facies. We suggest Tussaaq shear zone as a more modern term. The northern contact of PIC is locally intrusive (Figure 65-A) with a narrow contact aureole at tens to hundreds of metre scale and locally sheared with weak magmatic foliation in the granite that is parallel to S1 in the gneisses, indicating syn- to late-tectonic emplacement. The Tussaaq shear zone north of the PIC is likely one of the major structures of the orogen.

The southern contact of PIC is characterized by E to ESE-vergent reverse shearing of granite on top of paragneiss (Figure 65-B), as described by Rosa et al. 2016.

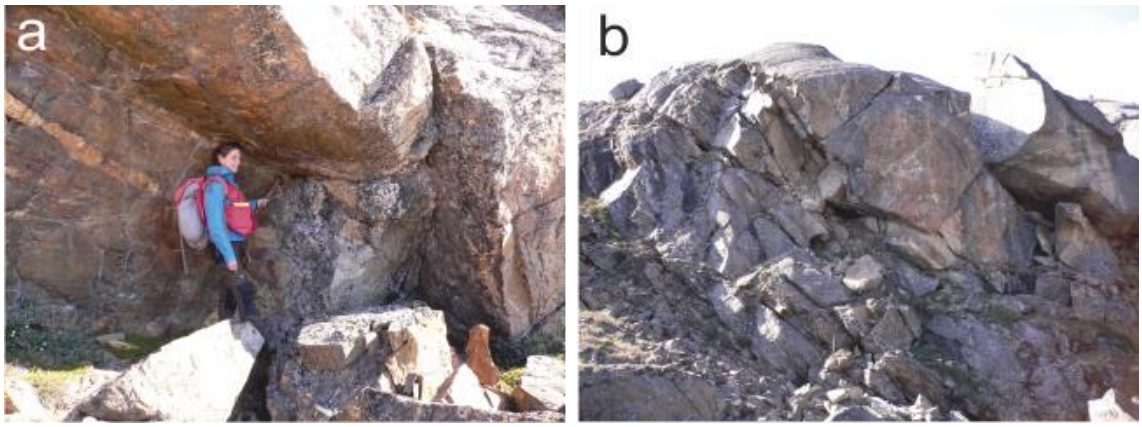

Figure 65. *A) Intrusive contact between what has been mapped as being the PIC on the right and Karrat paragneiss to the left. The monzogranite cuts across the S1 foliation and shows no evidence of metamorphism or deformation; B) East-vergent shear zone at the southern contact of the PIC, where orthopyroxene-bearing tonalite is thrust on top of orthopyroxene-bearing paragneiss*.

Kangiusap Kuua-Ukkusissat Fjord Domain

Along Ukkusissat Fjord, from north to south starting from the Ukkusissat Dome (Henderson and Pulvertaft 1987), a series of gneiss, quartzites, amphibolites and meta-greywackes of greenschist-amphibolite facies grade occur, followed to the south, by higher metamorphic grade schists and abundant granite sheets and again meta-sedimentary and meta-volcanic rocks of greenschist-amphibolite facies grade. The higher-metamorphic grade area with several generations of granite sheets outcrops in an area of extreme alpine topography. The structural relationship between the rocks of different metamorphic grade remains unclear. In the map sheet, all these different rocks are uniformly mapped as Nûkavsak Formation. The southern greenschist-amphibolite facies area is characterised by NW-vergent S-, Z- and M-type chevron folds at tens of metre scale. These folds are separated by axial planar shear zones, yielding a large-scale crenulation cleavage structure (Figure 66-A). The crenulation cleavage is also developed at a centimetre-scale in the schist of the Nûkavsak Formation (Figure 66-B). The fold axes are near-horizontal trending NE-SW, perpendicular to the SE-plunging mineral stretching lineation. These structures are refolded by open upright folds with N-S trending fold axis, which are related to ENE extension along a granite intrusion to the west and distal compression in the east (see Rosa et al, 2016; Figures 66-C,D). Thus, D1 deformation is characterised by F1 NW-vergent chevron folds and NW-vergent shear zones that formed during NW-SE compression and could be related to D1 structures to the north of PIC. The NNW-trending upright folds and ENE-vergent shear zones are related to D2 deformation.

Figure 66. *A) F1 chevron folds in schist of the Nûkavsak Formation between Inngia and Ukkusissat fjords. Note that chevron folds are separated by shear zones forming a large-scale crenulation fabric; B) The same fabric as shown in (a) developed at a smaller scale; C) Fold interference between F1 and F2 fold structures in schist of the Nûkavsak Formation; D) Fold interference as typically found along the northern shore of Karrat Island. This is likely fold interference between F2 and F3.*

Umiammakku-Inngia Fjord Domain

In the area of Karrat and Qeqertarsuaq islands and Kussinersuup Aaffaa, F1 and F2 structures are in turn overprinted by the NE-vergent Kigarsima Nappe resulting in extremely complex fold interference patterns (F3; Figure 66-D). This is the structure that is described as “overfold” in earlier publications.

The meta-greywackes of the Nûkavsak Formation are intruded by pegmatites that were sampled in 2015. Dating of samples collected in the Karrat Island (Figure 67) can help constrain the timing of thrusting and folding of Kigarsima that clearly post-dates the intrusion of the pegmatites.

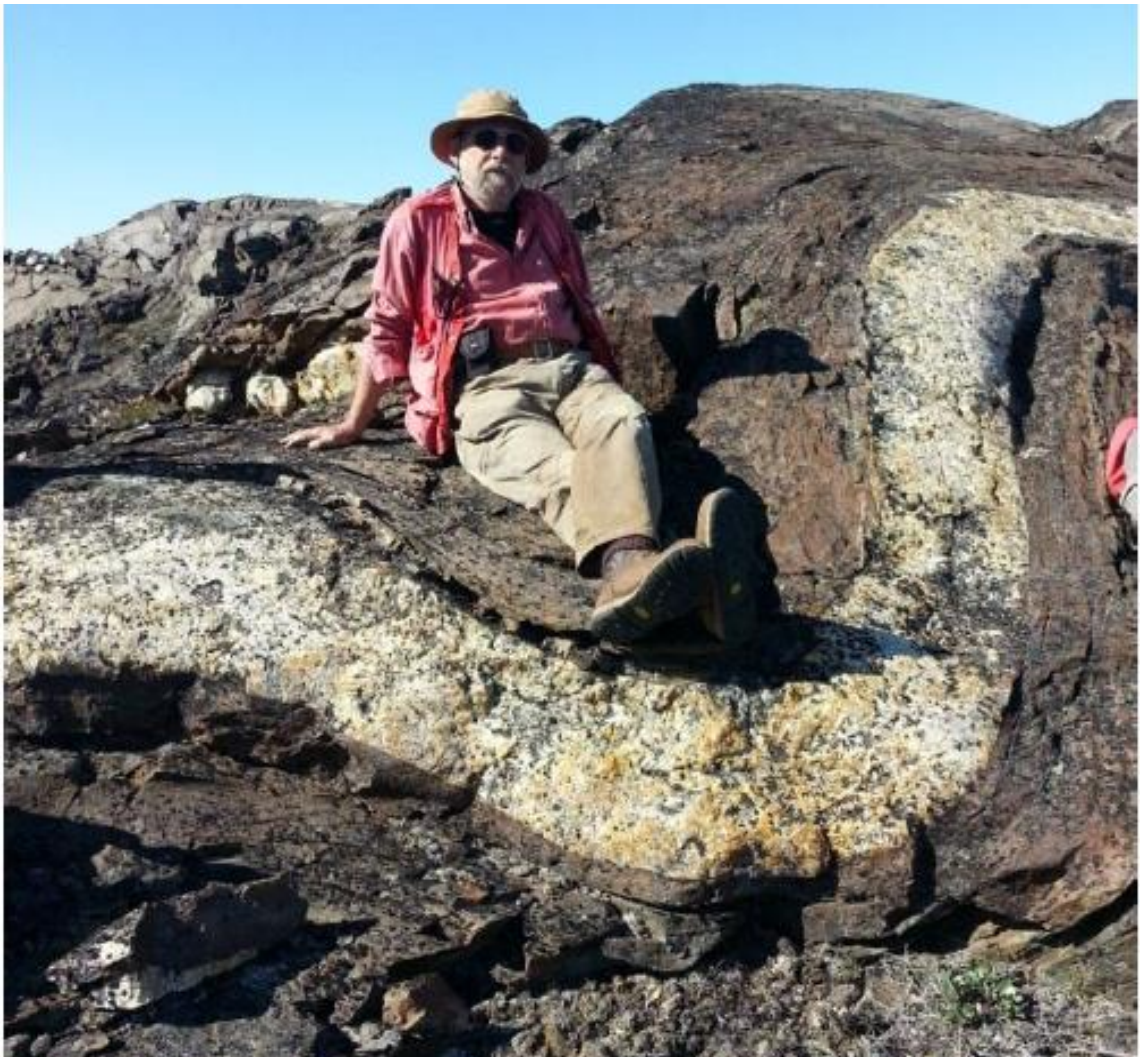

Figure 67. *F3-Folded pegmatitic intrusion in the Nûkavsak Fm on Karrat Island.*

Alfred Wegeners Halvø-Kangerlussuaq Fjord Domain

The Kigarsima Nappe is an overturned isoclinal fold emplaced during NE-SW compression and with a NE-directed tectonic transport (Figure 68). In the footwall of the Kigarsima Nappe, pegmatites intrude meta-greywackes of the Nûkavsak Formation (Figure 69) suggesting, as shown in the Karrat Island (Figure 67) that the thrusting event post-dates the emplacement of some pegmatite veins/dykes.

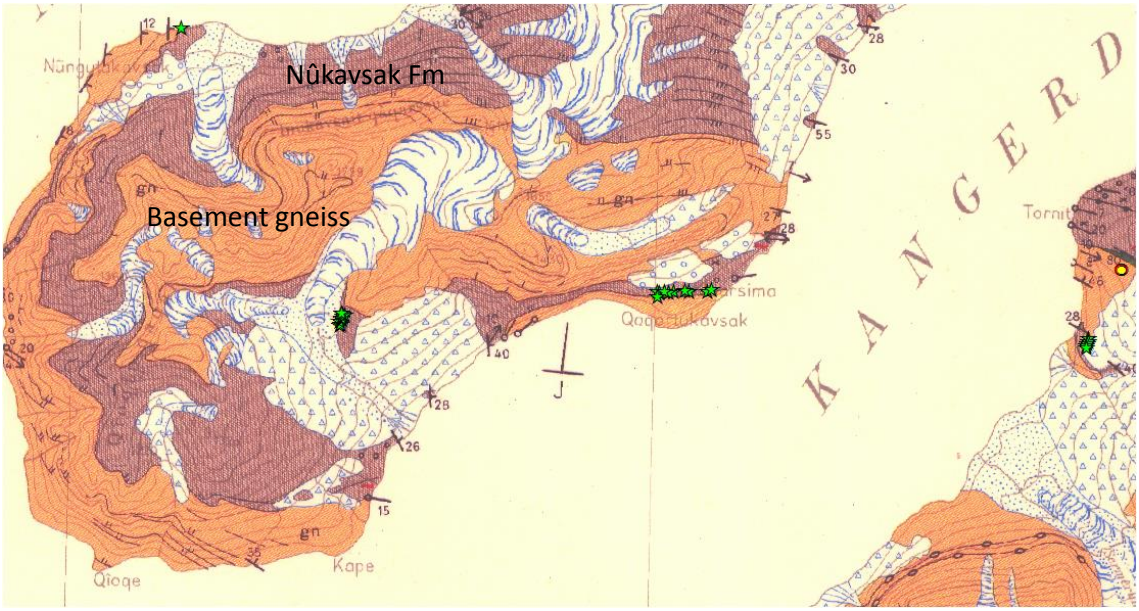

Figure 68. *Geological map of the Kigarsima area (from Henderson and Pulvertaft, 1987).*

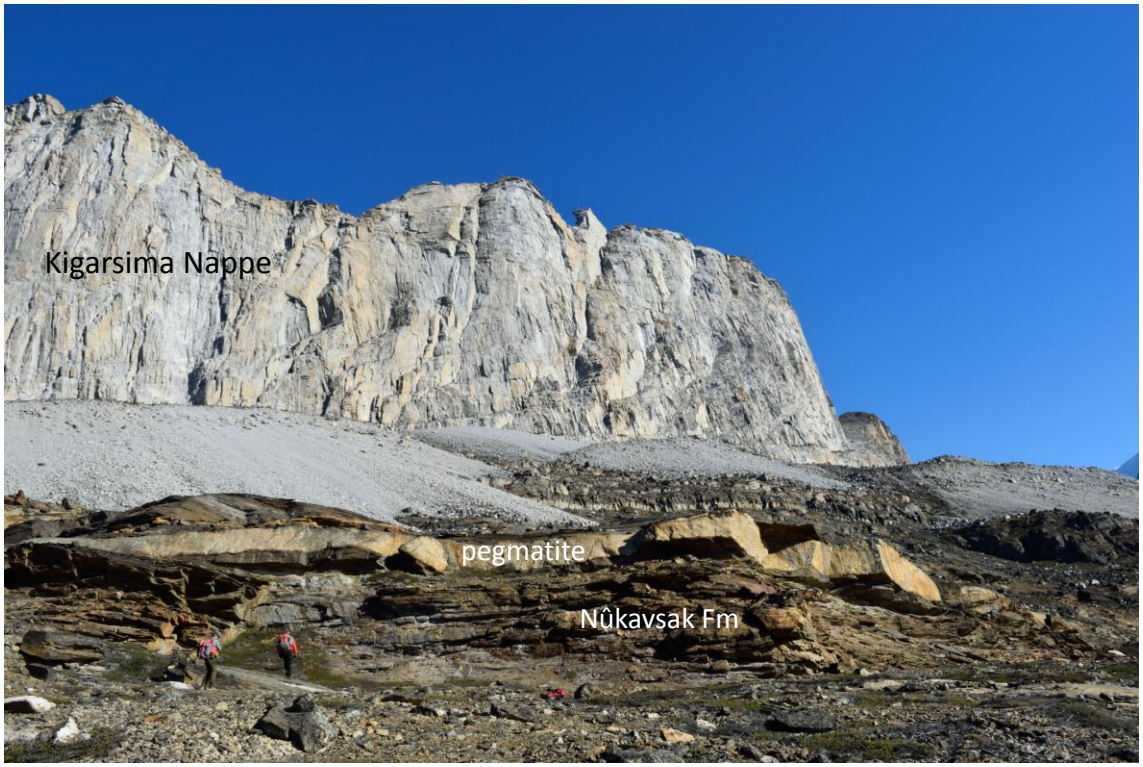

Figure 69. *The intrusive pegmatite and the Nûkavsak Fm meta-greywackes folded together in the footwall of the Kigarsima Nappe at Kigarsima.*

Nunaarsussuaq-Maarmorilik Domain

The structural setting of the southern part of the Karrat area, in the Maarmorilik-Kangerlussuak sector, is characterized by two main compressional stages as suggested in the previous report (Rosa et al. 2016).
In South Lakes (Figure 70) the sedimentary cover is deformed with NW-SE oriented isoclinal recumbent folds well visible at the South Lakes (Figure 71).

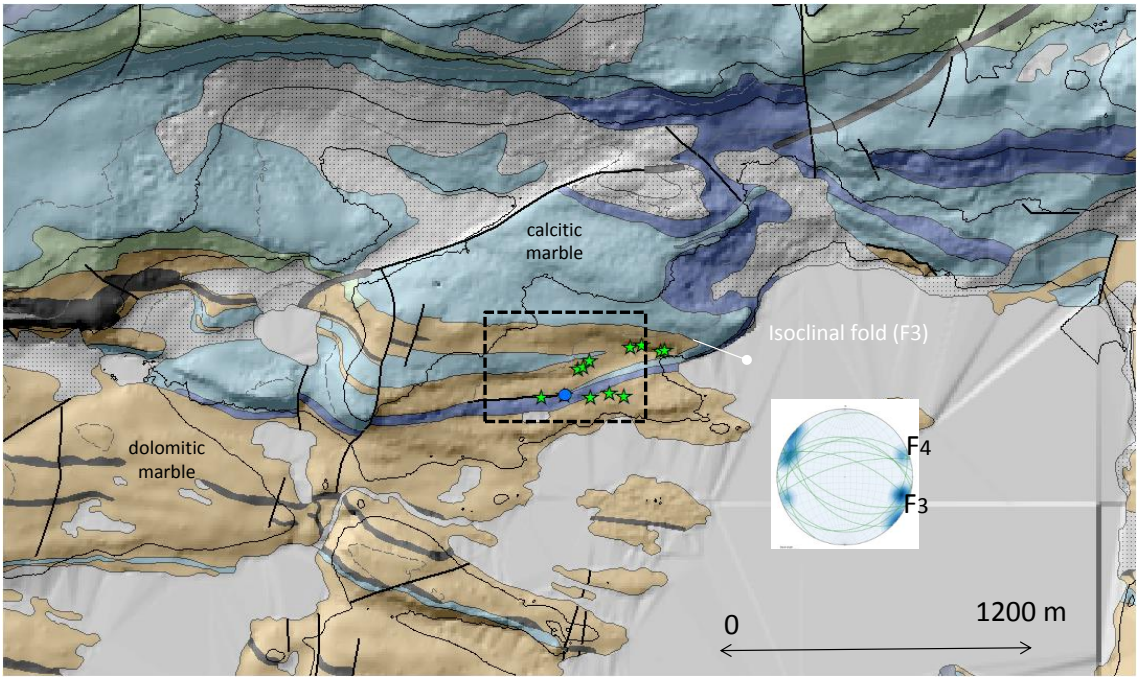

Figure 70. *Geological map of the South Lakes area (after King, 1981). Calcitic-dolomitic marbles form the recumbent isoclinal fold that belongs to the Kigarsima event (F_3). Lower hemisphere stereoplot shows bedding and fold axes collected in the field (green stars). Inset refers to Figure 71.*

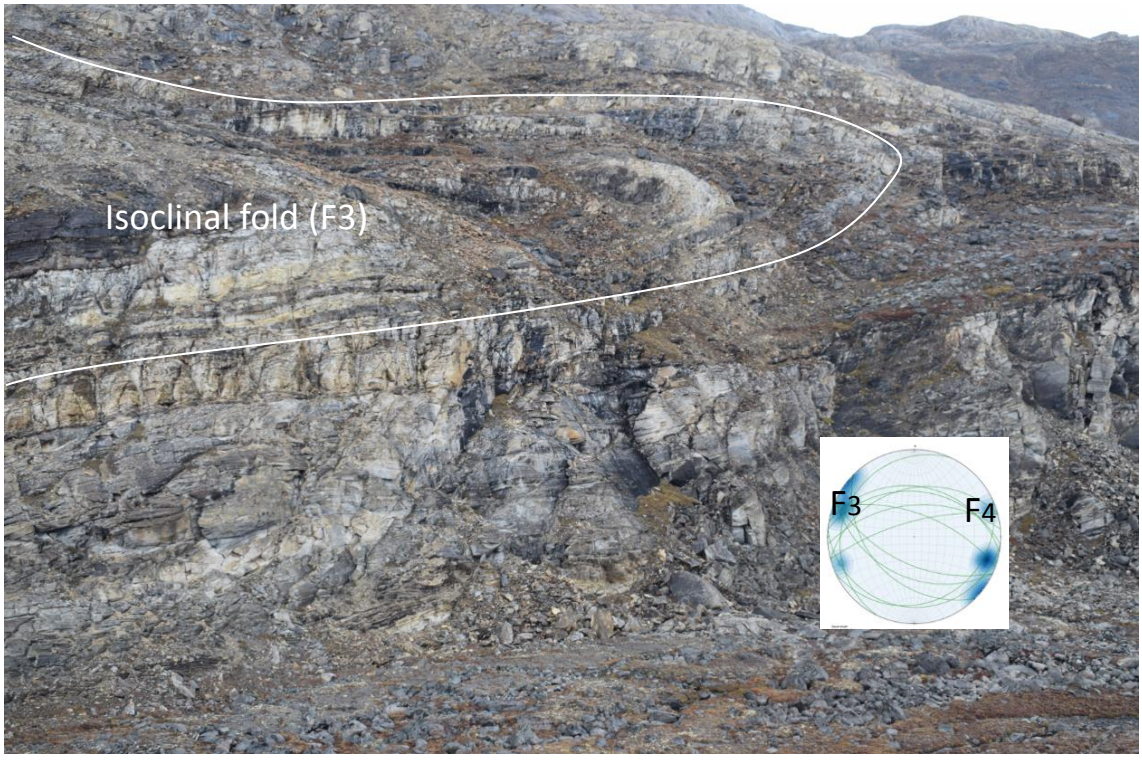

Figure 71. *Folded calcitic-dolomitic marbles in the South Lakes area (see Figure 70 for location).*

In the Nunngarut Plateau (Figure 72) NE-dipping top-to SW shear zones were visited (Figure 73) and mylonitic marbles were found (Figure 74). Both shear zones (thrusts) and the orientation of fold axes suggest NE-SW compression that is coherent with the Kigarsima Stage (D3).

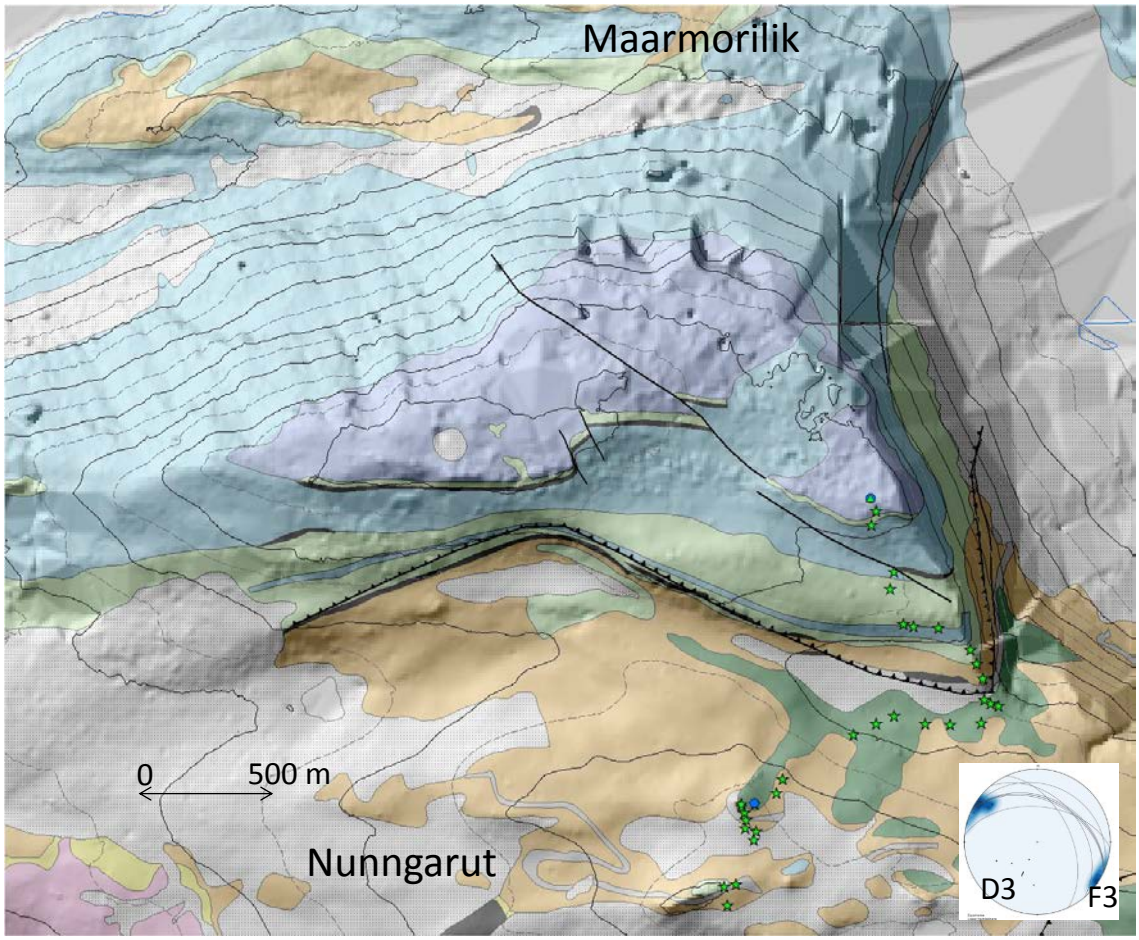

Figure 72. *Geological map of Nunngarut (modified after King 1981). The thrust fault mapped with black triangles represents a major NE-dipping top-to the SW (D_3) shear zone separating calcitic marbles above from dolomitic marbles below the contact. Bottom-right, lower hemisphere stereoplot showing D3 thrust planes and F3 fold axes collected in the area. Green stars, GPS waypoints.*

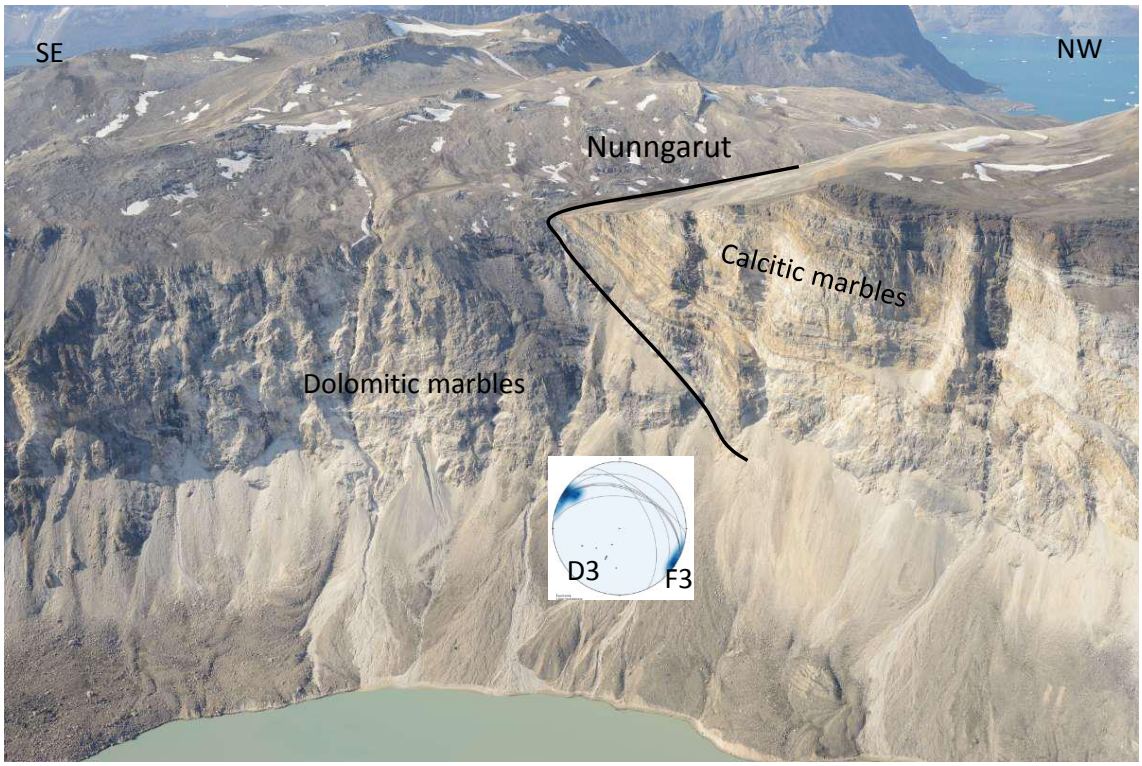

Figure 73. *Oblique photos of Nunngarut taken from the NE showing the thrust contact between calcitic marbles and dolomitic marbles.*

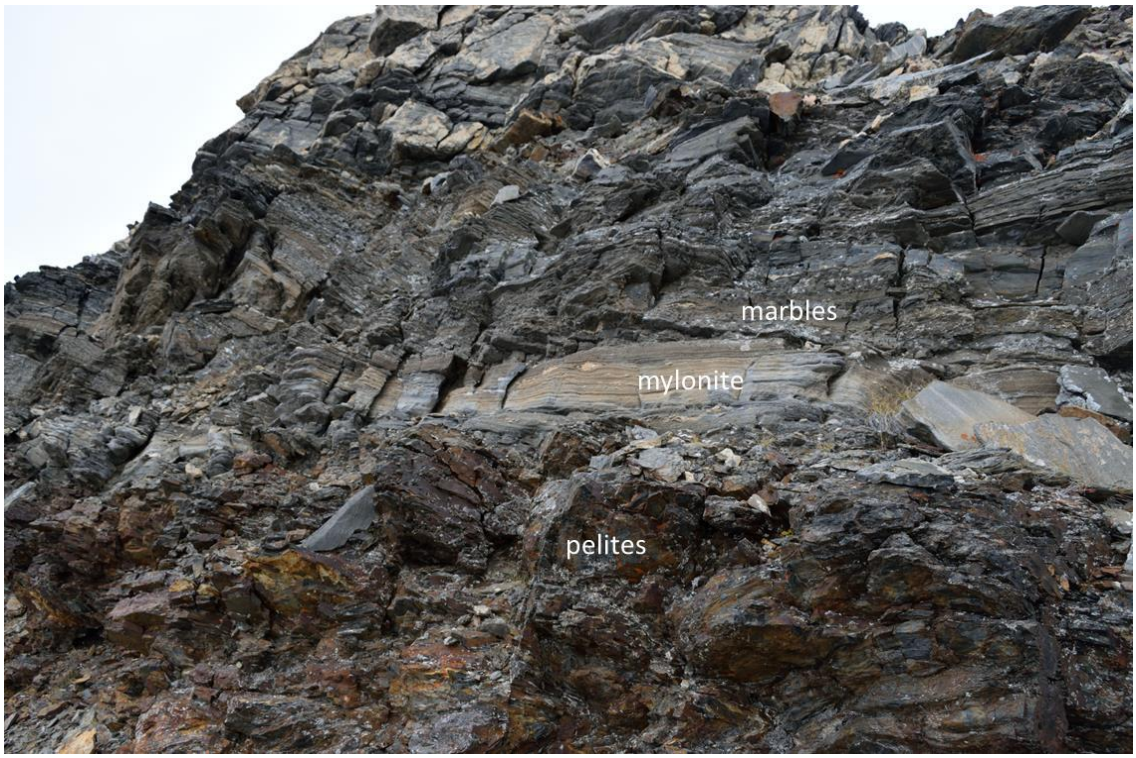

Figure 74. *Mylonitic marbles at the top of the sequence in Nunngarut, above pelitic layers.*

The Maarmorilik Stage introduced in the last report (Rosa et al. 2016) is represented by folds and thrusts involving both Archean rocks and meta-sedimentary cover with ENE-WSW trending reverse faults and fold axes during NNW-SSE to NW-SE compression.
The best example of D4-thrust and related fold structures is exposed at the western end of Nunngarut where Archean rocks and marbles of the Mârmorilik Formation are in tectonic contact along the NW-dipping Nunngarut Thrust (Figures 75 to 77).

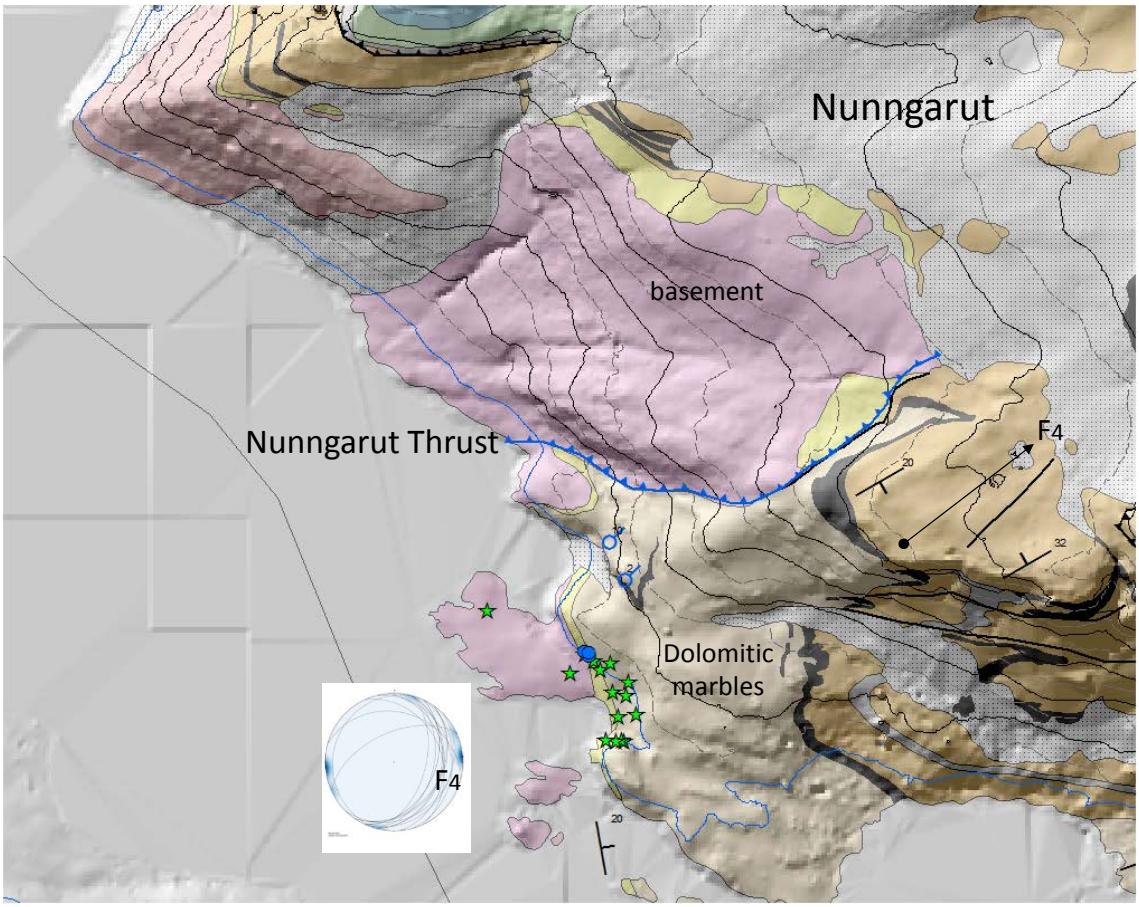

Figure 75. *Geological map of the Tasiussaq area (modified after King et al. 1981). The NW-dipping SE-directed Nunngarut Thrust with Archean rocks in contact with dolomitic marbles. The lower hemisphere stereoplot represents bedding of the marbles and fold axes. Green stars, GPS way points.*

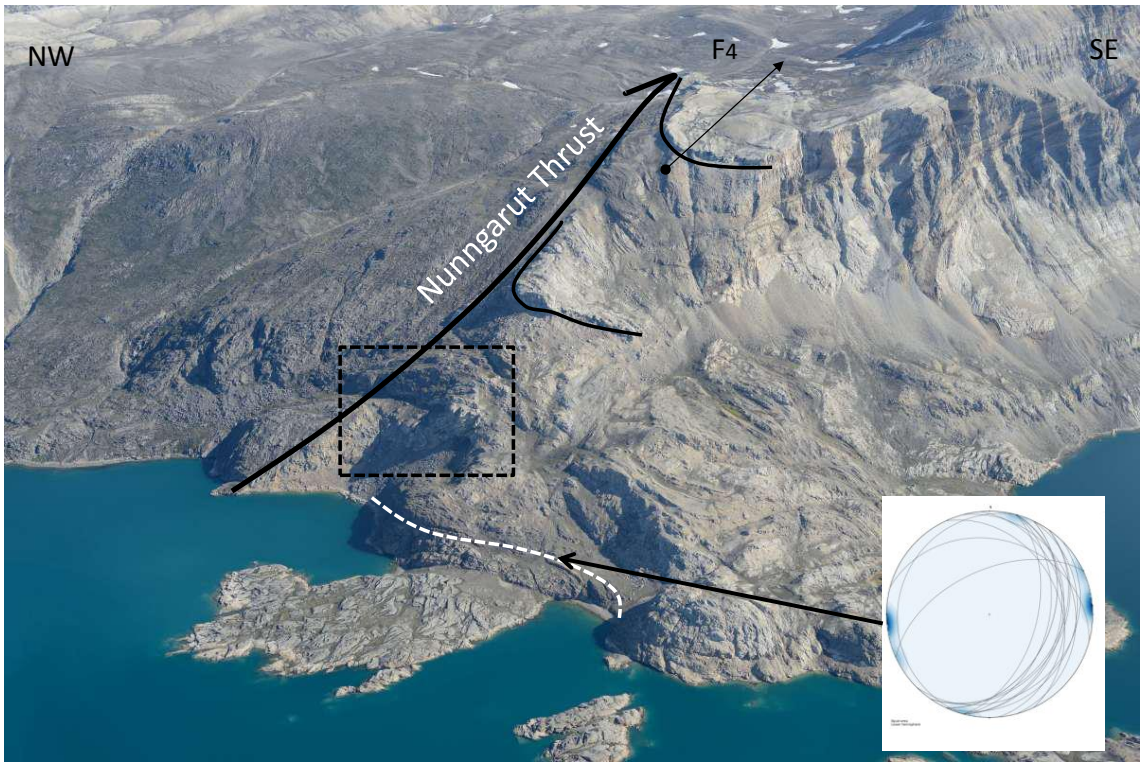

Figure 76. *Oblique photo of Nunngarut taken from the SW showing the geometry of the Nunngarut Thrust with Archean rocks to the left (NW) and folded marbles to the right (SE). The lower hemisphere stereoplot represents bedding of the marbles and fold axes. White dashed line= basal contact of the Mârmorilik Formation. Black dashed line=inset of Figure 77.*

Figure 77. *Detail of the contact between Archean rocks and D4-folded marbles along the Nunngarut Thrust. See location in Figure 76.*

Economic Geology

Nûkavsak/Kangilleq VMS

Allen and Harris (1980) noted that there is a spatial association between semi-massive sulfide horizons in the Nûkavsak Formation and the Kangilleq Formation. They also noted that continuous semi-massive sulfide horizons appear to occur on top of, or along strike from, subaqueous mafic volcanic rocks, suggesting these to represent VMS-type mineralisation.

In the northern Karrat region, previous work (Thomassen & Lind 1998) identified anomalously high zinc and copper in a stream sediment survey conducted in Northeast Nuussuaq. For this reason, a detailed evaluation of the area near the original sample location was conducted. Massive sulfide was found in outcrop comprising a minimum strike length of 400 m and a minimum thickness of 10 m (between N 74.30589/W 56.28057 and N 74.30386/W 56.27914). The massive sulfide mineralisation occurs between two quartz-biotite-sillimanite paragneiss units interpreted to be part of the Nûkavsak Formation. The upper contact of the meta-volcanic unit, which hosts the mineralisation, with the overlying paragneiss is sharp, but irregular, and the lower contact is not exposed. The lower paragneiss unit is in faulted contact with an orthogneiss (Archean basement?) unit (Figure 78).
The mineralisation is hosted by a very fine-grained quartz-amphibole ±biotite± sillimanite± sericite schist with rare primary volcanic textures preserved in the form of white lapilli (10-20vol%, 1-7 mm across) and crude bedding. More distal (>20 m along strike) to the mineralisation, primary textures are well preserved, and include bedding and lapilli-sized clasts (Figure 79).
The massive sulfide consists of 40-50vol% fine-grained pyrrhotite and 30-40vol% fine-grained pyrite, 1-3vol% fine-grained sphalerite and 10-20vol% fine-grained quartz (Figures 80-82). Locally the coarse pyrite ‘stringers’ cross-cut bedding (Figure 83). The massive sulfide is strongly foliated and shows local centimeter-scale folding.
In summary, the massive sulfide mineralisation in Northeast Nuussuaq appears to be replacing mafic volcaniclastic rocks suggesting it represents volcanogenic massive sulfide (VMS) – type mineralisation. The massive sulfide, which was found in four separate outcrops (all believed to be at the same stratigraphic horizon), may constitute one continuous lens or several separate lenses. The massive sulfide lenses have a maximum exposed thickness of 10 m; however, all four exposures terminate in >50 m of overburden (rusty scree) at the lower contact. Given the potential for the massive sulfide to continue at depth or even at surface under the scree, this area should be further explored through drilling or an airborne electromagnetic survey to evaluate the mineral potential further.

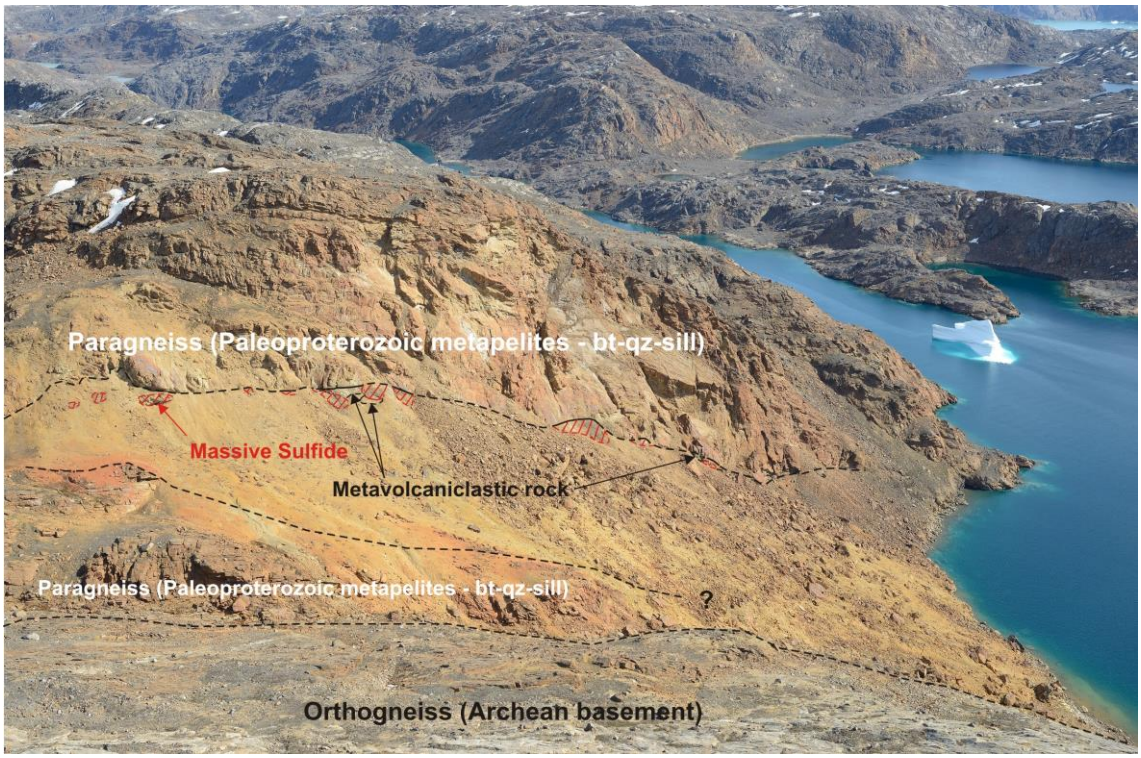

***Figure 78**. Geology of the Northeast Nuussuaq massive sulfide occurrence superimposed on an outcrop photo.*

***Figure 79.** Mafic lapillistone along strike (~20 m) from massive sulfide.*

Figure 80. *Massive sulfide lens (below dashed line).*

Figure 81. *Massive sulfide, detail.*

Figure 82. *Weathered massive sulfide with coarse, bedding parallel pyrite 'stringers' (arrows).*

Figure 83. *Pyrite 'stringers' (along pencil length) cross-cutting mafic lapilli-tuff.*

In the southern Karrat region a known occurrence of sulfide mineralisation within the Nûkavsak Formation, in the Central Kangiusap Kuua area, was revisited in order to complete a stratigraphic section within the host meta-volcanic rocks and massive sulfide mineralisation to gain a better understanding of the stratigraphy, distribution of mineralisation and ore-forming environment.

As outlined in the volcanology section, the Central Kangiusap Kuua area contains a thick (~100 m) sequence of dominantly mafic volcanic rocks, capped by a several metre thick felsic breccia, which hosts the sulfide mineralisation, and a strongly silicified cap rock. Stringer to semi-massive to massive sulfide (pyrite, pyrrhotite ± sphalerite, chalcopyrite; Figures 84 and 85) are hosted by felsic breccias near the top of the section/meta-volcanic package. Mapping of outcrops south of the main exposure of sulfide mineralisation revealed another exposure of mineralised felsic breccia identical to the main sulfide exposure and that changes in facing direction within the meta-volcanic rocks suggest the stratigraphy is tightly folded about NE trending fold axes that repeat the mineralised horizon and overlying zone of silicification three times (Figure 86).

Figure 84. *Massive sulfide (pyrite ± pyrrhotite ± sphalerite) mineralisation.*

Figure 85. *Pyrite stringers in silicified volcaniclastic rock.*

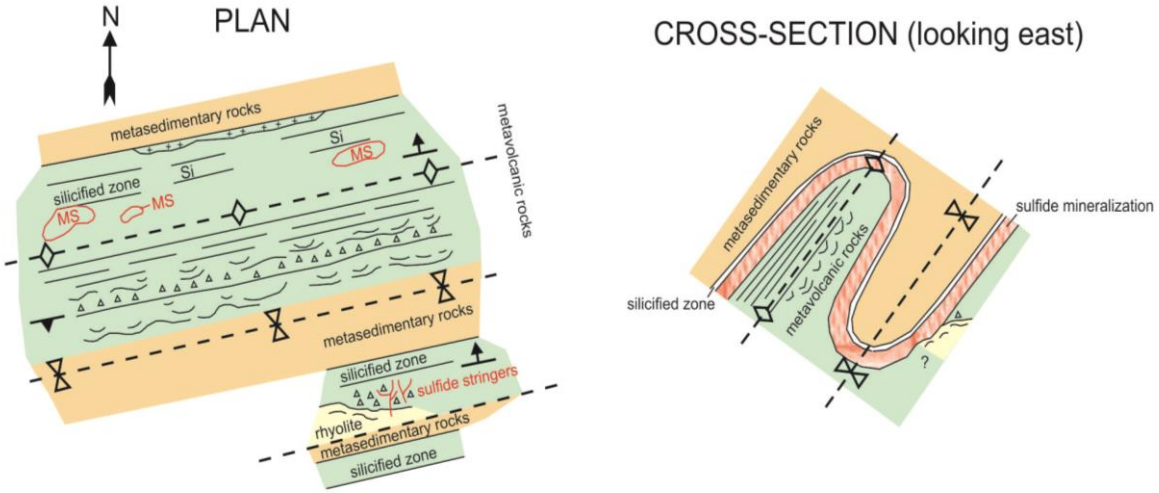

Figure 86. *Field sketches of the main rock types and sulfide occurrences in Central Kangiusap Kuua area, which outline the major structures in the area. Note that the sulfide mineralisation, previously recognised at only one horizon is repeated through folding.*

Similarly to what was documented in Northeast Nuussuaq, the massive to stringer-style sulfide mineralisation at Central Kangiusap Kuua occurs at the top of a sequence of mafic volcaniclastic rocks, just below meta-pelitic rocks of the Nûkavsak Formation, but in this locality appears to be replacing a felsic breccia unit. This along with a semi-conformable

zone of strong silicification and the sulfide texture and mineralogy suggests it also represents VMS-type mineralisation.

Analytical results on massive sulfide and gossan samples collected at Northeast Nuussuaq and in Central Kangiusap Kuua, as well of those collected in other VMS occurrences, namely at Anchorage #2, Rinks Isbræ, Umiamakku Glacier, SW Kangilleq Fjord (across from Karrat island), Qingarssuaq, Kigarsima, Nunatak 1, and Kangerlussuakassak valley, are plotted in Figure 87 and included in Table 5. The table shows that these massive sulfides and gossans, hosted by the Nûkavsak/Kangilleq formations, are base metal poor (typically <0.3% Cu+Pb+Zn), while the ternary diagram shows that their base metal contents are particularly low relatively to their Fe and S concentrations, compared to some samples from the Qaarsusassak and Marmorilik formations, in line with what was suggested in Rosa et al 2016).

Nevertheless, since this time-stratigraphic horizon represents a period of VMS-formation on (or just below) the seafloor, and because it is known that massive sulfide horizons can display zonations from barren to gold and/or base metal-rich zones, these horizons represent good targets for future base metal exploration in the Karrat region.

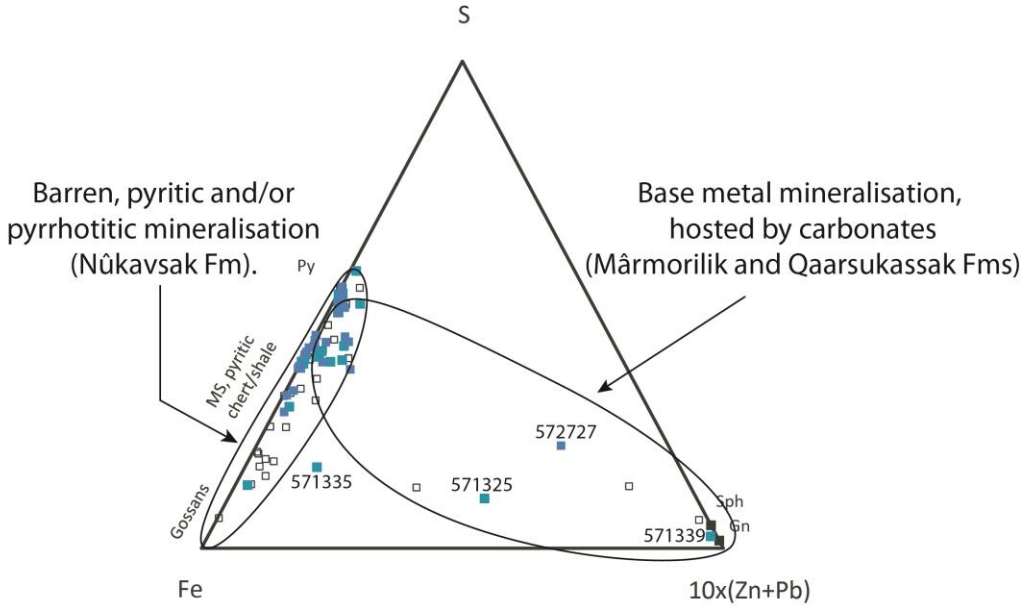

Figure 87. *Fe-S-10x(Zn+Pb) ternary diagram, with discrimination of signatures of base-metal mineralisation hosted by marbles of the Mârmorilik Formation or the Qaarsukassak Formation, and of the rusty weathering zones hosted by the Nûkavsak Formation. White symbols are samples collected in 2015 (reported in Rosa et al,,2016), blue symbols are samples collected in 2016.*

Table 5. *Summary of analytical results obtained through sodium peroxide fusion ICP-OES (Actlabs, Toronto, Canada):*

	Coordinates			Cu	Fe	Pb	S	Zn
Sample #	Lat	Long	Stratigraphic unit - Location	%	%	%	%	%
562036	71.239867	-51.031529	Reworked Qaarsukassak Fm? / Nukavsak? - Nunatak 1	0.143	30.50	0.005	20.20	0.004
562037	71.239870	-51.031500	Reworked Qaarsukassak Fm? / Nukavsak? - Nunatak 1	0.001	25.40	0.045	28.40	0.006
567823	73.774813	-56.151979	Undifferentiated Karrat Group - Anchorage 2	0.030	48.40	<0.001	28.90	0.005
567850	71.875903	-53.994302	Nukavsak/Kangilleq Fm - Central Kangiussap Kuua	0.011	35.40	<0.001	27.50	0.013
567851	71.880113	-53.997629	Nukavsak/Kangilleq Fm - Central Kangiussap Kuua	0.011	52.80	<0.001	34.60	<0.001
567853	71.871788	-53.981443	Nukavsak/Kangilleq Fm - Central Kangiussap Kuua	0.006	4.01	0.001	1.96	0.008
567854	71.872864	-53.982820	Nukavsak/Kangilleq Fm - Central Kangiussap Kuua	0.025	30.50	0.004	22.10	0.046
567860	71.738051	-51.474075	Nukavsak/Kangilleq Fm - Rinks Isbræ	0.086	44.40	0.010	29.40	0.306
567864	71.506080	-52.708129	Nukavsak/Kangilleq Fm - SW Kangilleq Fj, E of Karrat Ø	0.013	22.20	<0.001	23.60	0.086
567905	74.305891	-56.280568	Undifferentiated Karrat Group - NE Nuusuaq	0.111	27.10	0.006	22.70	0.371
567909	74.304716	-56.280688	Undifferentiated Karrat Group- NE Nuusuaq	0.110	24.20	0.004	20.70	0.273
567911	74.303863	-56.279140	Undifferentiated Karrat Group - NE Nuusuaq	0.080	26.80	0.002	20.60	0.129
567930	73.772702	-56.163760	Undifferentiated Karrat Group - Anchorage 2	0.038	52.00	< 0.001	36.40	< 0.001
567972a	71.875864	-53.994261	Nukavsak/Kangilleq Fm - Central Kangiusap Kuua	0.010	38.70	< 0.001	22.70	< 0.001
567972b	71.875864	-53.994261	Nukavsak/Kangilleq Fm - Central Kangiusap Kuua	0.007	36.10	< 0.001	28.10	0.001
567976	71.877055	-53.995215	Nukavsak/Kangilleq Fm - Central Kangiusap Kuua	0.016	49.90	< 0.001	33.70	< 0.001
567977	71.880162	-53.997624	Nukavsak/Kangilleq Fm - Central Kangiusap Kuua	0.014	51.00	< 0.001	33.80	< 0.001
567980	71.872551	-53.982418	Nukavsak/Kangilleq Fm - Central Kangiusap Kuua	0.028	34.30	0.004	25.70	0.019
567986	71.592614	-51.557584	Nukavsak/Kangilleq Fm - Johannes Brae glacier	0.002	29.30	< 0.001	34.00	0.002
571306	72.067147	-51.898613	Nukavsak/Kangilleq Fm - Umiammakku Glacier nunatak	0.056	26.20	0.002	16.30	0.043
571314	71.738508	-51.464109	Nukavsak/Kangilleq Fm - Rinks Isbræ	0.060	47.60	0.013	32.70	0.216
571315	71.736791	-51.475662	Nukavsak/Kangilleq Fm - Rinks Isbræ	0.097	41.10	0.006	27.70	0.168
571316	71.506053	-52.706144	Nukavsak/Kangilleq Fm - SW Kangilleq Fj, E of Karrat Ø	0.026	12.90	0.003	5.46	0.041
571317	71.506620	-52.707884	Nukavsak/Kangilleq Fm - SW Kangilleq Fj, E of Karrat Ø	0.011	22.20	0.001	21.70	0.093
571318	71.506065	-52.707782	Nukavsak/Kangilleq Fm - SW Kangilleq Fj, E of Karrat Ø	0.063	44.80	0.003	31.90	0.222
571320	71.506065	-52.707782	Nukavsak/Kangilleq Fm - SW Kangilleq Fj, E of Karrat Ø	0.001	22.60	0.002	24.70	0.008
571321	71.506393	-52.708000	Nukavsak/Kangilleq Fm - SW Kangilleq Fj, E of Karrat Ø	0.047	26.30	0.003	18.90	0.373
571322	71.500518	-52.729977	Nukavsak/Kangilleq Fm - SW Kangilleq Fj, E of Karrat Ø	0.002	5.47	0.012	7.44	0.004
571323	71.500470	-52.730584	Nukavsak/Kangilleq Fm - SW Kangilleq Fj, E of Karrat Ø	0.114	19.40	0.014	15.50	0.231
571325	71.371811	-51.651570	Qaarsukassak Fm - Kangerlussuakassak valley East	0.003	2.35	0.265	0.59	0.019
571326	71.371515	-51.649538	Qaarsukassak Fm? - Kangerlussuakassak valley East	0.013	13.90	0.004	8.56	0.010
571332	71.189710	-52.220938	Nukavsak /Kangilleq Fm - Kigarsima	0.043	35.40	0.001	22.60	0.020
571334	71.361790	-51.515080	Qaarsukassak Fm - paleovalley N of Qaarsukassak ridge	< 0.001	9.44	0.063	6.44	0.031
571335	71.361912	-51.516530	Qaarsukassak Fm - paleovalley N of Qaarsukassak ridge	0.013	3.52	0.003	0.84	0.067
571339	71.090979	-50.968352	Mârmorilik Fm - Ark showing	0.012	0.95	6.030	1.90	1.530
571343	71.240824	-51.033133	Reworked Qaarsukassak Fm? / Nukavsak? - Nunatak 1	< 0.001	38.00	0.448	42.80	0.007
571344	71.306797	-50.740435	Qaarsukassak Fm? - Nunatak 2	0.001	16.00	0.026	16.90	<0.001
572705	71.222721	-51.361478	MS in Kangerluarssup Sermia	< 0.005	25.00	<0.01	25.80	0.140
572706	71.222756	-51.361863	MS in Kangerluarssup Sermia	< 0.005	6.04	<0.01	6.26	<0.01
572719	71.384770	-52.116842	Nukavsak/Kangilleq Fm - Qingarssuaq	0.084	10.70	<0.01	7.40	0.200
572722	71.384395	-52.105077	Nukavsak/Kangilleq Fm - Qingarssuaq	< 0.005	19.80	<0.01	22.10	0.020
572723	71.385006	-52.106755	Nukavsak/Kangilleq Fm - Qingarssuaq	0.024	24.00	<0.01	24.80	0.050
572725	71.384916	-52.106435	Nukavsak/Kangilleq Fm - Qingarssuaq	0.012	19.50	<0.01	18.90	0.070
572727	71.332508	-51.438486	Qaarsukassak Fm - Discovery	0.015	18.20	<0.01	18.60	5.160
572736	71.384297	-51.678137	Nukavsak/KangilleqFm - Kangerlussuakassak valley East	0.051	26.10	<0.01	15.40	0.020
572739	71.384297	-51.678137	Nukavsak/KangilleqFm - Kangerlussuakassak valley East	0.019	15.90	<0.01	7.35	0.010
572742	71.384268	-51.677630	Nukavsak/KangilleqFm - Kangerlussuakassak valley East	0.018	20.50	<0.01	8.17	0.050

Qaarsukassak Formation

The work carried out in 2015 led to the proposal that the sedimentary package hosting the mineralisation at the Discovery zone of RTZ (Coppard et al. 1992) has unique characteristics and should be erected as a distinct stratigraphic unit, the Qaarsukassak Formation. The name comes from the deposition on Archean rocks around the Qaarsukassak ridge, in Kangerluarsuk Fjord (Rosa et al. 2016). Calcite marbles and (tremolite-)dolomite marbles of this formation appear to be spatially associated with the distribution of Zn-Pb mineralisation at the Discovery and Kangerluarsuup Sermia showings, and therefore its distribution was

preliminarily mapped out using the oblique stereo photographs acquired in 2015, for follow up in 2016.
This follow up, however, revealed that the Qaarsukassak Formation has a rather restricted distribution, and may be confined to the immediate surrounding of the Qaarsukassak ridge and possibly to Kangerluarsuup Sermia and nunataks to the East. This formation appears to be absent in Qingaarssuaq and across Kangerlussuaq Fjord, where it appears that the Nûkavsak Formation and its rust zones lay directly on top of Qeqertarssuaq Formation, so that mapping possibly requires revision. Likewise, in Kigarsima and in Kangerlussup Sermerssua, the Qaarsukassak Formation was not identified, and it appears that the Nûkavsak Formation overlies Archean gneiss.
The Qaarsukassak Formation can been seen on top of Archean rocks from Kangerlussuakassak valley, in the NW, through the Discovery zone where it was described (Rosa et al, 2016), to Discovery South, in the SE. Throughout this interval, the Qaarsukassak Formation occurs in discontinuous outcrops, because of its deposition in paleovalleys (Guarnieri et al, 2016), as highlighted by the distribution of dolomite marbles documented through the hyperspectral survey (Figure 7). In the few places where positive zinc zap response was obtained, chertified samples were collected, even if it was not always easy to trace the source for the response. The analytical results are included in Table 5. Sample 571339 was collected at the known Discovery locality, where sphalerite is clearly visible. Analysis of samples collected elsewhere within the Qaarsukassak Formation yielded relatively low absolute Zn and Pb concentrations, but two samples (571325, from Kangerluarssuk valley and, to a lesser degree, 571335, from the paleovalleys locality to the East, mentioned by Guarnieri et al, 2016) have relatively high base metal concentrations considering their S contents, thereby contrasting with the barren pyritic and/or pyrrhotitic mineralisation so far identified in the Nûkavsak Formation (Figure 87).

The limited distribution of the Qarssukassak Formation may partially be caused by the inference of its deposition in steep paleovalleys, rather than in a wide open basin. Furthermore, parts of the Qaarsukassak Formation might have also been tectonically transported to the East during D3. In this case, the sequences observed in the nunataks towards the East could represent upper stratigraphy of the Qaarsukassak Formation and mineralised horizons could still be found there. Furthermore, stream sediment anomalies with >400 ppm Zn in the clay fraction (Steenfelt et al., 1998), occur to the East and uphill from the Discovery showing cannot be accounted for by this showing. These stream sediment anomalies are also unlikely related to sulfidic horizons within the Nûkavsak Formation, which have not yielded significant base metal grades to date, and have only yielded more modest stream sediment anomalies. This opened the exciting hypothesis that the top of the Qaarsukassak Formation crops out to the East and could account for the stream sediment anomalies. Therefore, landing on several nunataks in the inland ice was attempted, but could only be carried out at the following three nunataks, which were briefly checked for indications of mineralisation:

-Nunatak 1 (N71.2398 / W51.0313) cannot account for the stream sediment anomalies mentioned above, due to its location and glacier movement. Nevertheless, a ground check was made because this nunatak includes a rusty sequence, between what has been mapped as Archean gneiss to the West and Nûkavsak Formation to the East. The base of the sequence is an undeformed felsic rock, possibly still part of the Archean. This is overlain by a poorly sorted (gravel to boulder) polimict breccia with marble, quartzite, chert, and possible quartz-phyric volcanic rock clasts, dominantly angular to subangular, set in a very

coarse sand matrix. Up to 1 m-thick lenses of massive pyrite or laminated pyrite and black siliceous shale occur throughout the breccia, which is also cut by pyrite veinlets (possible stockwork?). However, no positive zinc zap responses were obtained in this sequence. Among the analysed sulfide samples, only one (571343) stands out, with a modest Pb concentration of 0.45% (Table 5). This deposit appears to represent reworked Qaarsukassak Formation or Kangerluarssup Sermia sequence lithologies, possibly during volcanic activity. The sulfides could be part of a VMS system, developed concomitantly with volcanism during Kangilleq/Nûkavsak time. The analytical results of these massive sulfide samples are therefore included with the Nûkavsak Formation mineralisation in Table 5.

-Nunatak 2 (N71.3059 / W50.7345, called Sorte Nunatak and visited by King (1983)) appears to have a mafic dyke (Melville?) on its western part, and two grey horizons on its eastern part, where we landed. The lowermost and more easily accessible horizon was checked and shown to consist of ~10 m-thick calcitic marble, with pockets of coarse pyrite. In between the marble, there are phyllites with rusty horizons of chert and pyrite. However, encrustations in the marble and in the rusty horizons failed to yield positive responses with zinc zap. It is unclear whether this outcrop corresponds to the Qaarsukassak Formation or to the Kangerluarsuup Sermia sequence (Rosa et al. 2016). Since it is from this nunatak that a moraine trail emerges, which could be responsible for the stream sediment anomalies described above, till sediments were collected along the moraine, in order to attempt to constrain the source of the anomaly. However, analysis of the collected till sediment clay fraction revealed these to not be anomalous in base metals. Furthermore, the single pyritic sample collected revealed no significant base metal contents (Table 5). It therefore appears unlikely that this nunatak can account for the stream sediment anomalies further down the glacier. Instead, the source for these stream sediments anomalies, likely lies underneath the ice.

-Nunatak 3 was visited briefly despite its poor outcrop (N71.2981/W50.9196). It includes the contact between Archean gneiss to the West and Nûkavsak Formation metagreywackes to the East. No signs of mineralisation were identified. A relatively undeformed felsic rock was collected between these two map units, which could be part of the Archean basement.

A Mississippi-Valley Type (MVT) origin is suggested for the Zn-Pb mineralisation in the Qaarsukassak Formation, which consequently would have formed at the same time than the mineralisation in the Mârmorilik Formation. This is based on proximity of the Qaarsukassak Formation mineralisation to the Archean rocks and its control by marble and chert horizons, the latter documenting silicification of evaporites, which can play a key role in MVT mineralisation as discussed below.

Mârmorilik Formation

Gypsum/anhydrite has been reported in calcite marbles of the Upper Mârmorilik Formation, in the Black Angel mine (Pedersen, 1980), and in calcite and dolomite marbles of the Lower Mârmorilik Formation, in the South Lakes area drill cores (Harris, 1984). If dolomitization of the Lower Mârmorilik Formation is explained by the popular brine-reflux model of Adams & Jones (1960), the existence of hypersaline brines, and presumably evaporites, would also be required. Other indirect evidence for the previous existence of evaporites includes the

presence, particularly in dolomitic marbles, of scapolite (Garde, 1978). This mineral has elsewhere been interpreted to form through the metamorphic reaction of plagioclase with halite and calcite (Mora and Valley, 1989). Spectral unmixing of the hyperspectral scenes of Black Angel Mountain (Figure 9) document the presence of scapolite-rich marbles above and possibly along the thrust mapped by Garde (1978), suggesting evaporite migration along thrust planes.

The significance of the presence of evaporites in the Mârmorilik Formation for MVT mineralisation is twofold. On one hand, carbonate sequences with evaporites are excellent locations for H_2S formation, through thermochemical sulfate reduction, and H_2S preservation/accumulation, due to the presence of only limited amounts of reactive iron. On the other hand, evaporite diapirism is an ideal way of generating structural traps where the generated H_2S and oxidizing metal bearing fluids can be trapped and react with each other, leading to base metal sulfide precipitation.

With this in mind, a better understanding of the distribution of possible evaporite horizons and diapirs and their relationship with mineralised localities was attempted. This was, of course, complicated by the fact that any evaporites have most likely been destroyed or dissolved by metamorphism and weathering. Nevertheless, a clast-supported monomictic breccia of siliceous pelitic clasts cemented by calcite (Figure 88) is thought to record the presence of an evaporite horizon. This breccia, mapped by Harris (1984), King (1983) and others as mottled pelite, and by Garde (1979) as “chert”-and/or semi-pelite banded marbles, was studied in the South Lakes area. These authors interpreted this breccia as having a tectonic origin, related to thrusting. However, while a tectonic overprint is possible in some locations, this breccia can also be interpreted as being a possible evaporite breccia, in which the pelitic clasts could have resulted from the rupture and *in situ* rotation of pelite beds, as the result of migration of evaporites that were originally interbedded with the pelite beds. Any residual sulfate that would have stayed behind, as matrix to the pelitic clasts, could have subsequently undergone thermochemical sulfate reduction through reaction with hydrocarbons derived from the pelitic clasts themselves or that could have migrated through the breccia, to generate the calcite that presently constitutes the breccia matrix. The thermochemical sulfate reduction would have also generated H_2S that would react with oxidizing mineralising fluids, leading to sulfide precipitation. This is supported by the fact that the Lower Mârmorilik Formation mineralised showings are hosted by (Nunngarut Plateau) or in the immediate vicinity (ARK, Myers, Garde and South Lakes Glacier showings) of this monomictic breccia (Harris, 1984).

If the clast-supported monomictic breccia records the original location of the possible main evaporite horizon, with which the significant Lower Mârmorilik Formation showings appear to be related, the identification of possible diapirs, derived from that evaporite horizon, could indicate even larger mineralised occurrences. This is because such diapirs would have been a large sulfate source for thermochemical reduction, and the deformation their ascension would induce as they moved up stratigraphy, across the Upper Mârmorilik Formation, or the folding/doming they would generate above or laterally to their emplacement level, would form excellent traps for both H_2S and mineralising fluids. While the Black Angel mine was not visited, the literature indicates that its orebodies are in such a favorable position, on the hinge of a D3 fold, underneath thick pelites that would have acted as barriers to evaporite and, subsequently, hydrocarbon and mineralising fluid migration. In this case, the evaporite rocks reported to occur at the Black Angel mine should be interpreted to be al-

lochthonous (diapir), rather than caused by a short marine regression during Upper Mârmorilik Formation deposition, as suggested by Henderson & Pulvertaft (1987).

Figure 88. *Garde's (1978) "mottled pelite" horizon, in South Lakes. It is hypothesised that this horizon could be an evaporite breccia.*

Intrusion related mineralisation

The Nutaarmiut island locality, known for malachite staining and anomalous Cu, Au and As values (Thomassen et al., 1999), was revisited. This led to the identification of a new intrusive unit, including gabbro, monzogranite or syenite and a hybrid rock of both endmember compositions, as described in the Intrusive Rocks section.
Sulfide blebs (chalcopyrite, pyrrhotite; Thomassen et al. 1999) occur mainly in the gabbro and hybrid rock and malachite staining is prominent (Figure 89-A). Polished slabs of the green layering demonstrate an abundance of chalcopyrite stringers, as well as a metamorphic overprint of small (~1 mm wide) deep red coloured grains consisting of a mixture of rutile and titanite (Figure 89-B). The working hypothesis for the Nutaarmiut gabbro complex is intrusion of mafic melt into quartzite, unmixing of (1) mafic melt (gabbro); (2) felsic melt (syenite or monzogranite); and (3) sulfide melt, preserved as blebs of chalcopyrite and pyrrhotite. The study of the degree of PGE-Au enrichment in the sulfide is suggested to evaluate the economic potential of this intrusion.

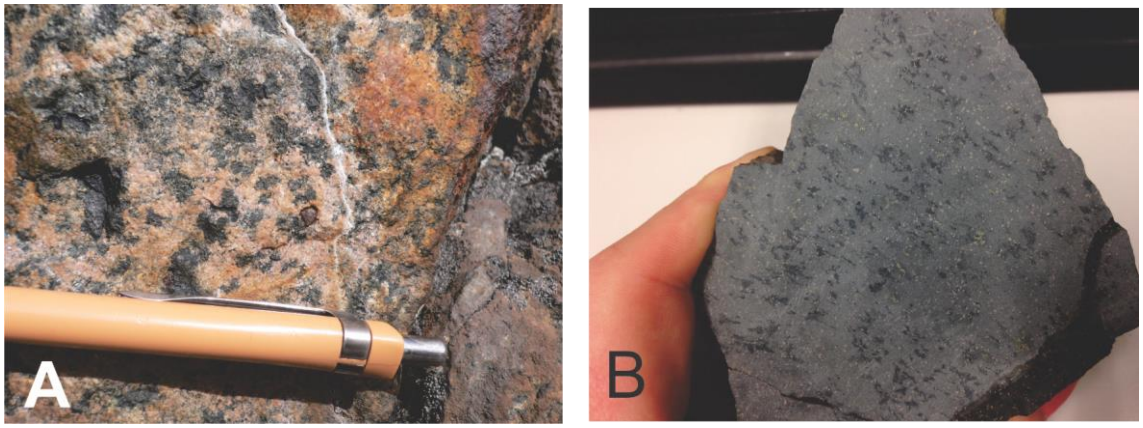

Figure 89. *Nutaarmiut gabro complex mineralisation: A) Sulfide blebs preserved throughout the intrusion; B) Polished slab of green layer. Preserves stringers of chalcopyrite and a metamorphic overprint of rutile and titanite.*

Preliminary conclusions and recommendations

Gaining a better understanding of the intrabasinal correlation of various units of the Karrat Group is critical to delineate the relative age relationship between units, which is elusive since several units are not in contact with one another, and to the interpretation of the basin tectonic setting in which the Karrat Group was deposited. This will also lead to insights as to how the various metal showings are related in space and time. The lowermost (several metres) of the Qaarsukassak and Mârmorilik formations preserve some primary sedimentary structures, but the remainder of those formations generally lack sedimentary structures, making reconstruction of their paleoenvironments challenging. The paleoenvironment of the lower Qaarsukassak and lower Mârmorilik formations appear to be different, since sedimentary structures suggest that the lower Qaarsukassak was deposited in a fluvial environment, whereas the Mârmorilik was likely deposited in a marine environment. The relative timing of deposition of these formations is uncertain, as is the hypothesis that the thin (<50 m) calcareous pelites and non-calcareous meta-sandstones above the Mârmorilik Formation correlate with the Nûkavsak Formation, which overlies the Qaarsukassak Formation in Kangerluarssuk Fjord. The latter can be tested with coarser-grained samples to be analysed for detrital zircon geochronology. The siliciclastic rocks above the Mârmorilik Formation have not been found to preserve sedimentary structures. The Nûkavsak Formation north of Maarmorilik does, however, preserve sedimentary structures as described herein, including scour structures, rip-up clasts, flame structures, cross-bedding, and graded bedding. These structures are consistent with normal marine deposition in a shelf setting. Rocks mapped as Nûkavsak Formation north of the area of Prøven are at higher metamorphic grade, contain no sedimentary structures, and appear to be relatively thin, though measurement of stratigraphic thickness is hampered by the intensity of deformation and lack of marker beds.
Investigations into the meta-volcanic rocks of the Kangilleq Formation have aided in understanding the volcanic history of the Karrat Group. Possible meta-volcanic rocks, seldom with primary volcanic textures, were identified in the northern Karrat area. These rocks could be similar to meta-volcanic rocks of the Kangilleq Formation in the southern Karrat area, but due to amphibolite grade metamorphism, this will need to be further tested by geochemical methods (whole rock trace element and isotope geochemistry). New investigations in the southern area document the concomitant eruption/deposition of the Kangilleq and Nûkavsak Formations established in Rosa et al. (2016). Detailed stratigraphic sections mapped at Qangattarsuaq revealed that volcaniclastic rocks are a more important component of the meta-volcanic package than previously recognised. Also documented are thick accumulations of pillow basalt (>200 m). The thickness and abrupt change from pillow basalts to volcaniclastic rocks suggest the presence of synvolcanic faults possibly outlining a synvolcanic subsidence structure at Qangattarsuaq. Finally, possible felsic volcanic rocks were recognized at Qangattarsuaq and Central Kangiusap Kuua suggesting that Kangilleq volcanism was of bi-modal character.

Little geochronology has been completed in the Northern Domain and so the relationship between lithologies, mineral assemblages and fabrics is critical to work out the orogenic history. Between Upernavik and Lille Renland, the two most prevalent lithologies are grey orthogneiss and grey to red paragneiss. Fieldwork demonstrated that these units, in most

places, were correctly mapped in the 70s and 80s. The regional metamorphic grade between Upernavik and Lille Renland is at granulite facies, demonstrating that this area represents the middle to lower crust of the Rinkian orogenic belt. The oldest lithologies in the area are Archean grey orthogneiss and migmatite, with only very few lenses of amphibolite and ultramafic rocks. Archean rocks preserve high-grade metamorphic mineral assemblages, which likely formed during Paleoproterozoic metamorphism at granulite facies in the deeper crust. No field evidence for multiple stages of high-grade metamorphism, such as intersecting leucosomes of different composition, was observed. One preliminary interpretation of this is that the Archean rocks could represent parts of Archean lower crust that were juxtaposed with Paleoproterozoic rocks and subsequently exhumed during Paleoproterozoic Rinkian orogeny.
High-grade metamorphism of both units was at similar grades and early with respect to juxtaposition along the retrograde shear zones. Extensional structures are minor and only locally observed, whereas the compressional shear zones represent the dominant structural grain north of Upernavik. Exhumation of the lower crustal rocks thus likely occurred during collision and crustal thickening prior to the relaxation of the orogen, possibly by channel flow.
The PIC intrudes the lower crust and post-dates most of the NW-vergent nappe tectonism in the north. It is, however deformed by the Tussaaq shear zone in the north, and thrust E/ESE in the south. The PIC includes a dark charnockite, and a hornblende-biotite granogranite is interpreted to correspond to a later intrusive phase. It contains abundant xenoliths of different compositions, including paragneiss and quartzite. Where the PIC intrudes quartzite (sitting stratigraphically below the paragneiss), there are skarn-like assemblages preserved with abundant garnet and clinopyroxene. Where the PIC intrudes paragneiss, the contact zone contains an increased volume of pegmatite dykes.
The early deformation, south of the PIC, is interpreted as related to NW-vergent D1 described in the Northern Domain. This relates to D1 in Rosa et al (2016). D2 is E-W extension near Archean orthogneiss at Kangiusap Kuua and distal compression further to the E. This deformation stage was assigned D4 in Rosa et al (2016), but clearly predates the Kigarsima stage, which folded the earlier structures. D3-deformation, described as D2 in Rosa et al (2016), is related to the NE thrusting of the Kigarsima Nappe, which clearly overprints all the other structures on Karrat Island and the peninsula to the SE. Toward the south the isoclinal D3 folds in Maarmorilik are overprinted by NW-SE compression previously assigned to D3 in Rosa et al (2016), and now relabeled as D4.

VMS systems related to Kangilleq Formation volcanism are extensive, but have so far only yielded low base metal concentrations. In contrast, the base metal-rich mineralisation in both the Qaarsukassak and Mârmorilik formations is probably related to a single, MVT, event. To better understand this event, the origin and distribution of breccia horizons of the Mârmorilik Formation, traditionally mapped as “mottled pelite”, should be studied and verified whether they could represent the result of the fragmentation of pelitic beds, concomitantly with the migration of interbedded evaporites, previous to or during folding. The migration and accumulation of evaporites in fold hinges could control the distribution of mineralisation, since evaporites could have acted directly, or indirectly, by controlling trapping of sour hydrocarbons, as a sulfur source for base metal-bearing fluids. Close integration of structural, stratigraphic and economic geology observations should be carried out to verify this hypothesis.

Drone-borne surveys can be helpful for specific targets. However, the applied instrument (multi-copter) was not really suited for the arctic environment and the intended area to survey. Here, application of a fixed-wing system with longer flight range is highly recommended. It can also be equipped with a multispectral camera in the VNIR range. In contrast, hyperspectral scanning/imaging of cliffs was revealed to be a powerful tool for large scale alteration mapping and follow up of specific target horizons e.g., distribution of tremolite-rich dolomite marbles at Qaarsukassak or identification of compositional differences in the marbles of the Maarmorilik Formation, that highlighted a fold and thrust structure at Black Angel Mountain. Despite the added logistical complexity for the deployment of instruments in the field, scanning selected scenes increased the in-depth understanding of spatial distribution of particular mineralogies. Thus, hyperspectral scanning should be continued on other targets to resolve specific questions.

Acknowledgements

The financial support from the Ministry of Mineral Resources (Greenland) and of GEUS is appreciated. The authors would also like to acknowledge the excellent working relation with Minna Martek´s crew; Poul, Angut and Henrik, as well as with Air Greenland's pilots, Carl Bostrøm and Petter Prydz Johansson. Finally, fruitful discussions with Stefan Bernstein, Jim Connelly, Adam Garde, Bjørn Thomassen and Agnete Steenfelt are also acknowledged.

Author contributions

EVS+RZI+SSAL wrote the Remote Sensing section, KT+CAP wrote the Archean section, CAP+MDE+EVS+CLA+SMT wrote the Stratigraphy section, KT+CLA wrote the Intrusive Rocks section, PG+JKOL+CLA wrote the Structural Geology and JKOL+MDE+DR+RZI wrote the Economic Geology section . All authors contributed to abstract and summary text and edited the report.

References

Adams, J.E., and Rhodes, M.L., 1960: Dolomitization by seepage refluxion: American Association of Petroleum Geologists Bulletin, v. 44, p. 1912-1921.

Allen, C. R. & Harris, C. J., 1980: Year end report 1979. Karrat Group reconnaissance programme, Mârmorilik area, West Greenland. (Period: May 1979-May 1980). Internal report, A/S Cominco & Greenex A/S, pp 34 (in archives of Geological Survey of Denmark and Greenland, GEUS Report File 20435).

Andersen, M.C. 1981: En geologisk Undersøgelse af den SV-lige del af Drygalskis Halvø, Umanak Fjord, Vestgrønland, med specielt henblik på radiometrisk aldersbestemmelse. Unpublished cand. scient. thesis, Geological Institute, University of Copenhagen, 164 pp

Bakker, W., 2014: Hyperspectral Python (HypPy), www.itc.nl/personal/bakker/hyppy.html
Canty, M. J., 2007: Image Analysis, Classification and Change Detection in Remote Sensing, 1 edn, CRC Press.

Clark, R.N.; Gallagher, A.J.; Swayze, G.A., 1990: Material absorption band depth mapping of imaging spectrometer data using the complete band shape least-squares algorithm simultaneously fit to multiple spectral features from multiple materials. Proceedings of the Third Airborne Visible/Infrared Imaging Spectrometer (AVIRIS) Workshop, v. 90-54, pp. 176–186.

Clark, R.; Swayze, G.; Wise, R.; Livo, E.; Hoefen, T.; Kokaly, R.; Sutley, S., 2007: USGS digital spectral library. U.S. Geological Survey, Digital Data Series, 231

Coppard, J., Swatton, S. & Harris, C. J. 1992: Karrat exclusive exploration licence. 1992 year end report. Internal report, RTZ Mining and Exploration Ltd., pp 19 (in archives of Geological Survey of Denmark and Greenland, GEUS Report File 21297).

Cudahy, T.; Jones, M.; Thomas, M.; Laukamp, C.; Cacetta, M.; Hewson, R.; Rodger, A.; Verral, M., 2008: Next Generation Mineral Mapping: Queensland airborne HyMap and satellite ASTER surveys 2006-2008. Technical report, CSIRO.

Escher, J.C. (compiller), 1980: Map sheet no. 4, Upernavik Isfjord, 1: 500.000, Geological Map of Greenland, Geological Survey of Greenland.

Escher, J.C. & Stecher, O., 1978: Precambrian geology of the Upernavik-Red Head region (72°15'-75°15'N), northern West Greenland. Rapport Grønlands geologiske Undersøgelse 90, 23-26.

Gaffey, S.J., 1985: Reflectance spectroscopy in the visible and near-infrared (0.35 to 2.55 μm): Applications in carbonate petrology. Geology, 13, 270–273.

Garde, A.A., 1978: The Lower Proterozoic Mârmorilik Formation, east of Mârmorilik, West Greenland. Meddelelser om Grønland 200(3), 71 pp

Grocott, J. & Pulvertaft, T.C.R. 1990: The Early Proterozoic Rinkian belt of central West Greenland. In: Lewry, J.F. & Stauffer, M.R. (eds): The Early Proterozoic Trans-Hudson orogen of North America. Geological Association of Canada Special Paper 37, 443–463.

Guarnieri, P.; Partin, C.A.; Rosa, D., 2016: Palaeovalleys at the basal unconformity of the Palaeoproterozoic Karrat Group, West Greenland. Geological Survey of Denmark and Greenland Bulletin 35, 63–66

Harris C.J. 1984: Report on the 1983 South Lakes Diamond Drilling Programme, Greenex A/S (in archives of the Geological Survey of Denmark and Greenland, GEUS Report File 20366).

Harris, C.J. 1986: GREENEX A/S 1985 Year End Report – Plateau - South Lakes. Unpublished report, Greenex A/S (in archives of the Geological Survey of Denmark and Greenland, GEUS Report File 20518).

Henderson, G., Pulvertaft, T.C.R., 1967: The stratigraphy and structures of the Precambrian rocks of the Umanak area, West Greenland. Meddr Dansk Geol Foren, 17, 1-20.

Henderson, G., Pulvertaft, T.C.R. 1987: Geological Map of Greenland, 1:100 000, Mârmorilik 71 V.2 Syd, Nûgâtsiaq 71 V.2 Nord, Pangnertôq 72 V.2 Syd. Descriptive text, pp 72, 8 plates. Copenhagen: Geological Survey of Greenland.

Hunt, G.; Salisbury, J.; Lenhoff, C., 1971: Visible to near-infrared spectra of minerals and rocks: III. Oxides and hydroxides. Modern Geology, 2, 195–205

Jakob, S., Zimmermann, R. and Gloaguen, R., 2017: The need for accurate geometric and radiometric corrections of drone-borne hyperspectral data for mineral exploration: MEPHySTo - A toolbox for pre-processing drone-borne hyperspectral data. Remote Sensing, 9, 88

Keshava, N. and Mustard, J. F., 2002: Spectral Unmixing, IEEE Signal Processing Magazine 19(1): 44–57.

King, A.R., 1981: Report on prospecting and correlation programme, in the Maarmorilik Fomration, West Greenland. Greenex A/S (in archives of the Geological Survey of Denmark and Greenland, GEUS Report File 20419).

King, A.R., 1983: Report on prospecting and correlation programme, in the Maarmorilik Fomration, West Greenland. Greenex A/S (in archives of the Geological Survey of Denmark and Greenland, GEUS Report File 20386).

Mora, C.I., Valley, J.W., 1989; Halogen-rich scapolite and biotite: Implications for metamorphic fluid-rock interaction. American Mineralogist, 74, 721-737

Nutman, P.A., Dawes, P.R., Kalsbeek, F. & Hamilton, M.A. (2008). Palaeoproterozoic and Archaean gneiss complexes in northern Greenland Palaeoproterozoic terrane assembly in the High Arctic. Precambrian Research 161, 419-451.

Pedersen, F.D., 1980: Remobilization of massive sulfide ore of the Black Angel mine, Central West Greenland. Economic Geology, 75, 1022-1041.

Rogge, D., Bachmann, M., Rivard, B., & Feng, J. (2012). Spatial Sub-Sampling Using Local Endmembers for Adapting OSP and SSEE for Large-Scale Hyperspectral Surveys. IEEE Journal of Selected Topics in Applied Earth Observations and Remote Sensing, 5, 183-195.

Rogge, D.M., Rivard, B., Zhang, J., Sanchez, A., Harris, J., & Feng, J. (2007). Integration of spatial–spectral information for the improved extraction of endmembers. Remote Sensing of Environment, 110, 287-303.

Rosa, D., Guarnieri, P., Hollis, J., Kolb, J.,Partin, C., Petersen, J., Sørensen, E.V, Thomassen, B., Thomsen, L., and Thrane, K., 1986: Architecture and mineral potential of the Paleoproterozoic Karrat Group, West Greenland Results of the 2015 Season, Geological Survey of Denmark and Greenland Report, 2016/12.

Steenfelt, A., Thomassen, B., Lind, M. & Kyed, J., 1998: Karrat 97: reconnaissance mineral exploration in central West Greenland. Geology of Greenland Survey Bulletin 180, 73–80.

Thrane, K., Baker, J., Connelly, J & Nutman, A., 2005: Age, petrogenesis and metamorphism of the syn-collisional Prøven Igneous Complex, West Greenland. Contribution to Mineralogy and Petrology 145, 541-555.

van der Meer, F., 2004: Analysis of spectral absorption features in hyperspectral imagery. International Journal of Applied Earth Observation and Geoinformation, 5, 55–68

Zhang, X., Pazner, M. and Duke, N., 2007: Lithologic and mineral information extraction for gold exploration using ASTER data in the south Chocolate Mountains (California), ISPRS Jounal of Photogrammetry and Remote Sensing 62: 271–282